Computer Instrumentation for Voltage Contrast Measurement in the Scanning Electron Microscope

Philip Nye

PhD thesis, University of Edinburgh 1990

Abstract

The scanning electron microscope is widely used in industry as a tool in both development and production stages of integrated circuit manufacture, firstly for very high magnification topographical inspection of circuits and secondly for various diagnostic techniques in which the electron beam interacts in some way with the circuit.

The most used of these techniques is voltage contrast, in which the scanning electron microscope is used to measure voltages and waveforms within the operating circuit. There are an increasing number of systems available for making voltage contrast measurements.

This thesis describes the designing, building, interconnecting and operating of instrumentation to improve the speed and accuracy and above all the usability of a computer based voltage contrast scanning electron microscope.

A fast and efficient technique was developed for making accurate quantitative measurements on ICs which avoids the problems of drift due to contamination and charging which usually hamper voltage contrast instruments in real situations. Studies of the mechanisms of oxide charging and its effects on readings are made.

Finally a scheme for integration of these methods into a fully computerised scanning electron microscope is proposed.

Acknowledgments

Many thanks to my supervisor Alan Dinnis for support and guidance throughout this work. Thanks also to James Goodall for technical assistance during the experimental work.

I am grateful to The Science and Engineering Research Council who funded most of the research described here.

Declaration

This thesis has been composed entirely by me and the work described in it is my own.

Contents

List of Abbreviations and Symbols	Page 7
Chapter 1 - Introduction	Page 9
The SEM - a brief description.	1.1
The Electron Gun	1.1.1
Electron lenses	1.1.2
Scanning	1.1.3
The Secondary Electron Detector	1.1.4
Applications of the SEM in electronics.	1.2
Voltage Contrast	1.3
DC Techniques	1.3.1
Logic Mapping	1.3.1.1
Quantitative Voltage Measurement	1.3.1.2
AC Techniques	1.3.2
Stroboscopy	1.3.2.1
Sampling	1.3.2.2
Direct Measurement	1.3.3
Chapter 2 - Background	Page 20
Spectrometers	2.1
Electronics	2.2
Sources of Error in Voltage Contrast	2.3
Contamination	2.3.1
Oxide Charging	2.3.2
Chapter 3 - Spectrometer Development	Page 28
Initial Experiments	3.1
Alternative Electron Detectors	3.2
Deflection Electrode Development	3.3
Conclusions	3.4

Chapter 4 - Electronic Instrumentation Page 35

Scanning 4.1
Scan Generator 4.1.1
Design details 4.1.1.1
Counters 4.1.1.2
Clock and Timing 4.1.1.3
TV Rate Scanning 4.1.1.4
Cursor 4.1.1.5
Microprocessor 4.1.1.6
RAM and alphanumeric display 4.1.1.7
Video Processing 4.1.1.8
GPIB 4.1.1.9
Front Panel 4.1.1.10
Construction 4.1.1.11
Software 4.1.1.12
Alphanumeric display 4.1.1.13
Operation 4.1.1.14
Improvements 4.1.1.15
Scan Coils 4.1.2
Construction 4.1.2.1
Operation 4.1.2.2
Scan Amplifiers 4.1.3
Design Criteria 4.1.3.1
Output Stage Design 4.1.3.2
Phase Splitter and Output Drivers 4.1.3.3
Feedback 4.1.3.4
Summary 4.1.3.5
Improvements 4.1.3.6
Scan rotation 4.1.4
Electronic Measurement of S-Curve Shift 4.2
Successive Approximation Circuit 4.2.1
Second Harmonic Detection Technique 4.2.2
Beam Chopping. 4.3
A Digital Delay Generator 4.3.1

Chapter 5 - Development of Computer System Page 66

Computer System Description 5.1
Summary of Control System 5.1.1
Superbrain computer 5.1.2
Operating System 5.1.3
General Purpose Interface Bus (GPIB) 5.1.4
Interface Hardware 5.1.4.1
Interface Software 5.1.4.2
System Hardware Configuration 5.1.5
Automated S-curve Detection 5.2
Second Harmonic Circuit 5.2.1
Direct Digital Connection 5.2.2
Software 5.2.3
Selection of Point For Measurement 5.2.3.1
S-Curve Sampling 5.2.3.2
Development of Processing Methods 5.2.3.3
Double Differentiation 5.2.3.4

Chapter 6 - Results Page 79

Specimen and Operating Conditions 6.1
First Testing 6.2
Linearity Test 6.3
Extraction Voltage and Oxide Charging 6.4
Theory 6.4.1
Experimental results 6.4.2
Effect of Scanned Area 6.4.2.1
Effect of Nearby Conductors on Oxide Charging 6.4.2.2
Oxide Potential and Voltage Contrast Linearity 6.4.2.3
Estimation of Absolute Value of Oxide Voltage 6.4.2.4
Conclusions 6.4.3

Chapter 7 - Conclusions, New Developments and Suggestions for Further Research Page 93

Conclusions 7.1
Spectrometer 7.1.1
Control Electronics and Computer 7.1.2
Summary 7.1.3
New Developments 7.2
Suggestions for Further Research 7.3
Improvements to Signal Processing Algorithm 7.3.1
A Proposal for a New Computer Based Electron Beam Tester 7.3.2
Theoretical Discussion 7.3.2.1
Optimisation 7.3.2.2
Microfield Compensation 7.3.2.3
Image Processing 7.3.2.4
Window Scanning 7.3.2.5
User Interface 7.3.2.6
AC Measurements 7.3.2.7
Work with Digital Equipment Corporation 7.4

Appendix 1 - The GPIB Page 102

Overview A1.1
Physical Medium A1.2
Logical Operation A1.3

Appendix 2 - The UCSD p-System Page 106

Description A2.1
Application of the p-System A2.2

Appendix 3 - The Digital Scan Generator Page 107

Introduction A3.1
Hardware A3.2
Main Board A3.2.1
Digital to Analogue Converter Boards A3.2.2
Video Processing A3.2.3
Front Panel A3.2.4
Remote Cursor Controller A3.2.5
Power Supply A3.2.6
Software A3.3
General A3.3.1
Front Panel Operation A3.3.2
Remote Control A3.3.3
Scan Rotation A3.3.4

Appendix 4 - The Superbrain/GPIB Interface Page 125

Appendix 5 - Voltage Contrast Software Details Page 127

Introduction A5.1
Program Structure A5.2
S-curve sampling A5.3
Convolution A5.4
Zero Crossing Detection A5.5

Appendix 6 - Published Papers Page 131

Digital Techniques for Improved Voltage Measurements
Extraction Field and Oxide Charging in Voltage Contrast Systems

References Page 143

Abbreviations

AC	Alternating current
ADC	Analogue to digital converter
BIOS	Basic I/O system
CMOS	Complementary metal-oxide-semiconductor (logic)
CRT	Cathode ray tube
DAC	Digital to analogue converter
DC	Direct current
DEC	Digital Equipment Corporation
e-beam	Electron beam
EBIC	Electron beam induced current
EPROM	Erasable programmable read only memory
ERCC	Edinburgh Regional Computing Centre
FET	Field-effect transistor
GPIB	General purpose interface bus - see Appendix 1
HPIB	Hewlett Packard interface bus - see Appendix 1
IC	Integrated circuit
IEEE	Institute of Electrical and Electronic Engineers (USA)
I/O	Input/Output
LS TTL	Low power Schottky TTL
LSB	Least significant bit
MFE	Microfield effect - see 7.2
MOSFET	Metal-oxide-semiconductor field-effect transistor
MSB	Most significant bit
Op-amp	Operational amplifier
oxide	see SiO_2
p-code	Pseudo code - see appendix 2
p-System	See appendix 2
PCB	Printed circuit board
pixel	Picture element
PSU	Power supply unit
PVC	Poly-vinyl-chloride
RAM	Random access (read/write) memory
ROM	Read only memory
S-Curve	See section 2.1
SBIOS	Simplified basic I/O subsystem
SEM	Scanning electron microscope
SiO_2	Silicon di-oxide
TTL	Transistor-transistor logic
TV	Television
UCSD	University of California, San Diego - see appendix 2

Units and Symbols

Units

A	Amp - electrical current
eV	Electron volt - electron energy
m	Metre - length
Hz	Hertz - frequency
s	Second - time
V	Volt - electrical potential difference
Ω	Ohm - electrical resistance

Other Symbols

E_S	Secondary electron energy
e	The charge on an electron
I	Electric current
I_b	Electron beam current
N	Number (of electrons)
R_F	Feedback resistance
V	Electric voltage
V+, V-	Positive and negative power supply voltages
Δf	Bandwidth (of voltage contrast system)
σ_V	Voltage resolution
Φ	Workfunction of material (usually the specimen)
ϕ_S	Surface potential

Chapter 1

Introduction

The scanning electron microscope (SEM) is now well established as a very versatile tool for functional examination and testing of complex integrated circuits (ICs) at various stages from prototyping to production. In this thesis two parallel lines of work are developed - firstly the improvement of existing electron energy spectrometers and associated electronics both in accuracy but more importantly in functionality and ease of use, and secondly the construction of computer control techniques for all important aspects of the SEM, with the aim of allowing quick and easy voltage contrast measurements under software control. These two themes are complementary and inter-link throughout their development.

Chapter 2 outlines the background to this research describing the state of previous research - its problems and successes.

Chapter 3 describes the development and construction of a particularly simple and economical electron spectrometer - which performs as well or better than many far more complex designs.

Chapter 4 is on electronic equipment for automatic control of the SEM: including a fully digitally controlled scanning system, developed to allow operation of the microscope by the central computer system, and a variety of circuits intended to interface to this computer.

Chapter 5 describes the computer control system which integrates control of the SEM with voltage contrast measurement via the spectrometer and electronics. In the first part software for general control is explained. The second half of the chapter then discusses the signal processing programs developed for digital measurement of secondary electron energy and their potential in high speed extraction of large quantities of voltage information.

Results obtained using this combination of electronics and software are detailed in chapter 6. Studies of the effectiveness of the apparatus are followed by an investigation with it into the mechanism of static charge accumulation on the specimen (oxide charging) and its influence on the accuracy of voltage contrast measurements.

The final chapter (chapter 7) contains conclusions from the previous work and suggestions for the direction of further studies. Also in this chapter is a brief description of some developments along these lines undertaken subsequently in collaboration with Digital Equipment Corporation and some comments on developments elsewhere in the field since conclusion of the project.

1.1 The SEM - a brief description.

A diagram of an SEM is shown in figure 1.1. it consists of an electron gun which projects a beam of electrons (e-beam) along the axis of a column to strike a target - the specimen. Between the gun and the specimen are a number of electron lenses which combine to concentrate the beam to a very small diameter spot ($\approx 1\mu m$) at the point where it strikes the specimen. At this point low energy ($\approx$10eV) secondary-electrons are emitted. Because of their low energy these electrons are easily attracted into an electron detector beside the specimen but the number reaching the detector will be depend on the shape of the specimen around the point where they are emitted (figure 1.2).

In order to produce an image the e-beam is scanned across the specimen in a series of lines (the raster) over an area of the specimen in a pattern similar (often identical) to that in ordinary TV. This scan is synchronised with the scan in a TV or cathode ray tube (CRT) screen while the output from the secondary electron detector modulates the brightness of the CRT; see figure 1.1. Thus the brightness of every point on the screen depends on the number of secondary electrons detected from the corresponding position on the specimen as it is scanned. The

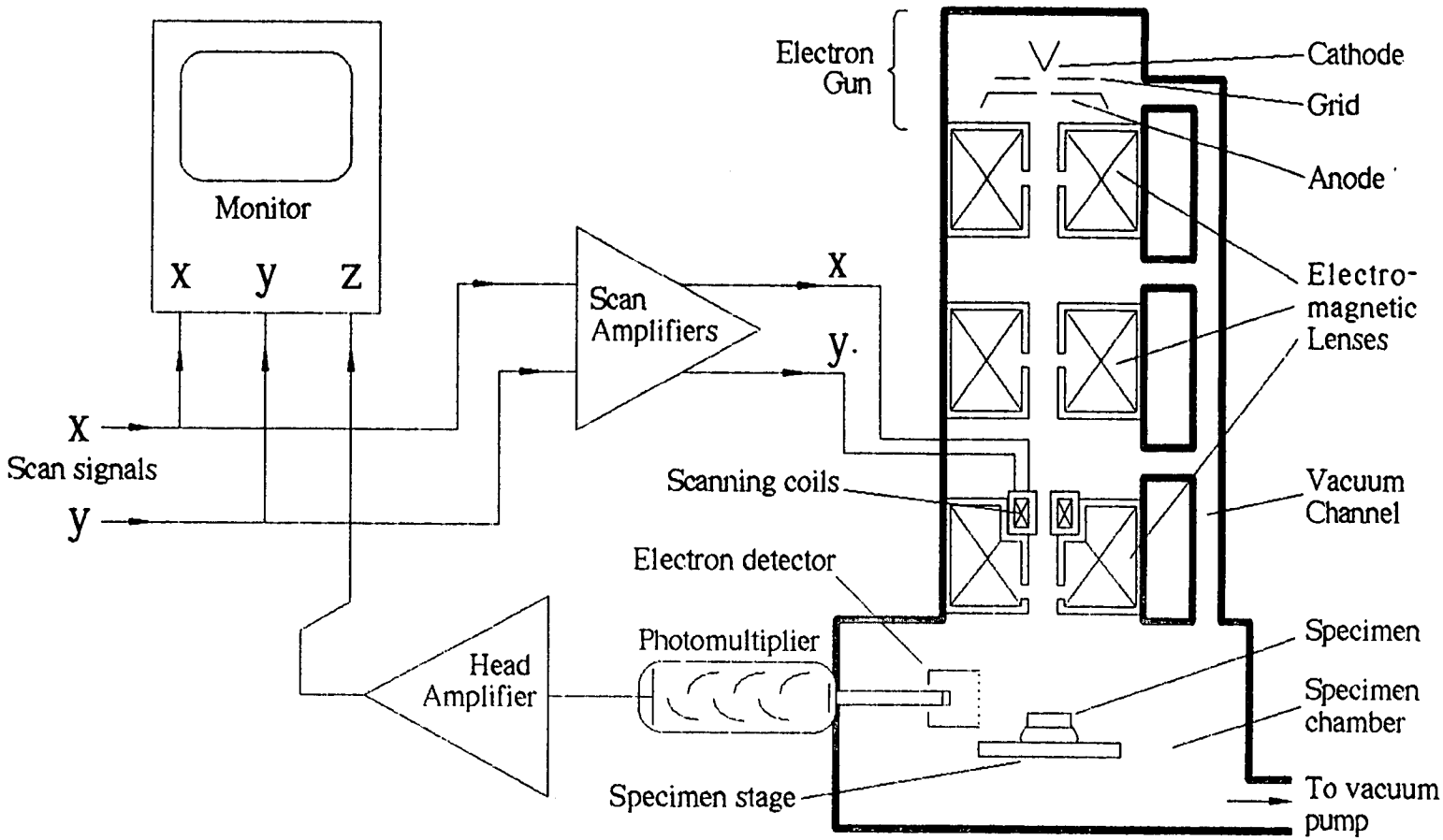

Figure 1.1. Simplified schematic section through a scanning electron microscope showing the major functional elements and electrical connections.

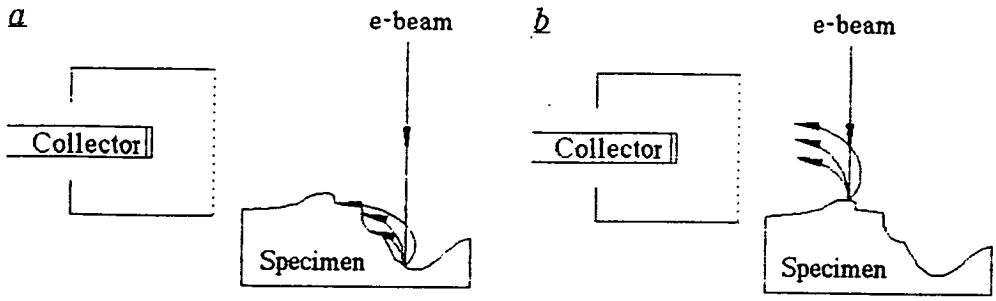

Figure 1.2 Effect of surface topology on secondary electron collection. In a. few secondaries will be collected owing to the obstruction between the point of emission and the collector and this region will appear dark - correspondingly in b. collection is efficient and the area will be bright.

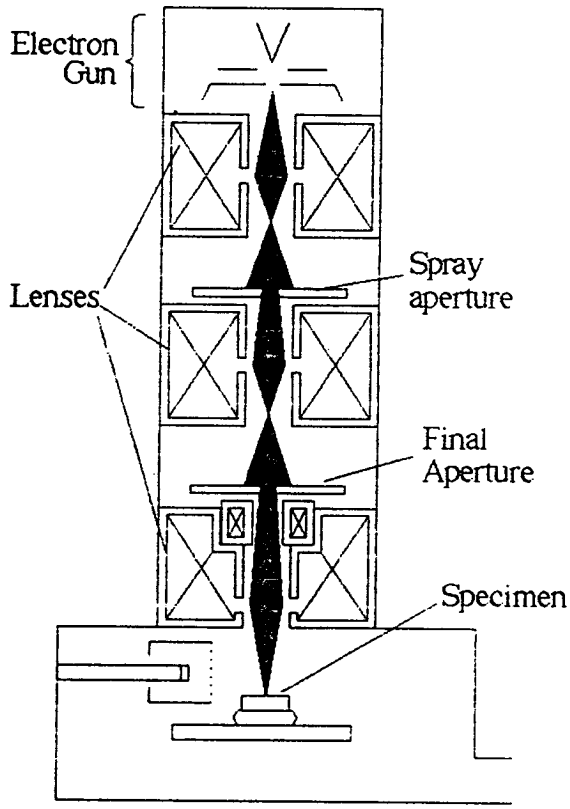

Figure 1.3 Schematic drawing of the electron optical path (e-beam in black) through the SEM showing the effect of the magnetic lenses and apertures in shaping the beam. The beam width is grossly exaggerated here; apertures usually being less than a millimeter in diameter and in many cases only a few microns.

visual image produced is rather as though the specimen were viewed from the direction of the electron beam with a light source in the position of the secondary electron detector.

In order to increase the magnification the area covered by the scan on the specimen is reduced while maintaining the full scan on the screen.

In order for the SEM to work the entire electron path including the specimen chamber has to be at high vacuum.

1.1.1 Electron Gun

This consists of a cathode which emits electrons which are then accelerated through a small hole in the neighbouring anode and projected along the axis of the column. A second electrode, the grid or Wenhelt, is usually provided to improve performance by forming a electrostatic lens effect. On most SEMs a hot V-shaped tungsten wire cathode is used: hot LaB_6 and cold field emission guns give superior results but are less robust and require a much better vacuum. A photocathode material illuminated by a laser beam has also been used as an electron emitter to produce very short pulses of electrons [1].

1.1.2 Electron lenses

Most SEMs have three electron lenses each of which converges the beam to a crossover, the final crossover being at the point where the beam strikes the specimen (figure 1.3). The smaller the spot produced at this point the better the resolution of the image.

The lenses can in theory be either electrostatic or magnetic and in most commercial SEM systems magnetic lenses are used. However combined electrostatic and magnetic lenses have been used to good effect in special purpose electron beam testers where very low beam energies are important.

1.1.3 Scanning

Again magnetic deflection is virtually universal. Scan coils are usually mounted just before the final lens and operate on a double deflection principle so that the beam is deflected to one side then back again, passing at an angle through the centre of the lens.

The electrical systems to drive the deflection coils are covered thoroughly in later chapters.

1.1.4 Secondary Electron Detector

The conventional Everhart-Thornley [2] secondary electron detector is shown in figure 1.4. The electrons are first attracted by the positive potential on the outer cage. Once they reach this they pass through the mesh and are then accelerated very strongly at the electro-luminescent scintillator. Each electron striking the scintillator at high energy produces a burst of several photons - the first stage of amplification - some of which pass along the light pipe where they illuminate the photocathode at the end of the photo electron multiplier (photomultiplier). This emits more electrons in response which are then multiplied by the photomultiplier to produce a cascade of electrons at its anode. The resulting anode current is amplified electronically by the head amplifier to provide an electrical signal for the display.

This detector while appearing complex has some extremely useful properties: Firstly, both the scintillator and the photomultiplier provide extremely high gain with very low noise compared with alternatives and this gain can be adjusted over a very wide range by simply changing the photomultiplier voltage. Secondly, the light pipe allows electrical isolation of the various components so with the specimen at 0V, the cage at around 200V to attract secondaries, and the scintillator at 10kV it is possible to have the photocathode at a large negative voltage (-1 or -2 kV) so that the photomultiplier's anode is once again at ground and no special isolation is required for the head amplifier.

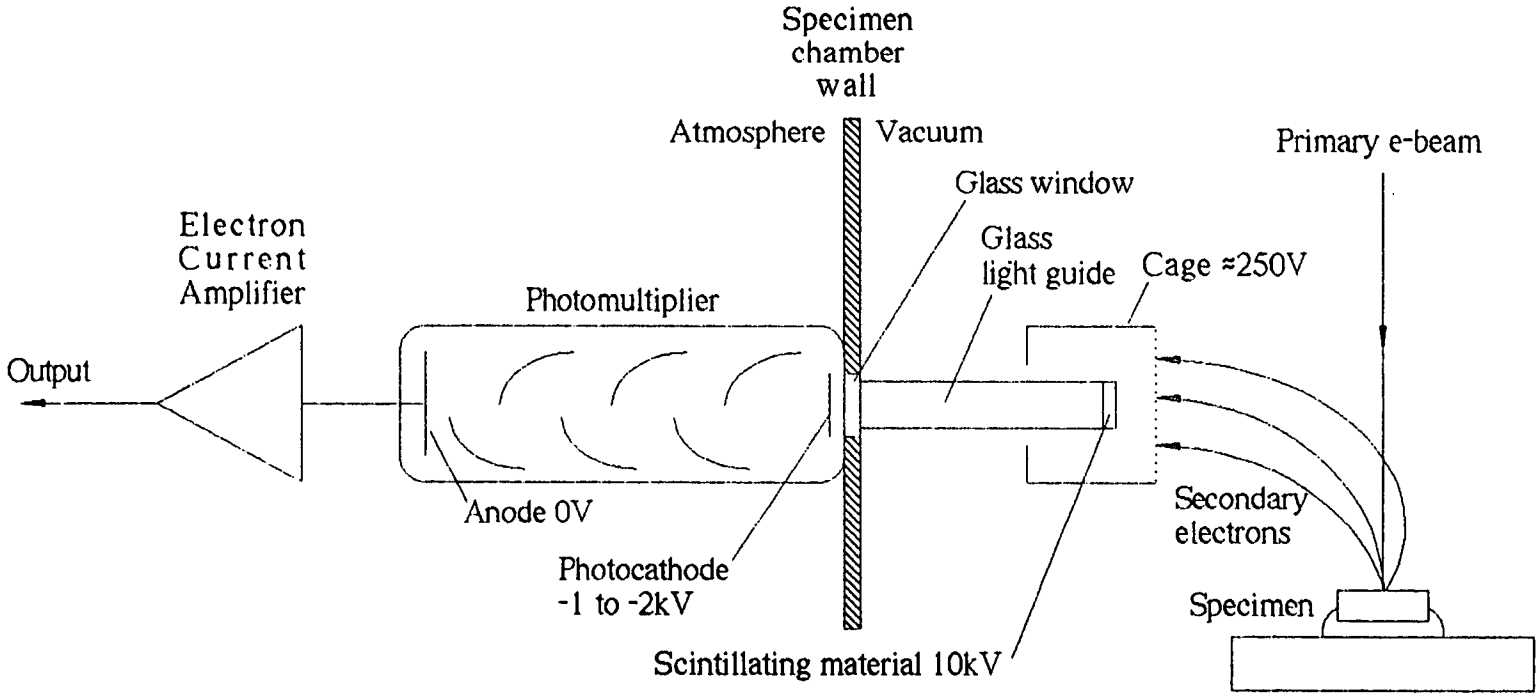

Figure 1.4. The Everhart-Thornley electron detector.

1.2 Applications of the SEM in electronics.

The SEM is very powerful for topological examination of a wide range of specimens. Carefully set up it can produce very high magnification pictures of objects with a wide depth of field, useful for physical examination of miniaturised ICs - but by making various changes it becomes the instrument for a large number of other applications.

When the e-beam strikes a specimen it not only produces secondary electrons but also a large number of other phenomena any of which can be used instead of the secondary electron detector to generate an image [3]. Thus pictures may be produced from backscattered electrons, e-beam induced current (EBIC), electro-luminescence, x-ray emission etc etc.

A further use of the SEM is as a general purpose steerable electron beam device. By replacing the line and frame generators with some other input giving general X,Y control the beam can be used for anything from simply pointing at a particular location - in order to make an x-ray analysis measurement for example - to e-beam writing using vector scanning to produce very fine patterns in resist before etching (commercial systems for e-beam writing grew out of more generalised SEMs).

1.3 Voltage Contrast

When the primary e-beam strikes the surface of a specimen secondary electrons are produced with a range of energies which can be described by the formula given by Chung and Everhart [4]:

$$\frac{dN}{dE_s} \propto \frac{E_s}{(E_s + \Phi)^4}$$

Where Φ is the workfunction of the specimen material and N is the number of secondaries with energy less than E_s. A typical curve of this form is shown in figure 1.5. If the specimen is not at the same potential as its surroundings the secondary electrons will be either repelled away from the surface or attracted back towards it producing an apparent shift in the energy distribution curve.

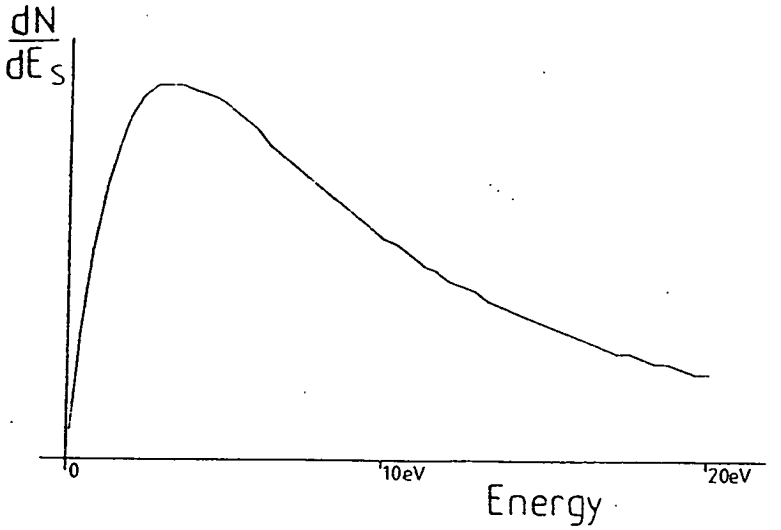

Figure 1.5 Typical secondary electron distribution curve.

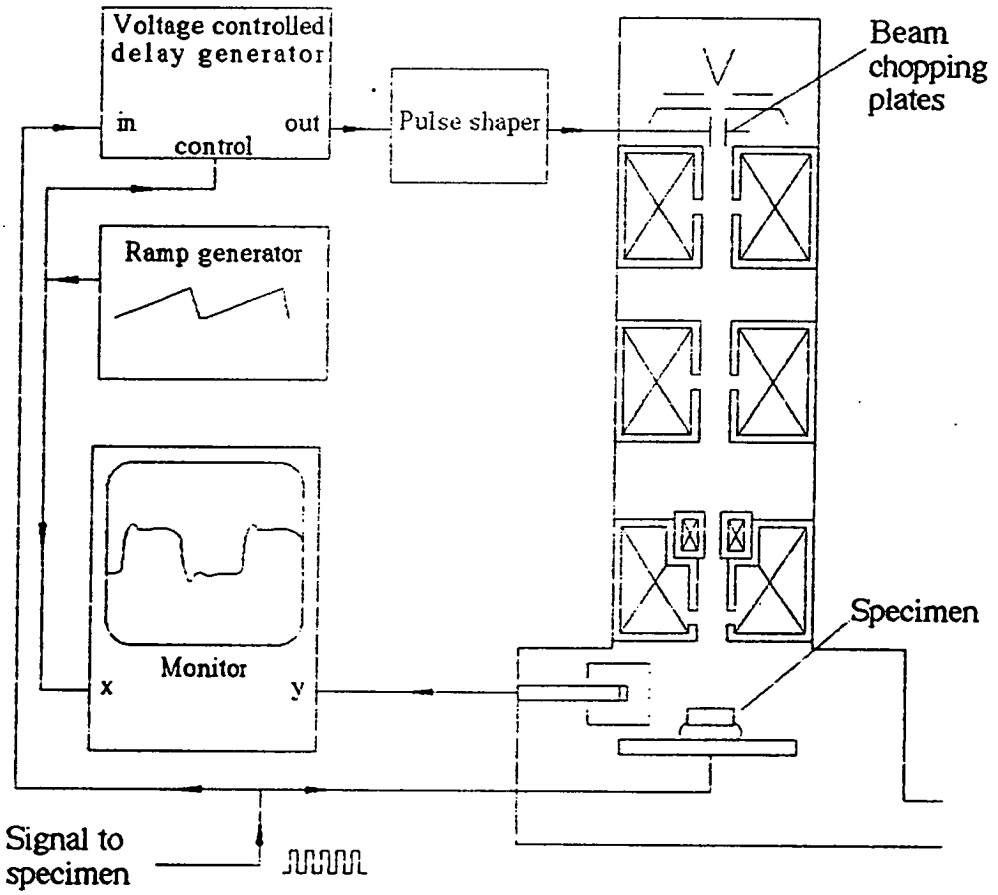

Figure 1.6 Sampling of AC waveforms using beam chopping- The ramp generator controls both the X input to the monitor and the beam chopping delay generator. The specimen signal is at a very much higher frequency than the ramp signal.

This shift will ideally exactly track the specimen voltage [5]. This phenomenon - voltage contrast - can be useful in a number of ways in examining ICs and there are a number of common techniques:

1.3.1 DC Techniques

1.3.1.1 Logic Mapping

This is the simplest form of voltage contrast and does not necessarily require an energy analyser. The IC is scanned in the normal way and tracks which are at a higher voltage appear darker as secondary electrons have more difficulty escaping from the surface. By careful setting of the operating conditions this can be made very striking - particularly on logic circuits where signals are (or should be) at either a high or low voltage and not at some intermediate state.

1.3.1.2 Quantitative Voltage Measurement

This uses a secondary electron energy analyser to measure the position of the energy distribution curve. By relating the position of the curve for a track at known voltage, with that for the point of interest, the shift and therefore the potential difference between the two can be deduced. This is rather analogous to probing the circuit with a voltmeter. In order to carry out a measurement the scanning operation must be stopped and the beam directed at a fixed point.

1.3.2 AC Techniques

When the signals on the IC are varying rapidly the previous techniques can not be used and the usual way to make measurements is to use some kind of stroboscopic or sampling technique - usually by pulsing the primary beam [6].

1.3.2.1 Stroboscopy

If the beam is pulsed on for short bursts synchronously with the signal on the IC and the picture scanned in the normal way then a logic state map can be produced as above with the IC "frozen" at some point in the cycle - this point can be changed by changing the phase relationship between the beam pulses and the IC signal.

1.3.2.2 Sampling

This works in a similar way to a sampling oscilloscope. The beam is directed at the point of interest and the beam is pulsed as before. As the phase angle between the beam pulses and the signal on the track is slowly changed so a trace of the signal throughout its cycle is generated. This process can be automated as shown in figure 1.6 [7].

1.3.3 Direct Measurement

A big problem with all beam pulsing systems is that for high time resolution a short beam pulse is necessary and as this gets shorter and the duty cycle decreases, so the output signal drops and the signal to noise ratio increases. This can be compensated using signal averaging of some sort at the expense of increased acquisition time.

Another method for medium frequency measurements which does not require beam chopping is to adjust the operating point to a region where the output from the secondary electron detector changes reasonably linearly with specimen voltage. This method gives real time viewing of the waveform but the accuracy is necessarily restricted and the frequency of measured signals is limited by the bandwidth of the detection system.

Chapter 2

Background

2.1 Spectrometers

Any attempt to measure voltages at the surface of an IC requires some system for measuring the energy of the secondary electrons emitted from the specimen - an electron energy spectrometer or analyser. Even for non-quantitative measurements, as often used for sampling or stroboscopic inspection, an electron energy spectrometer is often used to bias the operating region so that the output varies by the maximum possible amount (e.g. to maximise contrast in a logic state map), or in a near linear way (for fast AC or sampled waveforms; see 1.3.3), over the range of voltages encountered on any particular specimen.

The vast majority of spectrometers that have been described and virtually all those in use are "high pass" analysers (although some bandpass spectrometers have been developed[89]) in which only electrons with energy above a threshold value are detected[10]. The relationship between the detector output, proportional to the *number* of electrons reaching it, and the threshold level is given by a cumulative energy distribution curve - commonly referred to as an S-curve because of its shape. Ideally where all secondaries available are detected and the cut off level is acute the S-curve is the integral of the usual secondary energy distribution curve from high down to low energy (figure 2.1).

In order to extract the largest possible number of the secondary electrons originally emitted from the specimen, all spectrometers incorporate some kind of extraction electrode which accelerates the secondaries away from the complex fields at the surface into the retarding field region where they are decelerated again. This extraction ideally has no effect on measured energy but it is a critical part of the system.

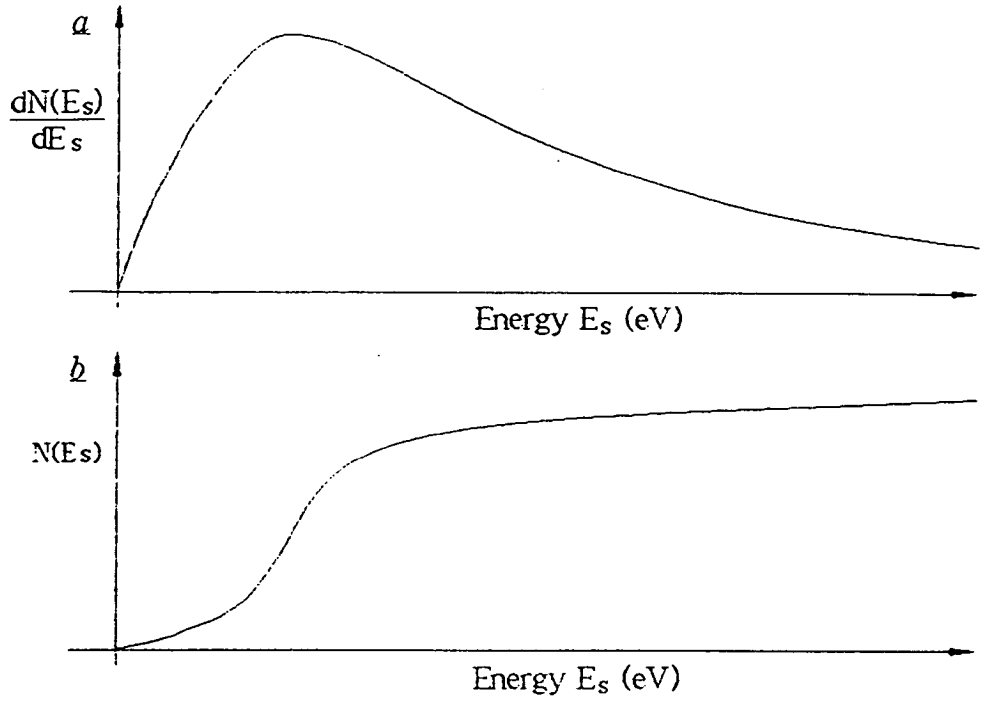

Figure 2.1 Secondary-electron energy distribution a. Is a typical energy distribution curve. b. Shows the cumulative energy distribution curve (the integral of a). The so called S-curve is in fact the result of integrating the energy distribution from from high to low energy.

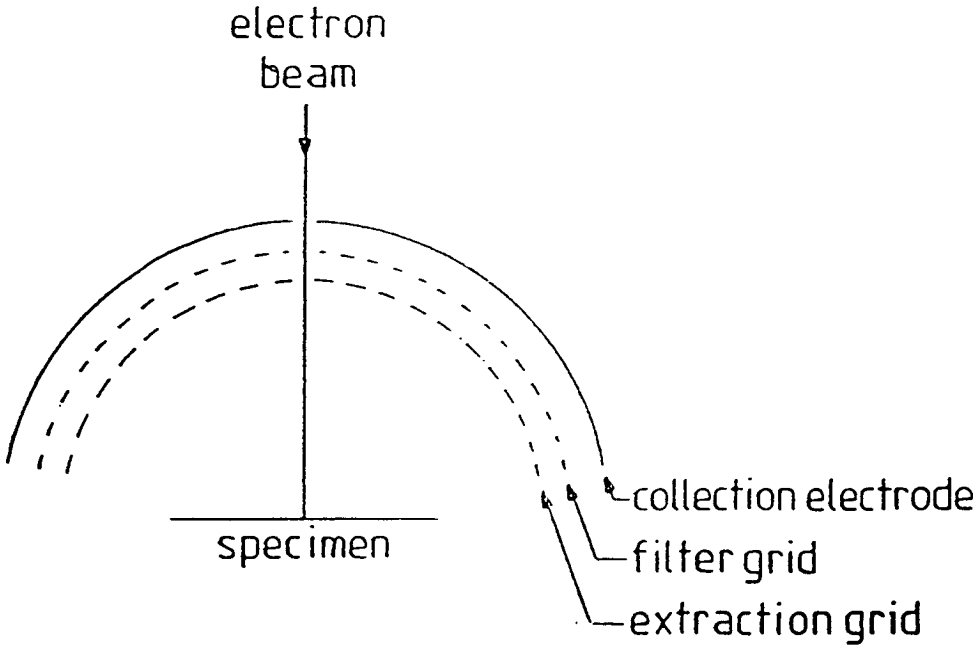

Figure 2.2 Schematic cross section through a retarding-field electron energy analyser with hemispherical grids.

Perhaps the simplest (conceptually) electron energy spectrometer is the one shown in figure 2.2[5]. In this analyser all the electrodes are spherically formed grids or plates centred on the point of emission so that electron trajectories will be always normal to equipotentials. The detection of those electrons which survive the retarding field is by direct measurement of the current into the collection electrode. Since this current is very small there is a considerable problem in amplifying this signal to a usable level without very high noise levels and/or narrow bandwidth. This leads us to a perennial problem in the design of energy analysers; the efficient detection of those secondaries which emerge from the filter stage.

The normal secondary electron detector in an SEM is the Everhart-Thornley detector (section 1.1.4). Both the scintillator and the photomultiplier provide very high gain and low noise amplification stages with wide bandwidth (5-10 MHz commonly but up to ten times this with specialist designs) and because the light pipe provides electrical isolation, the final output current can be close to system ground. The big problem though is that the usual geometry of the device is unsuited to the accurate "counting" of the very low energy electrons emerging from a filter grid which is usually close to the final lens (in order to reduce working distance).

The wide diversity of spectrometer designs is partly due to the secondary problem of detection of the filtered electrons and not to the primary one of accurate filtering. In general additional electrodes have been introduced which deflect the electrons towards the existing detector. In some cases the whole detector shape has been changed (sometimes quite drastically) in conjunction with the use of deflection electrodes[11]. Thus though a plethora of spectrometers have been described they mostly operate on similar principles. They are universally quite complex in mechanical construction and have been found to introduce many unpredictable inconsistencies such as astigmatism of the

primary e-beam due to asymmetries, dimensional inaccuracy and deviation, for reasons of practicality, from their theoretical design.

2.2 Electronics

Although development of spectrometers has been the subject of much research, comparatively little has been written about electronic techniques for making accurate measurements from their outputs. The major target of much of the work described in this thesis was to produce a usable quantitative voltage contrast system in which the e-beam can be used in a manner akin to a voltmeter to measure DC potentials accurately at any point of interest on the specimen. Voltage information manifests itself as a shift in the position of the electron energy distribution curve so what is needed is a means of accurately measuring the position of this curve.

Almost all common voltage contrast setups use high pass type spectrometer similar in principle to the one developed here so the output function is an S-curve rather than a simple distribution function.

The method commonly used and widely described uses a simple feedback arrangement whereby the analyser grid is adjusted to bring the output to a predetermined reference level (figure 2.3)[12]. This is very simple and appropriate filtering to remove noise is easy. It works so long as the S-curve maintains its shape and amplitude with voltage shifts - however it is obvious that variations in S-curve height even with no change in position will cause an output change.

A further problem with many systems is caused by irregularities imposed by most spectrometers at the high end of the S-curve. As the analyser grid voltage rises electrons pass through with higher and higher energies until some have sufficient energy to escape the collection system; giving rise to a falling off in the output. Any secondaries which collide with electrodes at these higher energies will in turn be more likely to generate secondary

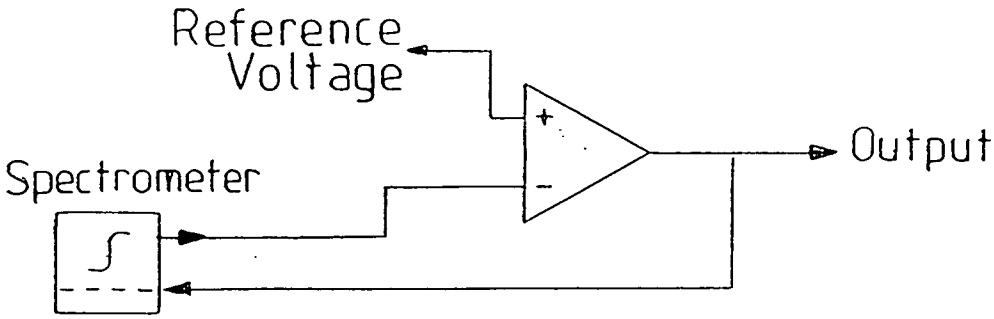

Figure 2.3 Simple feedback arrangement for tracking specimen voltage with a retarding field analyser.

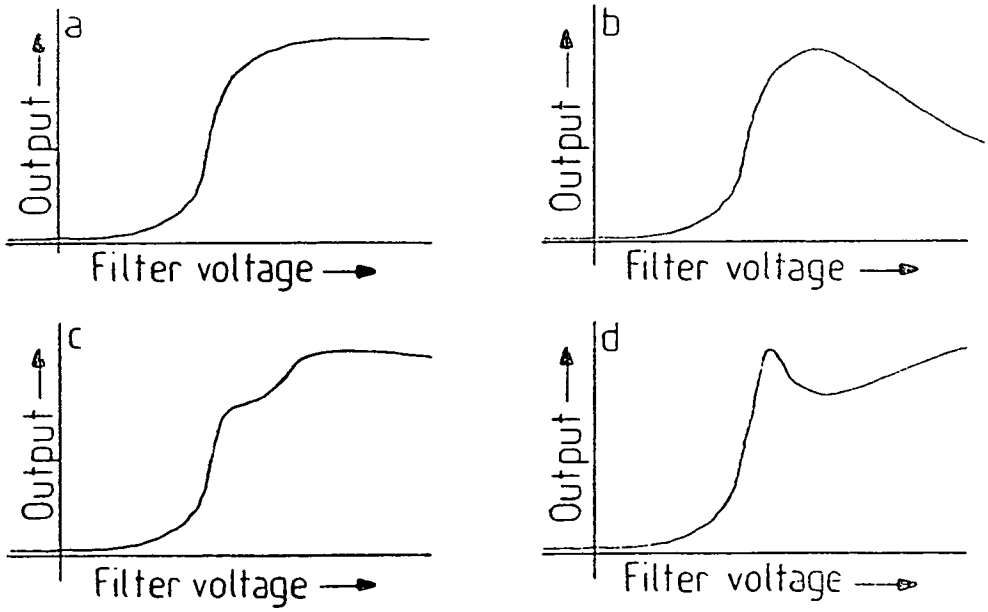

Figure 2.4 Examples of distorted S-curves seen experimentally. Reasons for some types of distortion are discussed in the text

emission themselves and these spurious "tertiary" electrons may further distort the output. Both these factors depend on the geometry and potentials of the spectrometer and the deflection and detection electrodes and produce unpredictable irregularities in the output which on some spectrometers appear uncomfortably close to the region of interest on the S-curve. Some examples of common distortions in the S-curve are shown in figure 2.4. Many circuits for S-curve tracking are liable to wild errors or latch up if their operating point wanders into this distorted region.

Despite the obvious limitations of this method then it is still the only one in common use. A modification occasionally used is to dynamically vary the reference voltage of figure 2.3 by sampling some point high on the S-curve to get an approximation of its amplitude before making a measurement. To do this automatically greatly increases the complexity of the circuit but can improve its accuracy considerably. It is however almost impossible to set up reliably under real conditions.

2.3 Sources of Error in Voltage Contrast

Making accurate voltage contrast measurements is very difficult - there are many sources of error which are unpredictable. Two perennial problems which I will discuss here are hydrocarbon contamination and oxide charging. Other common problems range from electron-gun brightness fluctuations at one end of the chain to electron beam damage to the specimen at the other.

2.3.1 Contamination

Traces of oily hydrocarbon in the vacuum of the specimen chamber condense in a thin film on any surface. When bombarded by the electron beam the molecules tend to polymerise to form a tough deposit. The longer the beam is directed at a point the thicker the deposit gets as stray molecules condense on the specimen and are incorporated. During normal scanning at

medium magnification this is not usually a problem as the electron dose at any point is small, but when the beam is "stopped" contamination buildup can be very rapid causing a drift in the output which can continue virtually indefinitely. In these circumstances it is very difficult to set up the conditions necessary to take readings and if the reading is not taken over a very short time ($\leqslant$0.1s) the drift during this time is likely to be significant.

The obvious way to minimise errors due to contamination is to avoid the contamination itself. Any hydrocarbon whose vapour pressure is not very low is a potential source - pump oil from vacuum pumps, plasticisers from plastic material, fingerprints and oil in mechanisms are common sources of trouble. Modern microscopes with turbomolecular pumps reduce contamination which can be caused by oil diffusion pumps, careful choice of materials for mechanisms in the vacuum (PVC insulation should be avoided at all costs) and general attention to cleanliness are also very important. Cooled baffles or "fingers" which act as condensers for the contaminants are a commonly used secondary method for reducing the problem.

Despite these precautions some low level of contamination is virtually inevitable and it is very common after making measurements at a point to observe a dark spot of contamination there on resuming scanning. Minimising the time spent taking a reading is the best way to get around this.

2.3.2 Oxide Charging

If any insulating material is within the viewing area it will accumulate a static charge which can play havoc with secondary (and even primary beam) electrons. Once again this problem is one of slow drift as during constant scanning steady state conditions are reached with charge leaking away as fast as it is deposited, but when the scan pattern changes the static charge pattern redistributes itself over several seconds. In most cases the best solution is to keep insulating material well away from the e-beam.

Trouble comes with integrated circuits though because large areas of their surfaces are composed of silicon dioxide ("oxide"). Detailed studies of the charging of exposed oxide are described in chapter 6, but generally to avoid problems any change to the scan pattern should either be kept as short as possible or should be held long enough for charging to reach a steady state - engendering a long delay.

Chapter 3

Spectrometer Development

3.1 Initial Experiments

One of the first problems encountered was the lack of a usable electron energy analyser so an initial design was developed empirically in several stages. Initially two flat grids (standard transmission electron microscope grids) were used as extracting and filtering electrodes, this is a much simpler construction than trying to build spherical elements and it is as easy to model and predict its behaviour. Initially the field of view was very restricted by the small overall grid size, and was further heavily obstructed by grid bars of both grids. These drawbacks were reduced when a source of superior grids was found. The new grids having a larger overall size (around 6mm useful diameter) and a convenient rectangular arrangement of the grid bars with high transparency. They also have a tab on the side which allows the two grids to be aligned in their mounting so that the bars of one do not coincide with the spaces of the other. A final improvement was to cut the centre bars out (a delicate operation with a scalpel) to give a clear view through the central area.

The final arrangement is shown in figure 3.1: The two grids are mounted in a circular hole cut out in a piece of copper clad circuit board with a notch cut to take the tabs on the grids, ensuring accurate alignment of the filter grid over the extraction grid. The grids are retained below by a sheet of thin brass shim bonded to the board and forming a completely flat lower surface which is kept at an even extraction potential. They are separated by a ring of nylon (a possible improvement would be to make this ring of a slightly conducting material which would ensure an even field between the two grids by eliminating any charging) and retained above by a circular spring clip (not shown in the diagram). The use of copper clad board allows conductors and

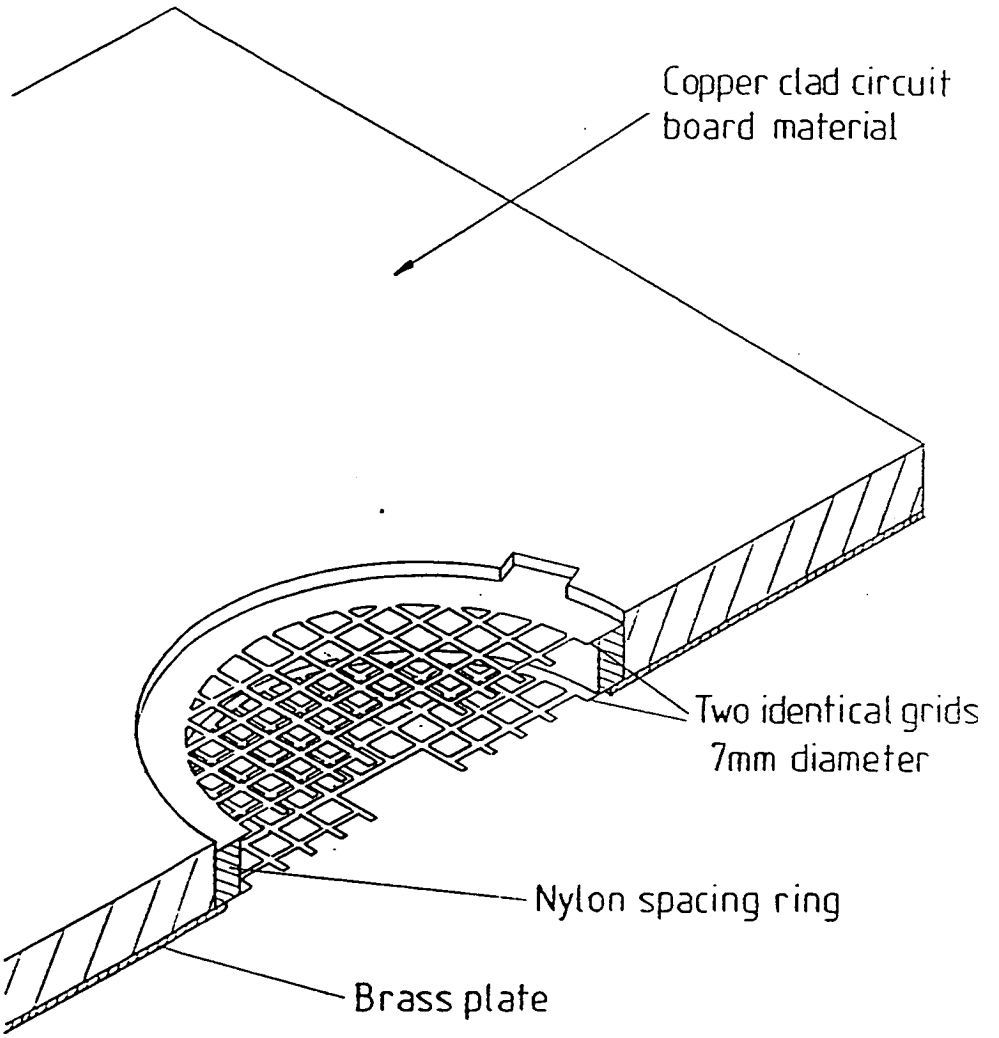

Figure 3.1 Sectional diagram of the prototype flat grid analyser based on printed circuit board construction techniques.

electrodes to be defined on the surface by standard printed circuit techniques.

This design whilst extremely simple has proved to be better for the subsequent development work than any of the others tried. Its construction is very cheap and reasonably easy, it is simple to mount in the specimen chamber and its flat laminar construction, particularly on the underside, with relatively few irregularities does not produce unpredictable or distorting fields (induced astigmatism of the primary beam is a severe problem with many analysers[13]). The main drawback is the restricted field of view ($\approx 1mm^2$) and for routine work in a production situation some method of increasing this would be required.

3.2 Alternative Electron Detectors

This analyser was first used with no deflection system at all and produced satisfactory S-curves provided that there was sufficient space between the top (filter) grid and the final lens polepiece, however this meant a long working distance with associated focusing and resolution problems. The S-curves were found to be somewhat unpredictable anyway and it was desirable to eliminate the possibility that this was due to some deficiency in the collection system.

When using a flat spectrometer of this kind the most desirable configuration for an electron detector would seem to be a flat plate parallel to the spectrometer and close to the final polepiece. This would eliminate all the problems of deflection into the conventional Everhart-Thornley collector. Three possible flat detection systems were considered: Direct measurement of electron current to an electrode, diode detectors, and microchannel electron multipliers.

Direct measurement of current whilst being simple in concept was rejected because of the problem of bandwidth and noise experienced with such amplifiers. Diode detection and microchannel plates both provide an initial stage of high gain, low noise amplification but both need to be held at a potential of

several kilovolts to give the low energy secondaries sufficient energy for reliable detection - this presents a considerable problem particularly when the output current has, for much of this work, to be detectable at frequencies right down to DC. The output amplifier would be required to operate at several thousand volts above ground potential and there must then be some kind of isolation system to translate its output to a useful level. Another drawback of both types of detector is that they are sensitive to contamination and need to operate at very high vacuum.

Despite these difficulties some investigation into using microchannel plates was made and the design shown in figure 3.2 was proposed. In this design the two grids of the analyser form a laminar structure with the microchannel plate and the collector electrode. Electrons which pass through the filter grid are accelerated into the lower face of the channel plate which is maintained at around 1kV; a potential of around 1-2kV across the plate causes multiplication and a cascade of electrons emerge from the upper side and are absorbed on the collection electrode which is connected to a current amplifier to provide the output. The guard tube is a low voltage electrode which protects the primary beam from the strong fields of the collection system. After some preliminary development work on this design it was abandoned when it was realised that a very large effort would be absorbed in developing this single component of the system and attention turned to improving the coupling between the newly developed analyser and the existing Everhart-Thornley detector.

3.3 Deflection Electrode Development

A spectrometer was designed by Khursheed[14] based on two flat grids with a complex deflection/extraction system. This analyser whilst performing excellently in simulation proved very difficult to construct and because of the many compromises made was found to be virtually unworkable due to large amounts of induced astigmatism and unpredictability of the local fields.

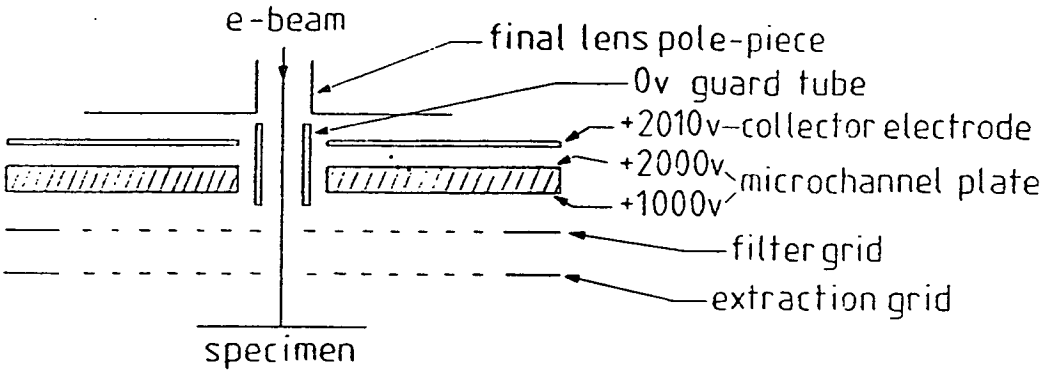

Figure 3.2 A design for a flat grid analyser using a microchannel plate electron multiplier as the detector.

Following Khursheeds work a substantially simplified deflection system was built onto my original analyser using some of the principles from his designs.

This new spectrometer (figure 3.3) is based on the printed circuit board design described above and has an upper deflection electrode curved in one plane only. This electrode is made of wire mesh rather than a solid material to minimise generation of spurious tertiaries by backscattered primaries or high energy secondaries striking it. The lower deflection electrode is simply a track on the top surface of the printed circuit board which forms the body of the two grid analyser. Finally a small compensation electrode is included which is fed with a cancelling signal to prevent movement of the primary beam due to the transverse component of the changing field between the upper deflector and the filter grid.

3.4 Conclusions

This arrangement was found to operate excellently in practice and was used for all subsequent studies and development work - it is simple and robust in construction, is easily mounted in the specimen chamber, and is close to the theoretical concept of flat parallel grids with few features to introduce non linearities - in particular it has a very flat extraction electrode with no obstructions to the specimen or non-linearities, and induced astigmatism is very low even at 500V primary beam energy.

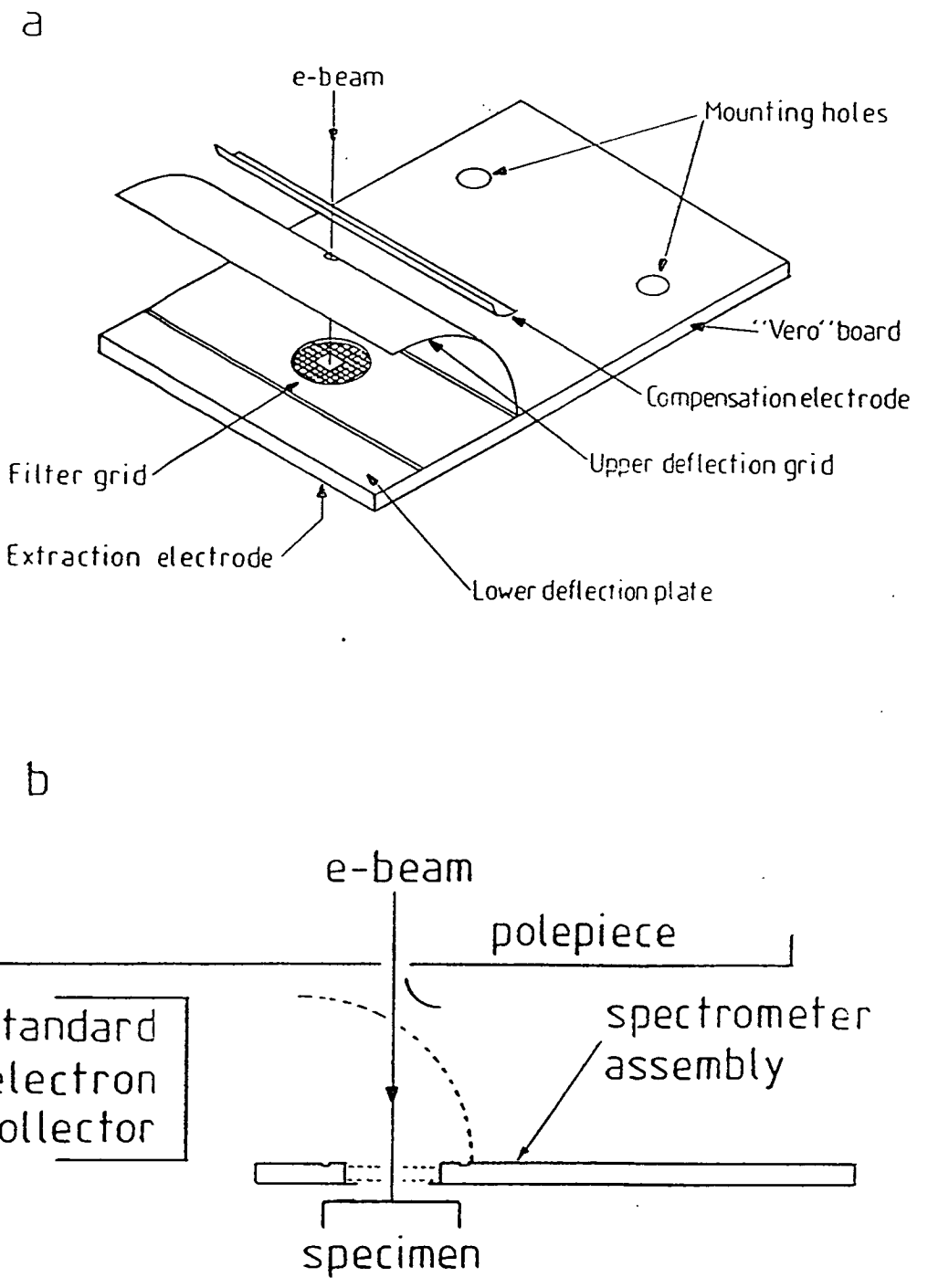

Figure 3.3 The final form of the printed circuit spectrometer. a. View of spectrometer. b. Cross section of the spectrometer in situ.

Chapter 4

Electronic Instrumentation

For a well integrated e-beam testing system it is essential that the computer has control over the major microscope functions as well as specialist voltage contrast functions. A great deal of work was done on designing circuitry for the microscope to allow digital control, as well as on new circuits for voltage measurement and control of beam chopping. While commercial microscopes are now often controlled internally by microprocessors, rarely is there any provision for remote operation or programming of them. The approach developed is intended from the outset to be generally applicable and to allow remote digital control in a flexible manner. Several new techniques or approaches were devised to achieve this and to improve on existing methods.

4.1 Scanning

An important component (*The* important component) of any SEM is the scanning system consisting of a scan generator, scan amplifiers and scanning coils. From the start it was evident that this system must be fully under the control of the central computer in any automated system; particularly control of the scanning mode and beam position; and since the existing system (on the Cambridge Instruments S2 microscope used at that time) was totally unsuitable for adaptation, design and construction of a completely new, microprocessor controlled scan generator was undertaken [15].

4.1.1 Scan Generator

4.1.1.1 Design details

The design was made to be as flexible as possible with all functions controlled by a dedicated microprocessor so that details of operation could be changed as new requirements emerged, by

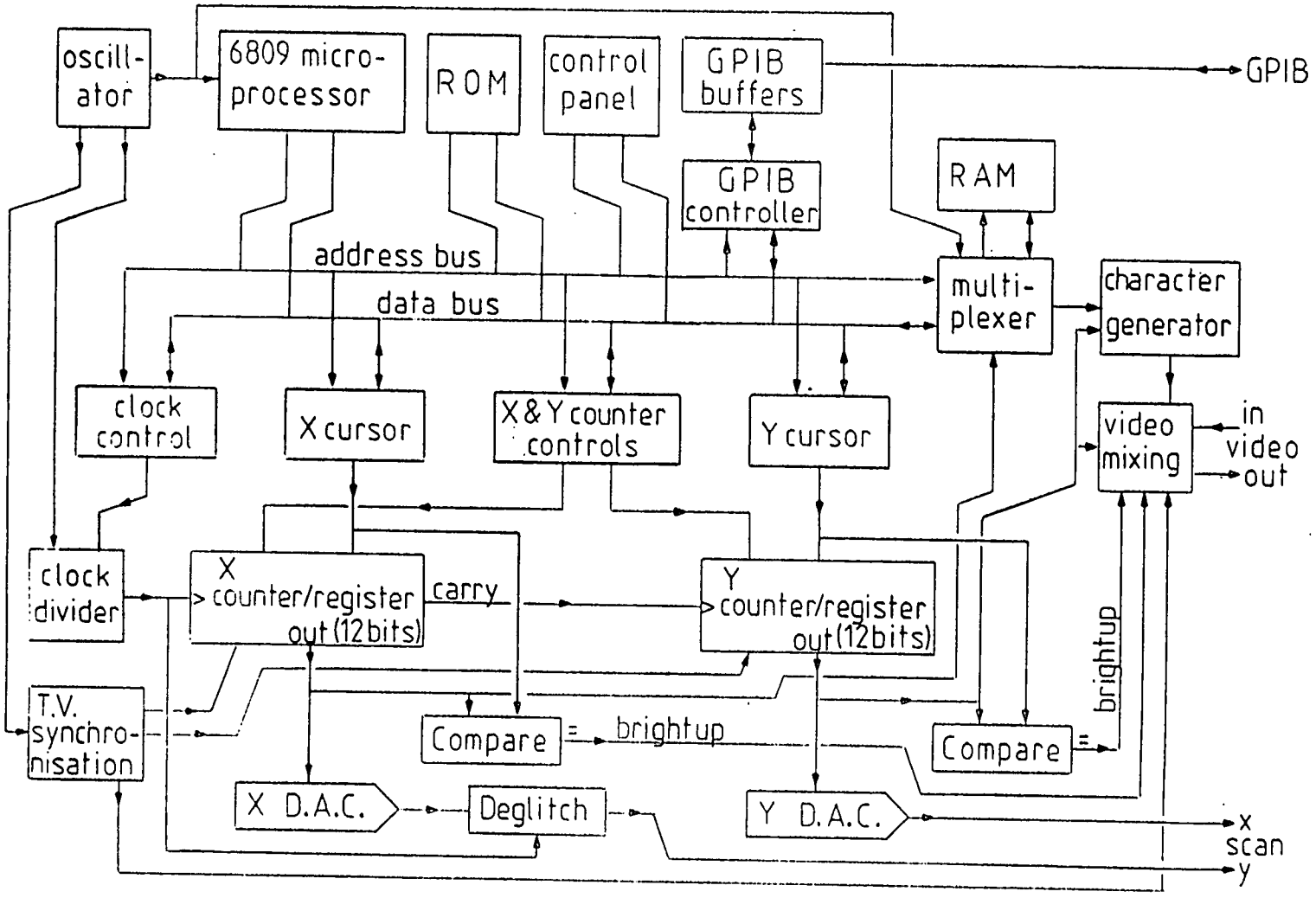

Figure 4.1 Block diagram of scan generator logic.

simply changing the software. The new scan generator would need to duplicate all the existing manual functions as well as providing new remote ones. A simplified block diagram of the final design is shown in figure 4.1.

4.1.1.2 Counters

The design centres around two high speed 12 bit binary counters/registers feeding high speed digital to analogue converters (DACs) for line and frame scans. These counters may be individually enabled or disabled; they may be individually set to increment by anything from 1 to 16 counts at each clock pulse so allowing a wide range of steps between zero and full scale; or they can be loaded with a preset value - the "cursor" value.

Extra logic allows the Y (frame) counter to disable itself on reaching maximum value until an external trigger signal is received. This allows single frame scans for photographic purposes (record mode).

4.1.1.3 Clock and Timing

A more detailed diagram of the timing logic is shown in figure 4.2. The master clock is a quartz crystal controlled oscillator operating at 10.25 MHz. This feeds to a clock divider circuit which divides the frequency by anything from 1 to 256 before driving the X counter, thus line rate is determined by a combination of the clock divisor and the X increment, frame rate is determined by the line rate and the Y increment. The master clock is also divided by two to provide a 5.125 MHz clock for the controlling microprocessor and by four to produce a 2.5625 MHz clock for the special TV sync pulse generator IC.

Two monostables produce flyback periods for line and frame ramps during which counting is inhibited (at zero) and the display blanked. These periods are fixed at 12μs (line) and 1200μs (frame) irrespective of scan rates.

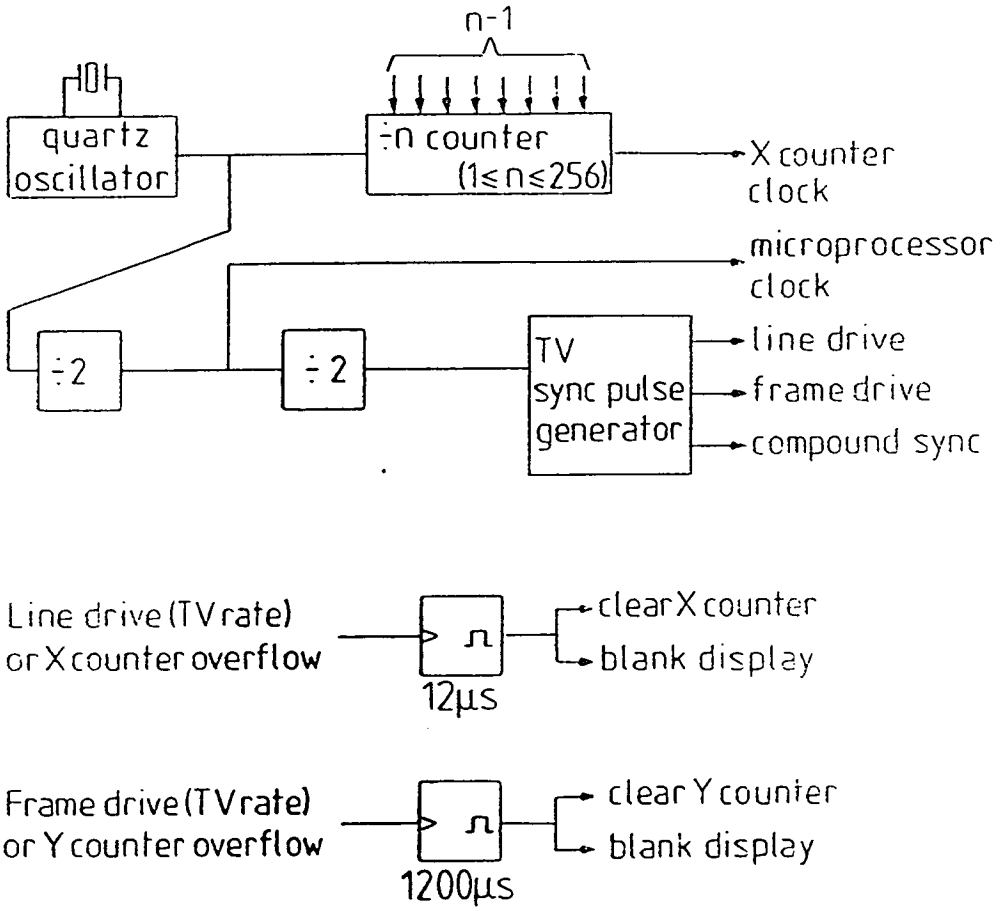

Figure 4.2 Detail of scan generator timing logic.

4.1.1.4 TV Rate Scanning

For TV rate scanning the TV sync pulse generator IC produces line and frame drive pulses which are used to reset the X and Y registers. The Y register is reset to zero at odd fields and to half the Y increment value for even fields giving a true interlaced scan. The sync pulse generator also generates 625 line standard mixed sync pulses which are subsequently added to the SEM output signal for driving into a standard TV monitor.

For all other scan rates the sync pulse generator is disabled allowing the counters to free run at whatever rate has been set by the clock divider and X and Y increment values. Note though that the flyback monostables ensure that they reset to zero each time so interlace is not possible at any other scan rate.

4.1.1.5 Cursor

The cursor values are stored in two 12 bit registers (X and Y) and spot mode or line scan are implemented by simply disabling the counters and loading them with the cursor values (for line scan only the frame counter is disabled). During normal frame scanning the binary outputs from the line and frame counters are continually compared with the cursor values and when they agree bright-up pulses are generated. This action produces a crosswire type cursor on the display indicating the position that the spot or line will be when spot mode or line scan are selected.

4.1.1.6 Microprocessor

The scan generator is entirely controlled by a dedicated Motorola 6809 microprocessor which sets all the necessary signals to control the counters, the X and Y count increments, the master clock divider and the cursor registers. The microprocessor is also connected directly to read only memory, the front panel switches and indicators, a General Purpose Interface Bus (GPIB) interface IC for remote control and via a multiplexer to random access memory.

4.1.1.7 RAM and alphanumeric display

The RAM is multiplexed between the microprocessor and the character generation circuitry so that bytes stored in 32 locations at the top of memory may be displayed as a single row of alphanumeric characters at the bottom of the SEM image.

4.1.1.8 Video Processing

Blanking signals are produced by the flyback monostables, the alphanumeric logic, and also during spot mode; brightup signals are produced by the cursor and alphanumeric circuitry. Both these are mixed with the raw video signal from the SEM head amplifier together with the TV compound sync pulses (when TV scanning is enabled) on a separate video mixer board. Cursor and alphanumeric brightup functions may be individually disabled if required.

4.1.1.9 GPIB

The GPIB (General Purpose Interface Bus) interface is controlled by a special GPIB interface IC (Motorola 68488) together with two GPIB standard driver/receiver ICs. All remote control functions are provided via this interface and depend entirely on the programming of the microprocessor.

4.1.1.10 Front Panel

The front panel has sixteen push button switches arranged as 11 scan rate switches, 4 major mode switches for visual, one shot (photo mode), line scan and spot mode, and a secondary function switch which allows the other buttons to be used for selecting minor functions (e.g. enabling or disabling the alphanumeric display). Finally a remote cursor control box with two knobs for moving the cursor position in X and Y directions can be connected via a single coaxial cable to the front panel. Again all the front panel functions depend entirely on the software stored in ROM.

4.1.1.11 Construction

The digital circuitry was constructed on a single board in the department from LS TTL using wire wrap connections. It worked after only minor modifications and corrections although some additional modifications were carried out later, particularly to the clock and timing circuitry, to improve operation.

4.1.1.12 Software

The software for the 6809 microprocessor was written, using a cross-assembler, on the departmental PDP11 computer and loaded into EPROMs. Although the initial hardware design included a serial interface for the 6809 with the intention of downloading program routines into RAM, in practice the development of the operating software outstripped progress in making the serial interface work properly and the latter was abandoned. The operating software was developed through many versions over a long period of use and the final result is a reliable interface which makes control of common functions either remotely or with the front panel very simple, whilst allowing more subtle and detailed control, when required, via the remote (GPIB) interface. The program also positions the cursor either in response to signals from the cursor position box or to any desired position specified via the GPIB.

Under front panel control the scan generator offers 11 different scan rates ranging between 625 line TV rate and a 60 second frame time for photographic purposes, in all these the crosshair cursor and alphanumeric displays can be enabled or disabled. The four main modes of operation are visual raster (continuous scanning), record raster ("one shot" frame scan) line scan and spot mode. The cursor value and therefore the position of the crosswires or of the electron beam in spot mode is controlled by a remote control box with two knobs for X and Y positions respectively. Secondary front panel functions allow for enabling and disabling of the crosswires and of the alphanumeric display.

Remote operation via the GPIB allows all the front panel functions to be easily duplicated as well as giving more detailed control if required.

4.1.1.13 Alphanumeric display

This is intended primarily for information to be displayed by remote control, allowing simple instructions or information to be shown. After switching on or resetting the scan generator the display region simply displays a message and software version number. The only display functions available from the front panel are enable and disable (allowing a larger picture area), clear the display area to blank space and display cursor position - the X and Y coordinates of the cursor are displayed numerically each in the range 0-4095 (0,0 at bottom left).

4.1.1.14 Operation

The completed scan generator was initially connected to the Cambridge Instruments S2 microscope together with the scan amplifiers and coils described below. The system produced a recognisable image on a TV screen but distortion in the form of vertical lines corresponding to major transitions of the X DAC indicated that some "deglitching" was necessary. These glitches are produced when the more significant bits of the counter change state and differences in the switching speeds from low to high and from high to low in both the output of the counters and the current switches in the digital to analogue converter itself, cause a momentary false value to be registered producing a spike in the digital to analogue converter output.

The usual way of deglitching a digital to analogue converter uses a sample and hold circuit at the output of the DAC which holds the previous value until the new one has settled (figure 4.3).

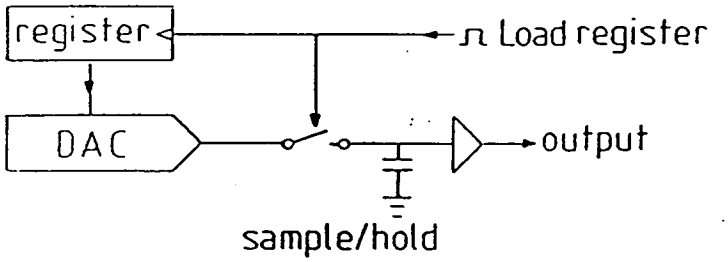

Figure 4.3 Deglitching the DAC output using a sample and hold circuit.

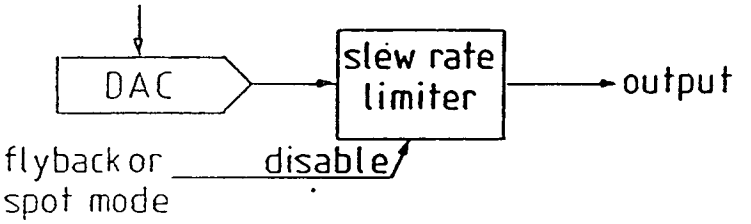

Figure 4.4 Deglitching technique using a slew rate limited amplifier.

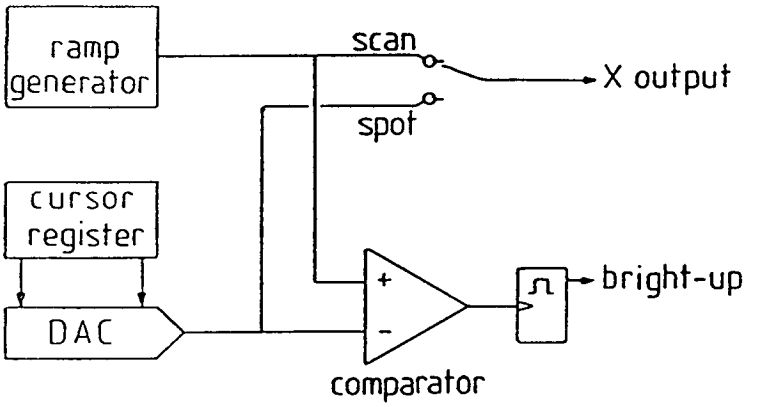

Figure 4.5 A circuit to generate cursor crosswires by analogue voltage comparison.

At the count rates used in the scan generator a very high speed sample and hold is necessary and though various arrangements were tried in all of them the sampling signal tended to feed through and distort the output.

The solution eventually used was to use a slew-rate limiting circuit on the DAC output which restricts the slew rate and so smooths out the glitches during the ramp but is disabled during flyback or in spot mode to allow full speed operation (figure 4.4). This circuit has not entirely eliminated the glitches but has reduced them to quite acceptable levels.

When a more modern microscope - a Cambridge Instruments S100 - was acquired the scan generator was adapted quite easily to drive it using its own scan amplifiers and coils. This simply involved changing the magnitude and offset of the analogue ramp outputs and some small modifications to the blanking and brightup logic to allow these signals to be fed directly into the new SEM's own video mixing circuits. Once connected the scan generator provides the full range of remote computer control facilities using the GPIB in addition to spot and line operating modes, neither of which was previously available on this very basic SEM.

4.1.1.15 Improvements

This scan generator has been used very extensively in the later work using remote control and has given few problems. It could be improved upon in several ways if it had to be redesigned from scratch: The main faults are caused by overcomplexity of the design - in an attempt to give versatility - and the need for very high speed and therefore expensive digital to analogue converters and the glitches they produce.

The design allows an extremely wide range of different scan rates of which only one or two are regularly used. For the vast majority of purposes TV rate is sufficient, provided that the detector and head amplifier have a good bandwidth - especially if a framestore with some kind of picture averaging is available. For

high resolution photographic purposes a single slow scan rate is also desirable. By restricting the scan rates to two or three the design can be simplified and more attention can be paid to making scanning at these two rates work very well.

The problem of glitches in the output could be removed by using an analogue ramp generator for the line scan and using the counter just to generate the timing signals and drive the character generation circuitry. This would also remove the need for highly expensive digital to analogue converters. The frame scan could remain as before since it operates at low frequency and all its glitches appear during line flyback. Digitally controlled spot mode could still be achieved by using a (lower speed) DAC and switching the output between this and the ramp generator. The cursor brightup pulses could then be generated in much the same way as before but using analogue rather than digital comparison, see figure 4.5. Alternatively brightup could be generated entirely by the timing circuitry but in this case there would be a problem of calibration to ensure that the position of the cursor crosswires while scanning is the same as that of the beam in spot mode.

The digital circuitry could also be vastly simplified by using a VLSI video controller IC which could replace most of the counting logic and the character generation circuitry. The Motorola 6845 appears to be ideal for the job.

4.1.2 Scan Coils

The existing scan coils in the S2 microscope were unsuitable being high impedance double deflection coils which are driven by thermionic valve scan amplifiers at comparatively low frequencies. For ease of construction it was decided to build after lens deflection coils as these need only be single deflection devices and are also more easily mounted in almost any microscope for experimental purposes. A further benefit is that there is no rotation of the scan with changing focus current in the final lens - the main drawback being the increased working distance required.

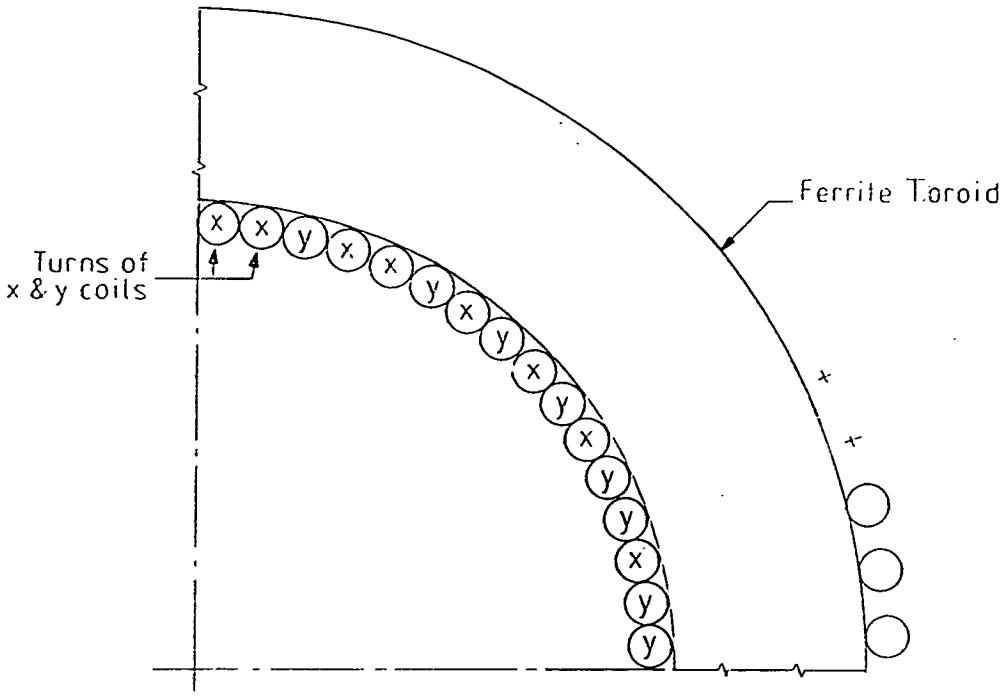

Figure 4.6 Section through one quadrant of the scan coils showing ordering of X and Y turns.

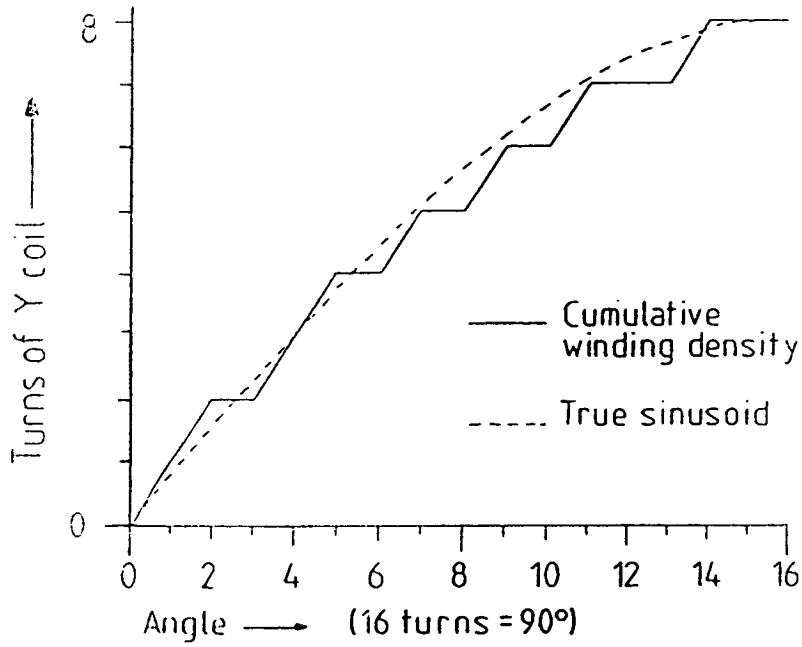

Figure 4.7 Integral of Y turns density around the deflection coil quadrant of fig 4.6.

4.1.2.1 Construction

The coils were wound on a small ferrite toroid. To achieve a linear deflection field in the central region the windings should be distributed sinusoidally around the toroid. Using a heavy gauge wire to withstand several amps of deflection current it was found that the inside circumference of the toroid used would take 64 close packed turns. The problem is how best to divide these turns between X and Y coils to achieve the best approximation to sinusoidal distribution. The arrangement used was arrived at empirically and one quadrant is shown in figure 4.6 (all four quadrants are similar with the directions of either X or Y turns reversed). Figure 4.7 shows the integral of the density of X turns over the quadrant against a true sinusoid.

Once these windings had been made the assembly was set into an aluminium plate 5mm thick which was simply bolted to the final polepiece of the SEM. As well as providing a mounting this plate acts as a heatsink. Connections were made via feedthrough connectors in the side of the vacuum chamber.

4.1.2.2 Operation

These coils worked excellently with the scan generator and amplifiers, described below, as a simple solution to providing high frequency scanning on the antiquated S2 microscope - however all modern SEMs have adequate coils for TV rate operation and as in general the benefits of before the lens deflection outweigh its defects there was no point in developing these coils further.

As mentioned above the distribution of turns was arrived at empirically and a more scientific method which minimised the deviation from a true sinusoid would have produced a different arrangement in this case and could be applied to coils with any desired number of turns. The use of "saddle wound" coils could also reduce the overall inductance without affecting the linearity of the deflection field.

4.1.3 Scan Amplifiers

4.1.3.1 Design Criteria

The job of the scan amplifiers is to take the scan ramp voltage from the scan generator as input and drive a corresponding deflection signal into the scan coils at the output. They must operate from DC (for spot mode) through to several hundred kHz for accurate TV rate scanning and, if required, for any vector scanning applications e.g. for rapid automated probing of ICs. They must also have a gain variable over a wide range as this is how magnification is varied.

Since the deflection of the beam is (ideally) directly proportional to the current passing through the scan coils, the output of the scan amplifiers must be a current which is not sensitive to variations in the load voltage due to the inductive nature of the load; i.e. the amplifiers must have a very high output impedance. This is the converse of most conventional amplifiers in which the output is generally considered as a voltage which should be insensitive to load current, and so have a low impedance. Because of the conventional ideal of low output impedance, most existing designs begin with a voltage amplifier design and linearise the output with large amounts of feedback. The amplifiers described here are a completely new design derived from an earlier model by my supervisor Alan Dinnis. They have an inherently high output impedance which is further linearised with the use of feedback - leading to a very stable design with good high frequency capability.

The scan coils used (see below) had comparatively few turns and were constructed from thick wire so their inductance was fairly low and their resistance negligible - the penalty for this being that a large current is required to generate the deflection necessary for low magnification scanning. Based on previous work a maximum current of around 3 to 5 amps was required and the amplifiers were designed to operate up to 5 amps.

4.1.3.2 Output Stage Design

Bipolar and FET type transistors both have an inherently high output impedance when operated in the common emitter (or common source) mode and the simplest output stage would be the class A design of figure 4.8*a*. This is however not feasible as the quiescent current is very large and the negative supply must be capable of sinking twice the maximum output current. Replacing the current source with a second, complementary, transistor produces the class B design of figure 4.8*b* in which positive and negative cycles are supplied by separate transistors. This circuit allows low quiescent power but has the disadvantage that two drive signals must now be generated.

MOSFET type power transistors were used for the output stage for a number of reasons: They require smaller drive current and less complex drive circuitry, they have better high frequency performance and since source and drain are isolated from the gate there is virtually no error produced in the feedback resistors (see below) as there would be due to base current with bipolar transistors.

4.1.3.3 Phase Splitter and Output Drivers

The output transistors, whose inputs have quite high capacitance, are driven via emitter follower buffers (in fact Darlington pairs were used) which are in turn driven directly from a phase splitter circuit (figure 4.9). It is this circuit which generates separate drive signals for the positive and negative output transistors. Also by adjusting the potentiometer, the quiescent current and crossover distortion may be optimised.

4.1.3.4 Feedback

The final circuit is shown in figure 4.10. A feedback signal proportional to the actual load current is generated by taking the difference between the voltages across the two equal feedback

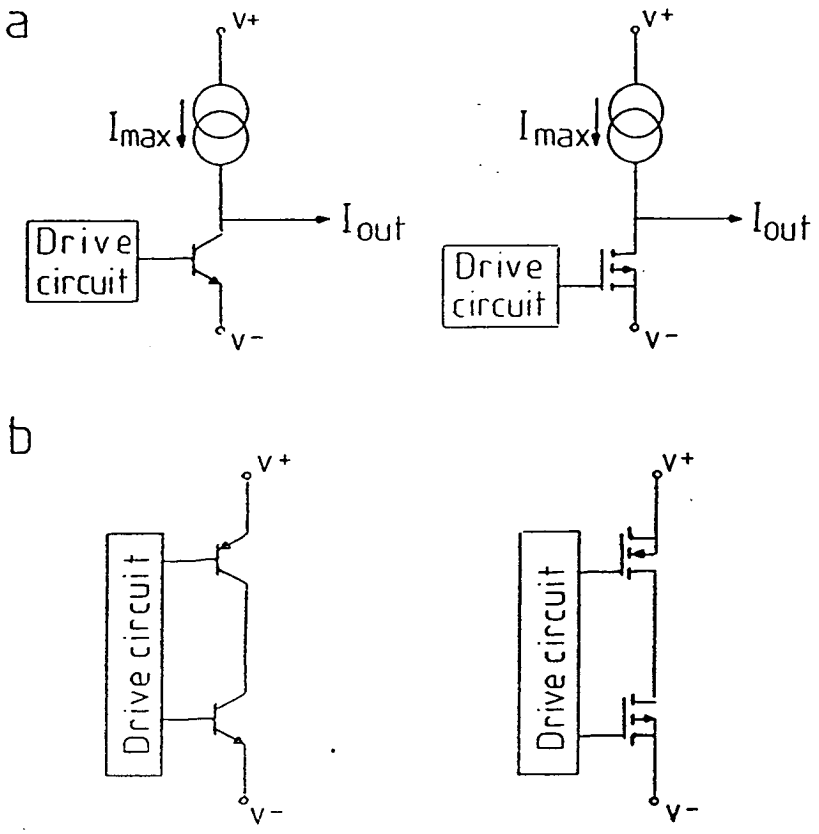

Figure 4.8 Simplified current amplifier output stages: a. Class A - Bipolar and MOSFET equivalents. b. Class B - Bipolar and MOSFET.

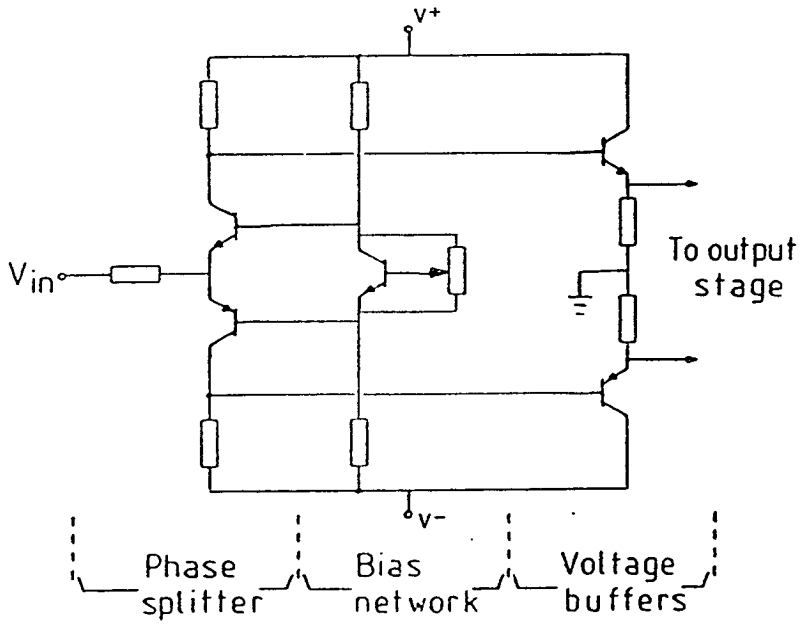

Figure 4.9 Circuit used for phase splitter and output transistor drivers in the scan amplifiers.

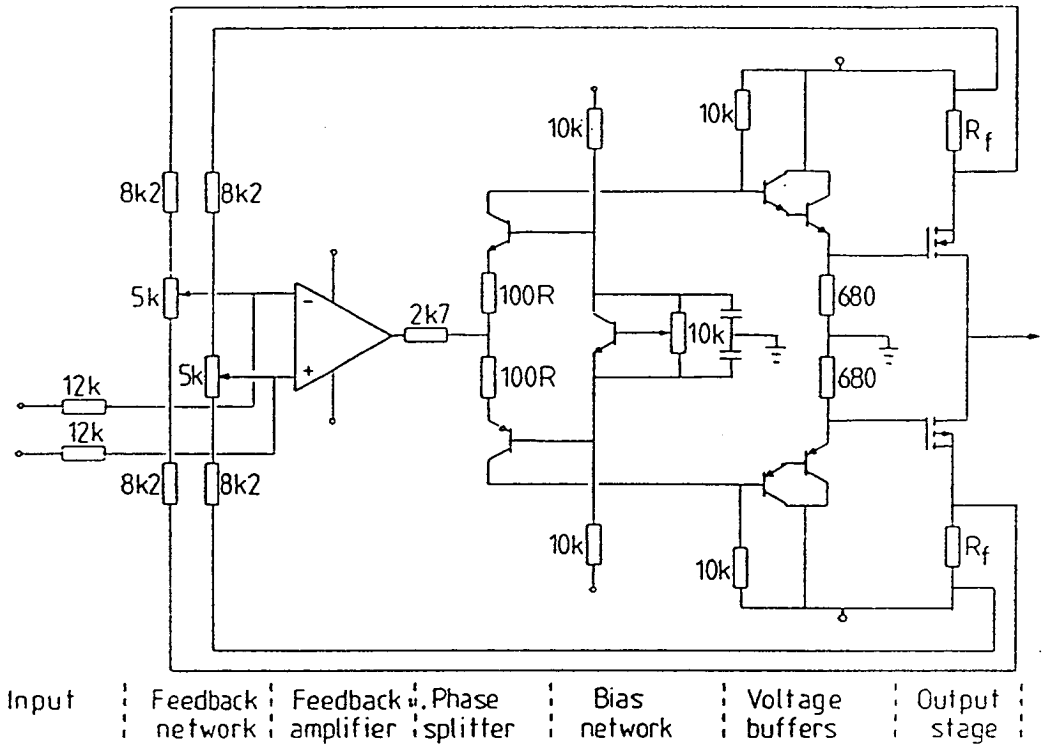

Figure 4.10 Complete circuit of scan amplifiers.

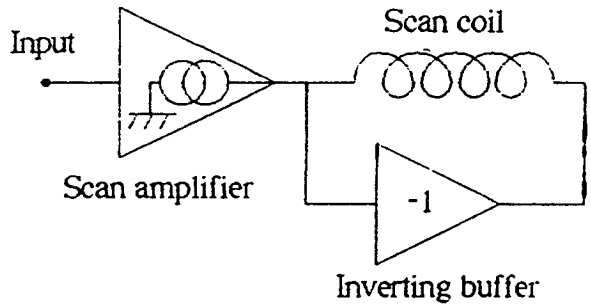

Figure 4.11 Slave amplifier connection for driving the return end of a scan coil in antiphase to improve speed.

resistors R_F. A simpler method would be to insert a small feedback resistor between the scan coil return and ground, however this connection is not always available and the method used does not require any external feedback connections, it does however assume that the feedback resistors are well matched.

Magnification is changed by a combination of switching the main feedback resistors for coarse control and by attenuation of the input signal for fine control and zoom.

4.1.3.5 Summary

All sections of the amplifier work from a 15volt stabilised power supply except the output section which is fed from an unstabilised 12V supply. The amplifiers have no trouble at all driving a deflection current up to 5 amps into the specially built coils at TV line rate and in fact flyback times observed indicate that much higher scan frequencies could be used.

4.1.3.6 Improvements

The basic design of this amplifier has been shown to work well and was used to good effect and no further practical work was done on the subject but a number interesting possibilities for improvement arise from this design.

With scan coils of higher inductance the voltage at the output of the amplifier will fluctuate further and clipping will occur as this approaches the power supply rails. Rather than simply increasing the supply voltage to cope with this an alternative is to drive the return end of the coil in antiphase. Since the feedback signal is generated inside the scan amplifier circuit this could be achieved by simply connecting a unity gain inverting voltage amplifier across the coil as in figure 4.11. Providing the input impedance of the inverter is high it will have no significant effect on the accuracy and would operate as a slave to the main amplifier.

Magnification is controlled by varying the output range of the scan amplifiers. Over a small range, up to about one order of magnitude, this can be done by attenuating the input signal but for larger changes it is necessary to alter the gain of the amplifier itself. The simplest way to vary the gain in this design is to change the feedback resistors R_F and this was done using electro-mechanical relays. An all electronic method would be more desirable for computer control giving better speed and reliability and simpler interfacing. An ingenious way I propose to do this is to use the same transistors for switching and as the output stages, using low power switching circuits to select between them. The circuit of figure 4.12 shows a design which does not require additional switching of the feedback connection and which allows the output transistors to be selected for their working range. This now allows very rapid, all electronic, switching of the gain, controlled by ordinary digital circuits.

Although this amplifier works well at the magnifications used for voltage contrast applications, for higher magnifications and very small output currents the amplifiers tend to become unstable. At low deflection currents this type of power design is inappropriate anyway so a solution would be to switch to a different amplifier. Due to the use of feedback resistors in the amplifier output rather than the return connection, a second amplifier could be connected in parallel with this one - the antiphase voltage booster of figure 4.11 could be included too. In this configuration whilst scanning at high magnification the high current amplifier could be fed with a DC signal to offset the scan to any position on a large specimen with no mechanical movement of the specimen necessary.

4.1.4 Scan rotation

To rotate the image of the specimen it is necessary to rotate the raster pattern of the beam in the microscope whilst retaining the same scan on the display. To achieve this rotation one of the

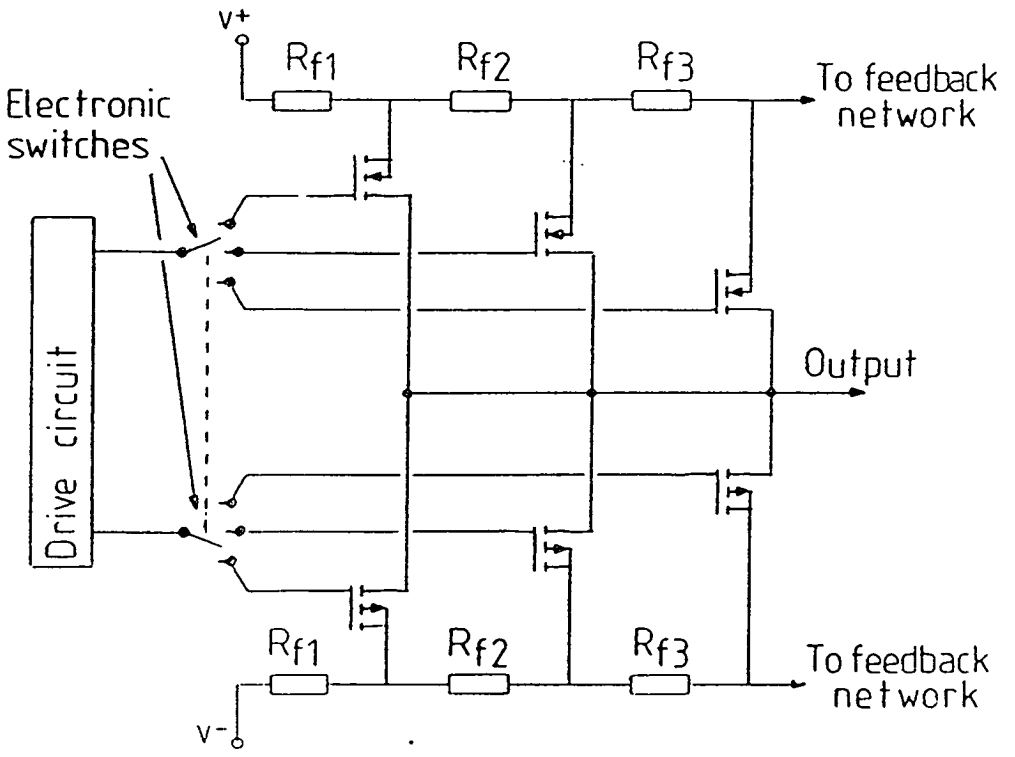

Figure 4.12 Circuit for fast low power switching of feedback elements in the scan amplifiers using the output transistors as switching elements.

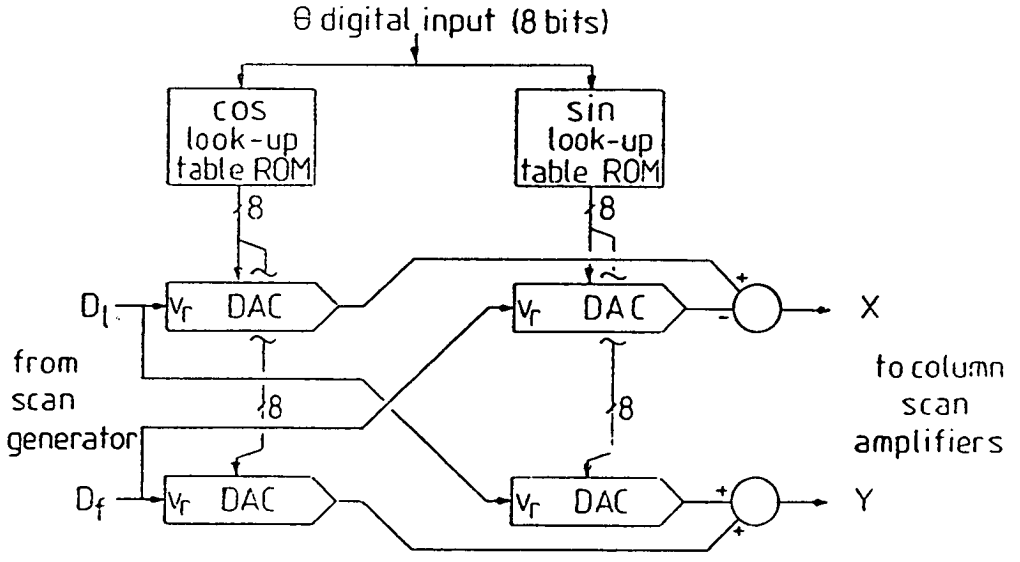

Figure 4.13 Scan rotation circuit using multiplying DACs. Dl and Df are the display line and frame deflection signals. Vr are the DAC reference voltage inputs.

simplest methods is to mechanically rotate the scan coils within the electron column and this method has been used in at least one range of commercial microscopes. A more elegant method is to perform the rotation electronically.

The equation used to do this is the usual mathematical rotation of axes transformation:

$$X' = X\cos\theta - Y\sin\theta$$
$$Y' = Y\cos\theta + X\sin\theta$$

In this case X and Y are the unmodified (display) deflection signals and X' and Y' are the rotated column deflection signals.

A circuit to realise this equation (shown in figure 4.13) uses four multiplying DACs to produce the four sine and cosine terms directly. In most digital to analogue converters the analogue output is derived from a reference voltage input, so that the output is proportional to the product of the digital input and the reference voltage. Multiplying DACs are designed to operate with a widely and rapidly variable reference voltage so that the output is the product of this analogue input and the digital input. Thus the X and Y ramps from the scan generator become the reference inputs to the DACs and the values of $\sin\theta$ and $\cos\theta$ are supplied as digital inputs. The outputs from the DACs are then added (or subtracted) using operational amplifier circuits which also serve to buffer the outputs. Values of $\sin\theta$ and $\cos\theta$ are produced by two lookup tables stored in ROM so θ can be input directly in digital form.

A version of this circuit was built to work with the digital scan generator by a Third year undergraduate project group under my supervision [16] and works well although the rotation caused some slight variations in magnification due to a lack of resolution in the DACs (12 or more bits would be preferable). However once again the purchase of the S100 microscope rendered this circuit redundant as this SEM had scan rotation built in.

An alternative approach with the all digital scan generator design would be to carry out the rotation transformation digitally and convert the result using DACs. This approach would prevent the use of an analogue ramp generator to avoid glitches as described in section 4.1.1.14 and the amount of rapid number crunching involved would be formidable in the most straightforward solution. A way around this would be to perform the multiplication using a lookup table stored in RAM and to reload the entire RAM with the appropriate values whenever the value of θ is changed; however the circuit would still be very complex.

4.2 Electronic Measurement of S-curve Shift

To measure voltages on an IC some means for accurately measuring the position of the S-curve is necessary. For purposes of computer manipulation this information must ultimately be available in digital form. Very little work has been done on this problem - most research being aimed at improving analysers rather than attempting to improve the quality of measurements from existing ones. A number of very different approaches were tried with varying degrees of success:

The common method used with high pass spectrometers is the feedback arrangement described in section 2,20 whereby the analyser grid is adjusted to bring the output to a predetermined reference level (figure 2.3). This works so long as the S-curve maintains its shape and amplitude with voltage shifts - however it is obvious that variations in S-curve height, even with no positional change, will cause an output change.

4.2.1 Successive Approximation Circuit

The first circuit constructed was simply an attempt to digitise this feedback process by interposing the spectrometer in the normal feedback loop of a successive approximation type analogue to digital converter. A block diagram of the arrangement is shown in figure 4.14a. A second version of this circuit was built in an

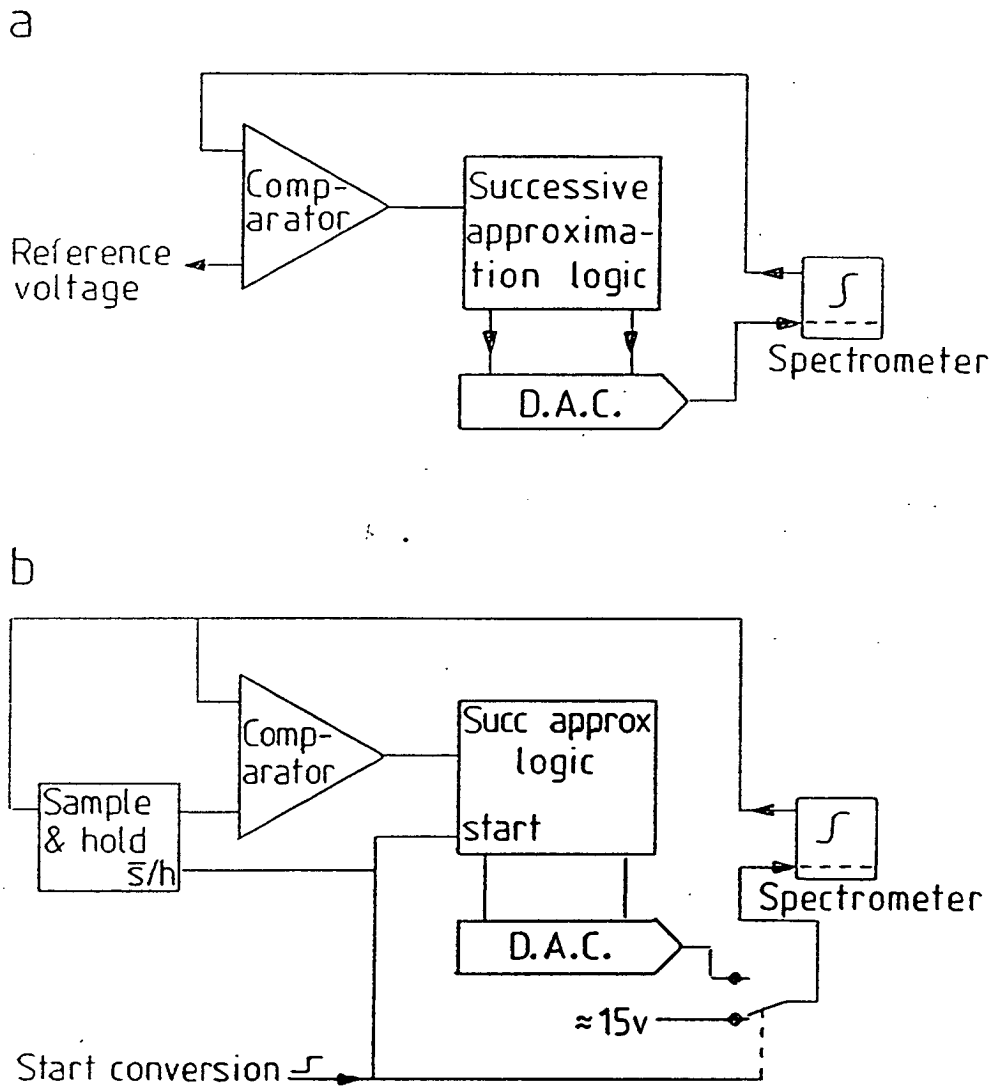

Figure 4.14 S-curve tracking by including the spectrometer in the feedback loop of a DAC. a. Basic circuit. b. With reference level compensation.

attempt to compensate for errors due to S-curve amplitude changes. This was done by setting the analyser grid voltage to a high value certain to be on the upper plateau of any S-curve in the operating range. The resulting output was taken as a measure of S-curve height and the reference level for the subsequent conversion was taken to be exactly half of this (figure 4.14*b*).

While both circuits were made to work they were found to be unreliable and hard to set up and operate. The nature of the successive approximation conversion algorithm means that the analyser grid voltage jumps about over a wide range and is easily upset by the distortions at the upper end of the S-curve mentioned above. The fact that the second circuit actually uses this upper region as a starting point to derive a reference level can compound the trouble if the S-curve is irregular.

These experiments showed that the successive approximation algorithm was unsuitable for these purposes - it would be better to either use a different digital algorithm (perhaps one which "ramps" up from a low voltage) or to use an analogue method and simply digitise its output. Subsequent improvements in spectrometer design and operating conditions - and therefore S-curve shape - might have made the circuits more practicable but no particular benefit from their use could be seen by this time.

4.2.2 Second Harmonic Detection Technique

A more complex method for S-curve detection relies on modulating the filter grid with an AC signal and synchronously detecting the second harmonic of this signal in the output waveform [17] (Figs 4.15 & 4.16). When the filter grid signal is centred at the point of inflection on the S-curve, the output waveform is approximately symmetrical above and below the average level. However as the S-curve is offset the output becomes flattened either above or below depending on the direction of the offset. Phase sensitive detection of the modulating signal's second harmonic gives a measure of this asymmetry.

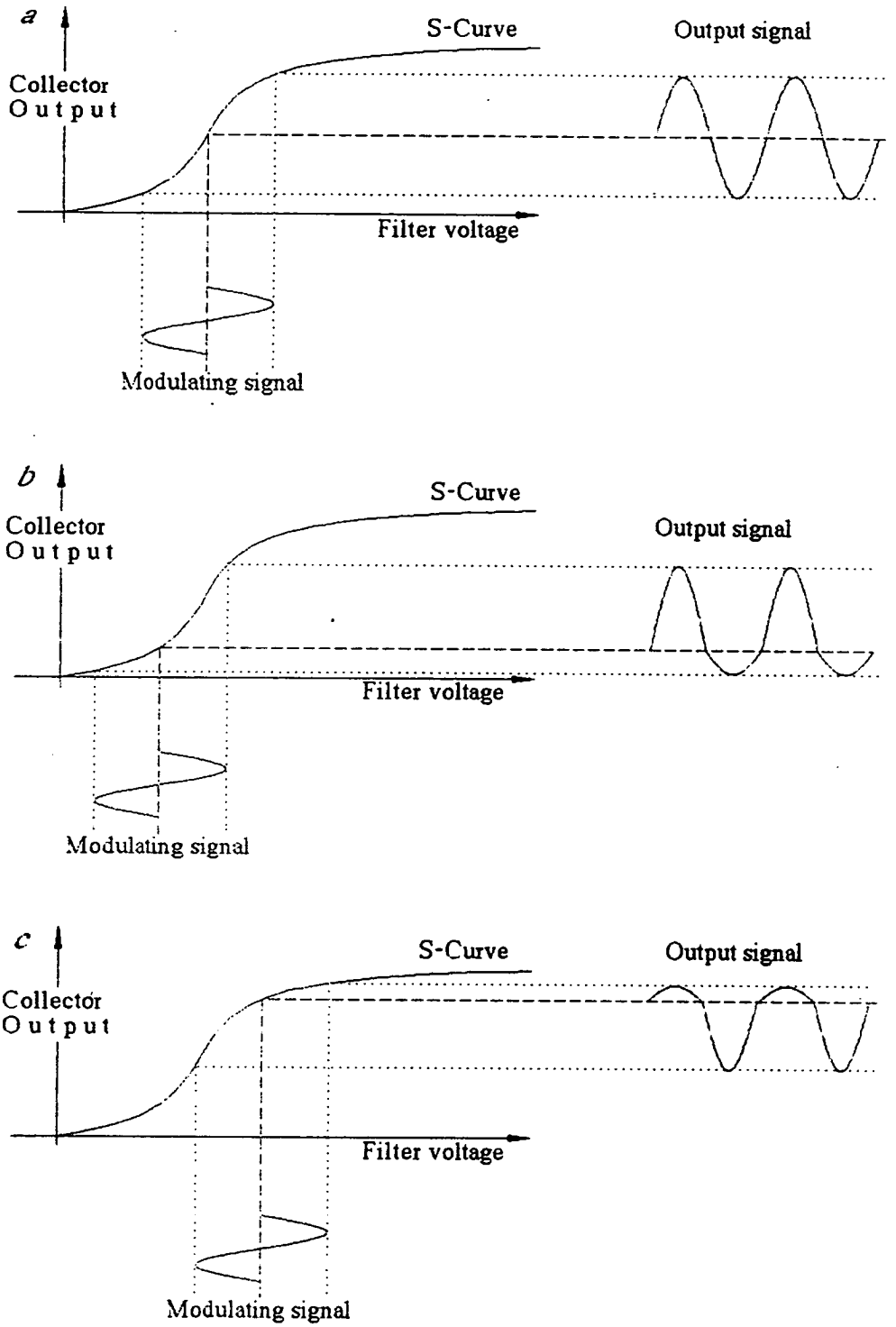

Figure 4.15 a-c. Modulating the grid signal with a sine wave produces an output which is flattened from above or below depending on the offset relative to the central part of the S-curve.

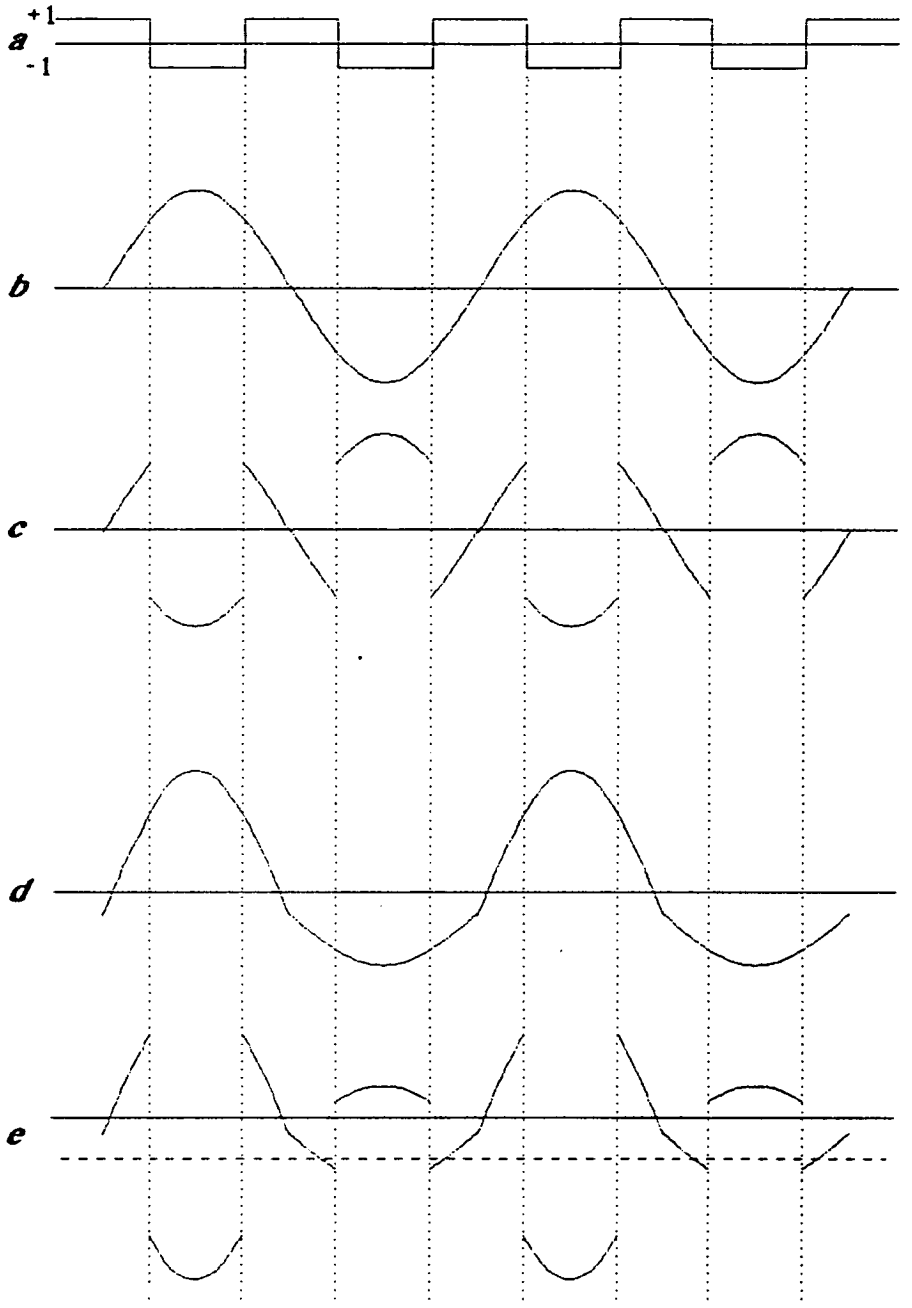

Figure 4.16 Synchronous demodulation of the second harmonic of the original sine wave produces a measure of this flattening a. Is the demodulating signal at twice the original signal frequency. b. is a symetrical output waveform with no second harmonic component at the requires phase angle and c. shows the output from the modulator whose mean level is zero. d-e. show what happens when an asymmetric flattened curve is demodulated - in this case the dashed line shows the DC mean level of the output curve.

This method has the great advantage that the output is theoretically independent of the amplitude of the S-curve. A further feature is that the output signal need not be DC coupled. Although not relevant in the present context, AC coupling could be invaluable if the analyser design necessitated output detection at a high voltage, as in some designs proposed in Chap 2, because isolation of the head amplifier output from processing electronics is generally much simpler for AC signals when a simple capacitor or transformer arrangement can be used. The narrow bandwidth that the information is carried in could also be useful for noise reduction.

Although sophisticated circuitry for second harmonic detection of S-curve shift was being developed concurrently by Brian Gilhooley [17] an extremely simple circuit based almost entirely on CMOS logic circuits was built to test the efficacy of the method and gauge its potential for further investigation and use in a computer based e-beam tester. The circuit is shown in figure 4.17. The signal to the filter grid is a triangle wave generated by a square wave oscillator and an integrator. This is added to a DC offset level which can either be provided externally or fed back from the detection electronics to provide S-curve tracking. A good approximation to second harmonic demodulation is provided by two CMOS analogue switches which select either the incoming signal or its inverse. The correct phase relationship between this detector and the grid signal is determined by a digital counter. The output of the demodulator is then smoothed and amplified to provide an output level and an error feedback signal to adjust the filter grid offset.

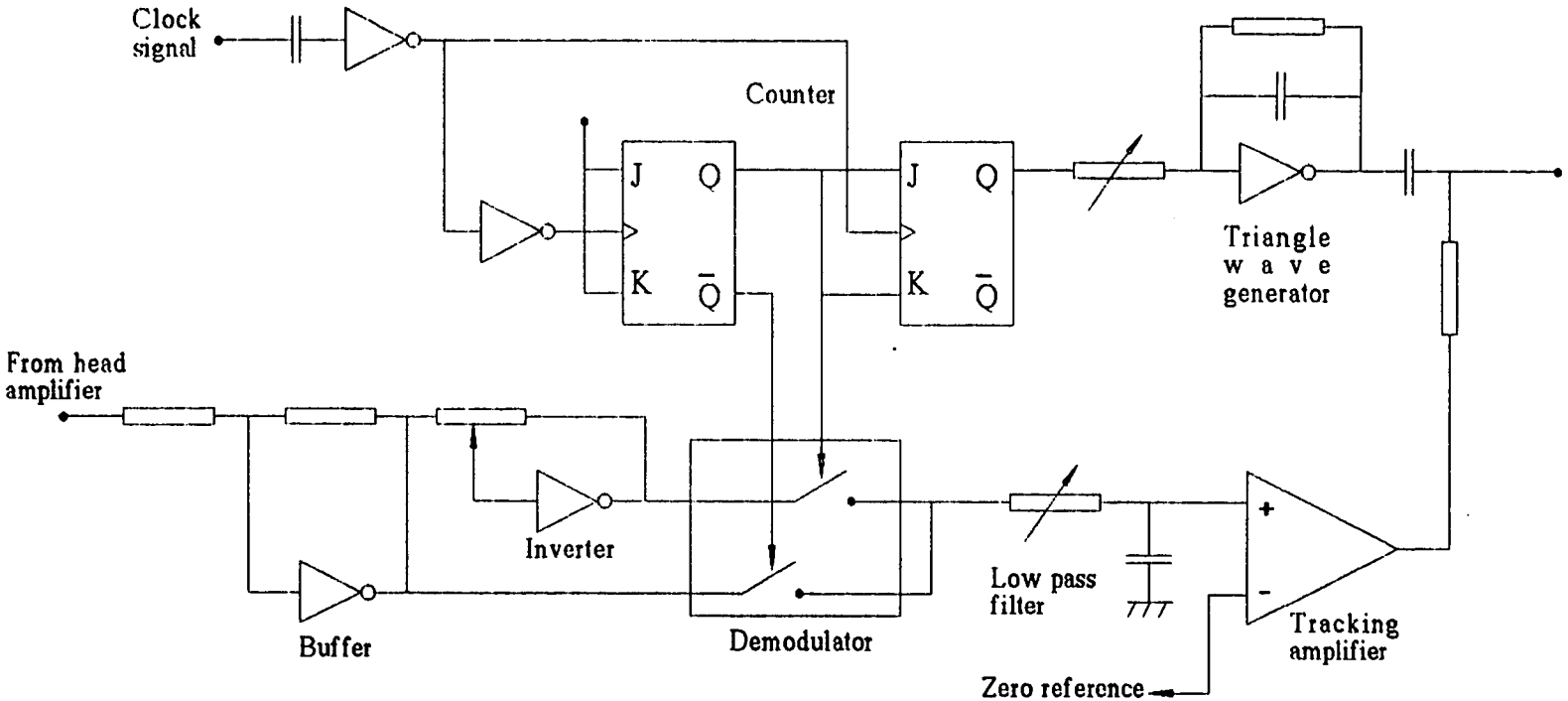

Figure 4.17. Original circuit for tracking s-curve shift using second harmonic detection. All active elements are CMOS logic devices - operating in linear modes in some cases - with the exception of a single operational amplifier.

Initial results from this circuit were very promising, (although it showed some tendency to latch up with irregular S-curves) and some attempt was made to link it into a digital feedback loop - described in the next chapter - but as Gilhooley was already working on a much more advanced version, little more was done. In the event a similar technique was eventually used in the all digital method described in chapter 5.

4.3 Beam Chopping.

Beam chopping for measurement of rapidly varying signals on ICs has been the subject of a vast amount of study and is beyond the scope of this project [18]. However, as with the rest of the e-beam testing system, it is obviously important that the chopping electronics should be under computer control. The main element of interest here is the delay generator which controls the phase relationship between the waveform on the specimen and the beam pulses (see figure 1.6). Some attention was given to methods for accurate digital control of very short delays.

4.3.1 A Digital Delay Generator

The main requirement of the delay generator is that it should produce any delay within a wide range to the accuracy of the smallest step. For longer delays (>50ns) it is very simple to do this using digital counters. The only real problem being that the oscillator driving the counter must start up uniformly with the trigger signal and cannot be free running. Use of higher speed logic can improve the resolution of counter based systems somewhat but for sub-nanosecond delays some other method is necessary. Several circuits had already been built at Edinburgh using analogue delay lines [19] with digital data selectors to switch between them.

To control very short delays digitally I proposed a different arrangement using binary weighted delays and Shottky TTL to switch between them. The full circuit of the binary weighted delay

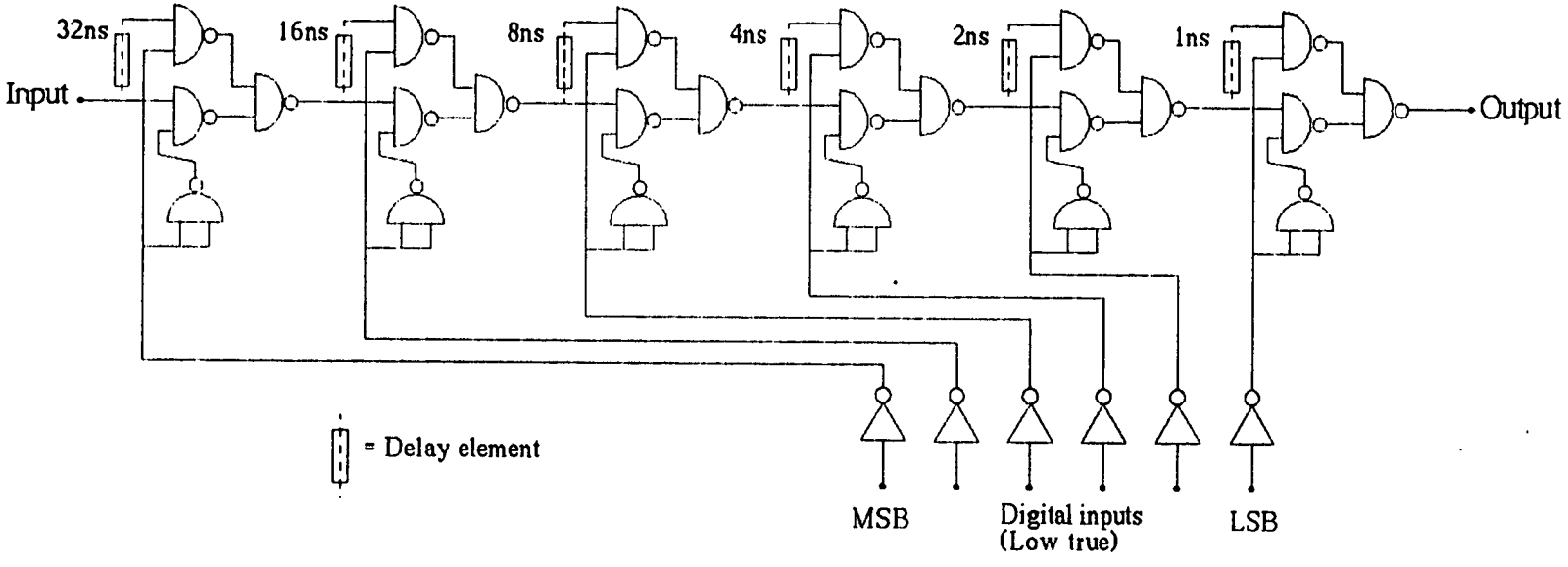

Figure 4.18. Circuit for delay generation using binary weighted delay elements. All logic gates are Schottky TTL.

generator is shown in figure 4.18. To avoid errors each stage is identically laid out on the circuit board. The delays are provided by lengths of co-axial cable trimmed to match each other. The high order bits of delay are provided by a counter based circuit matched to the same scale.

The binary weighted delay gave some problems in matching all the delay lines together and it was found that the matching was different for rising and falling edges so it has to be operated on the the same edge in all cases. A diagram of this circuit was given to British Telecom Research Laboratories who built and operated it with some success.

Chapter 5

Development of Computer Systems

5.1 Computer System Description

5.1.1 Summary of Control System

The computer control system used throughout the work was built up around a Superbrain microcomputer made by Intertec Data Systems. The choice of computer was based on storage and computing power and the recommendations of the Edinburgh Regional Computing Centre (ERCC). The UCSD p-System (see appendix 2,00) was also chosen as the operating system on the recommendation of ERCC.

At the time of purchase it was realised that this hardware and software combination would need modification and addition for the use envisaged, however in order to get a more suitable system a lot more money would have to be spent as other systems on the market even up to two or three times the cost would present a similar problem. In fact the final system has proved quite adequate for the control applications provided so far but further work would need a computer with much more processing power to handle signal and image processing.

5.1.2 Superbrain

The Superbrain is based around a Zilog Z80 microprocessor with 64 kbytes of RAM, and two 5¼" floppy disk drives. These are housed in a single terminal unit incorporating the keyboard and display screen. Two external serial interfaces are also included.

5.1.3 Operating System

The UCSD p-System is a complete program development system based around a pseudo-code or p-code interpretation program. All programs are compiled to p-code which is then interpreted at run time. This has the advantage of great program

portability at the object code level at the expense of execution speed. The system includes a screen editor, an assembler (although programs assembled to Z80 machine code will not be portable) and a sophisticated PASCAL compiler with many extensions and debugging facilities, as well as utilities for file manipulation and disc management.

5.1.4 General Purpose Interface Bus (GPIB)

5.1.4.1 Interface Hardware

To allow control of a large number of differing instruments the first priority was to add a GPIB interface (see appendix 1,00) to the Superbrain. No such interface was available commercially but, once circuit diagrams for the computer had been obtained, a very simple interface was designed using a Texas Instruments GPIB controller IC (TMS9914) which was new at about that time. The interface was mounted inside the Superbrain's cabinet and powered by the computers own 5V power supply. This has caused no problems on this particular Superbrain though I understand that other people have had trouble with the power supply being inadequate for normal use so the addition of extra circuitry could cause trouble.

After some initial trouble, traced eventually to faulty documentation from Texas Instruments, the circuit worked exactly as predicted. A more difficult problem was now to write a universal software driver for the GPIB.

5.1.4.2 Interface Software

A number of possible ways to control the GPIB were considered ranging from piecemeal machine code routines linked into PASCAL programs to full incorporation into the operating system. In the end the latter course was taken as it was felt that once the task was completed it would become very simple to write programs to use devices on the bus.

Input and output in the p-System is handled by a section called the BIOS (for Basic I/O Subsystem) in which the physical control of individual devices is isolated in a (necessarily) machine dependent section of machine code called the SBIOS (Simplified BIOS). The SBIOS consists of a standard set of routines with clearly defined calling parameters which are called via a table. Implementation of the body of these routines depends on the hardware available but there are entries included for up to 16 "User Devices" for which calling conventions are established but no assumptions are made as to their function. So if the GPIB drivers could be implemented to link these User Devices to instruments on the bus then these instruments could be accessed from any level of program by inbuilt I/O calls. In order to do this a complete new SBIOS was written over the course of around 1 year. The new version not only incorporated the GPIB drivers into the operating system but also improved the drivers for nearly all the other devices attached to the system (screen, keyboard, discs, printer, auxiliary serial interface etc, etc.

As it became clear that a major piece of software was being developed, interest was shown in it by ERCC's micro support unit and through them some commercial computer dealers. A deal was eventually agreed to sell the new SBIOS to a commercial company[20].

5.1.5 System Hardware Configuration

With the GPIB full remote control of the scan generator was now possible and several other GPIB devices were also purchased including a plotter and a Hewlett Packard multiprogrammer. The multiprogrammer is a rack mounting box containing a power supply, a GPIB interface and a simple backplane for which a range of cheap (by Hewlett Packard standards) interface cards are available to provide a wide range of functions such as analogue to digital or digital to analogue conversion, stepper motor control, pulse generation, timing etc etc. Alternatively simple circuits

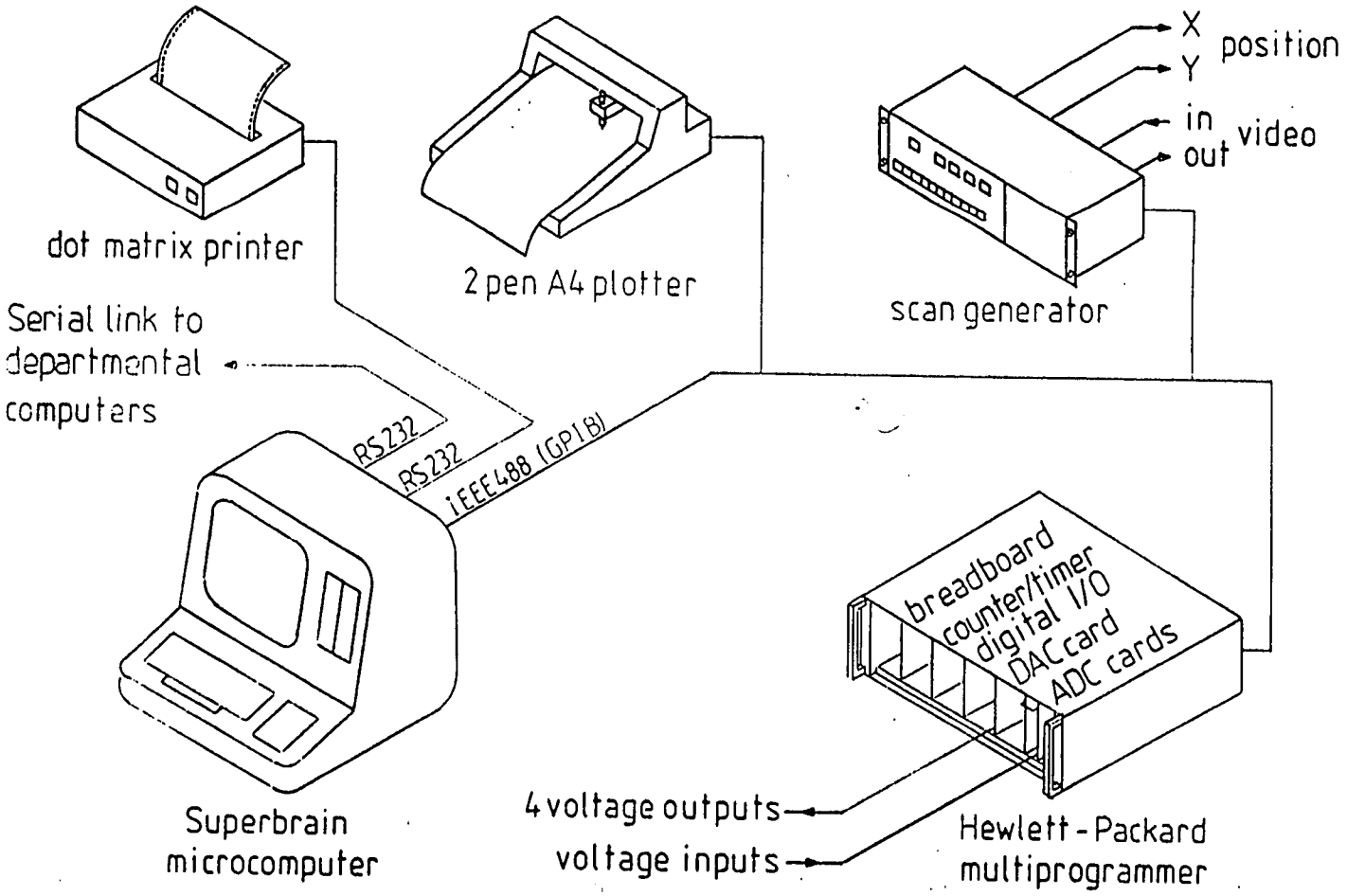

Figure 5.1 Block diagram of computer system.

could be built on "breadboard" cards and plugged into the multiprogrammer much more simply than building them with direct GPIB interfaces. This device was used for control and monitoring of most of the microscope circuitry, apart from the scan generator which has its own GPIB interface.

The final hardware arrangement is shown in figure 5.1. In addition to the SBIOS, special program modules were written (in PASCAL) to simplify control of interface cards within the multiprogrammer, of the plotter and of the scan generator which are the three main devices connected to the GPIB.

5.2 Automated S-curve Detection

5.2.1 Second Harmonic Circuit

By the time that the basic computer hardware assembly was completed work was being carried out on the second harmonic detection method for S-curve tracking (see section 4.2.2 and so the first use of the computer was as an element in this system. A version of the prototype circuit (figure 4.16) was built on a multiprogrammer breadboard card. The DC offset level was provided by one of the four DAC outputs and the detected second harmonic level was read by the ADC input; thus the loop could be closed and the S-curve tracked by suitable software. Two algorithms were tried; first a simple tracking scheme whereby the offset was adjusted one step at a time until second harmonic detection fell to zero. This worked in most circumstances but could latch up in the same way as the all analogue version described in the previous chapter. A second method worked in much the same way but started from the minimum offset value each time - which eliminated the latch up problem but increased the time taken. Both these routines operated very slowly since the offset was only adjusted by one step at a time and at each step the analogue circuitry had to settle before the new second harmonic value could be read.

Although drastic improvements on these routines could almost certainly have been made, the basic circuit was abandoned at this stage in favour of simpler hardware and a more software intensive scheme. By giving the computer direct control of the filter grid voltage and access to the detector output, a very wide range of techniques including all those described previously could be implemented in software and adjusted, where necessary, by simple program modification. The only penalty for this approach might be a reduction in speed but if necessary new hardware could be built once the measurement process had been refined. In the event speed was no great problem.

5.2.2 Direct Digital Connection

Digitising of head amplifier output is simply a matter of connecting it directly to the multiprogrammer's ADC input - experimentation showed that no filtering of the signal is necessary. Control of the filter grid voltage is not quite so simple, since the available DAC outputs only have a range of ±10.24 volts which is insufficient. However by using one DAC to provide an offset voltage for the others they could range through ±20.48 volts, subject to some restriction on their relationship to each other. Figure 5.2 shows the resulting connections - the computer can control the filter grid and two spare analogue outputs and digitise the electron detection level. This arrangement in conjunction with the computer system of figure 5.1 and connected to the S100 microscope were used for all the subsequent work on voltage measurement.

5.2.3 Software

Once the computer system had been put together and the physical links necessary for control of scanning and the spectrometer were established, various programs for voltage measurement were developed. Two approaches are possible: the first - direct real time simulation of more conventional analogue

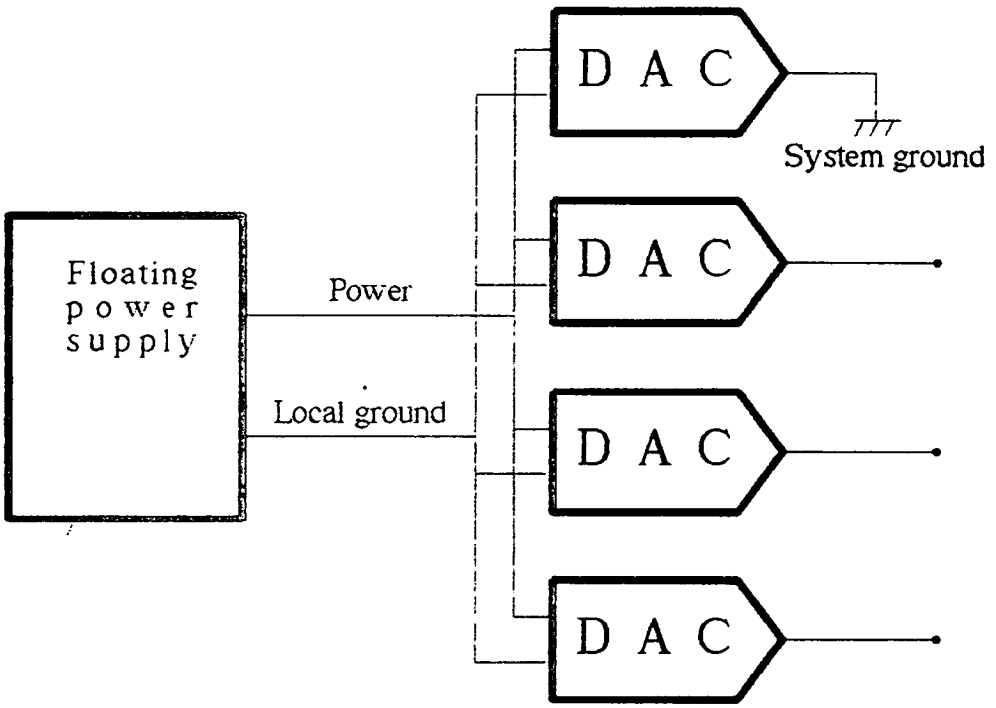

Figure 5.2 Connection of DACs to provide extended output voltage range. Connecting one output to system ground offsets the DAC card's local ground.

methods - was passed over in favour of simply sampling an S-curve in the shortest possible time and then processing it in computer memory. The first task tackled was to sample a complete S-curve from a point of interest on the specimen.

5.2.3.1 Selection of Point For Measurement

The resulting program modules first ensure that the scan generator is in visual display mode and turn on the cursor crosswires to allow the point of interest to be selected. This can be done either by using the existing remote control box for positioning the cursor or by using the cursor keys on the computer keyboard. In the end the latter technique was dropped as it was easier to use two knobs as input than repeated presses of the cursor keys - with a computer system incorporating some kind of pointing device (mouse, tracker ball, graphics tablet etc) it would be a simple matter to use this for cursor positioning.

5.2.3.2 S-curve Sampling

Once the position for measurement is defined the sampling process can be triggered by a single keystroke. The scan generator is switched into spot mode, positioning the beam at the predefined point, the filter grid is then held at a number of voltage steps in turn while the resulting detector output is read in and stored for each step. Finally the scan generator is switched back to visual mode. In the initial programs a graph of the sampled S-curve is immediately displayed on the screen.

The two routines for positioning the beam and sampling a single S-curve are at the heart of all subsequent programs described here. The display of the sampled S-curve is very useful for adjusting the various spectrometer voltages and the detector gain and offset. In the initial stages the filter grid sweep range and the number of steps were variable to allow experimentation. It was soon found that a voltage sweep of around 20 volts is ideal though the best offset depends on the particular conditions and settings of

such things as extraction voltage, primary beam energy etc. For most cases something like -5V to +15V works well. The number of steps sampled is a compromise between the time taken, storage space for the data and the accuracy required. More steps require a longer sampling time which can cause the old problems of drift in output due to static charge leaking away and contamination buildup. In this setup the time taken is dominated by processing time and could be improved with a faster computer or specialised hardware - the actual sampling time does not limit the speed so much - for a 21 point S-curve the sampling time is around 0.1s.

If a large number of S-curves are to be stored then the number of points sampled in each can create storage problems. The obvious disadvantage with using fewer sampled points though is the increase in the significance of noise and loss of accuracy.

Some experimentation was done sampling several S-curves, with a delay between each curve sampled, then averaging them to reduce noise levels. Although this succeeded it needed quite a few curves to be sampled before much improvement was apparent and this was extremely time consuming as a delay was required to allow re-establishment of equilibrium conditions before each S-curve was measured. It was felt that this method gave no particular advantage over simply using more sample points on a single S-curve. Careful setting up of the microscope can keep noise levels to a reasonably low level anyway.

5.2.3.3 Development of Processing Methods

Once an S-curve has been sampled and stored the problem is to calculate its position. Time is no longer a critical factor as the beam can now be turned off or left to scan. obviating the usual problems caused by long setup and acquisition times. Level detection analogous to the conventional feedback method would be simple but is subject to the same inaccuracies, further degraded by quantisation and interpolation errors.

To experiment with other processing methods a set of program options allowing definition of an operator, convolution with the sampled curve and graphing of the result were added to the original program.

The convolution integral is often viewed as the time domain expression of frequency domain filtering by simple multiplication of frequency spectra. A signal $F(t)$ when applied to a system will produce a corresponding output $F'(t)$ which is the convolution of $F(t)$ with the transfer function of the system $G(t)$. In this case the signal and transfer function - described by the chosen operator - are arrays of points and so discrete convolution is used and the time variable is simply the index into the array. In its discrete form the convolution integral becomes:

$$F'_n = \sum_{i=0}^{n} G_{n-i} F_i$$

All graphs in this and subsequent chapters show series of discreet sampled points connected by straight lines and do not represent continuous data.

A number of results are shown in figure 5.3. In the first case (b) a simple block operator has been used to smooth the raw sampled data. The second operator performs exactly the same function as the simplified second harmonic detection circuit of section 4.2.2. In the third example the simplest two point differential operator has been used and it can be seen that the resulting curve whilst looking something like the ideal energy distribution curve is also very noisy. Direct measurement of the position of the maximum of this curve would not be useful.

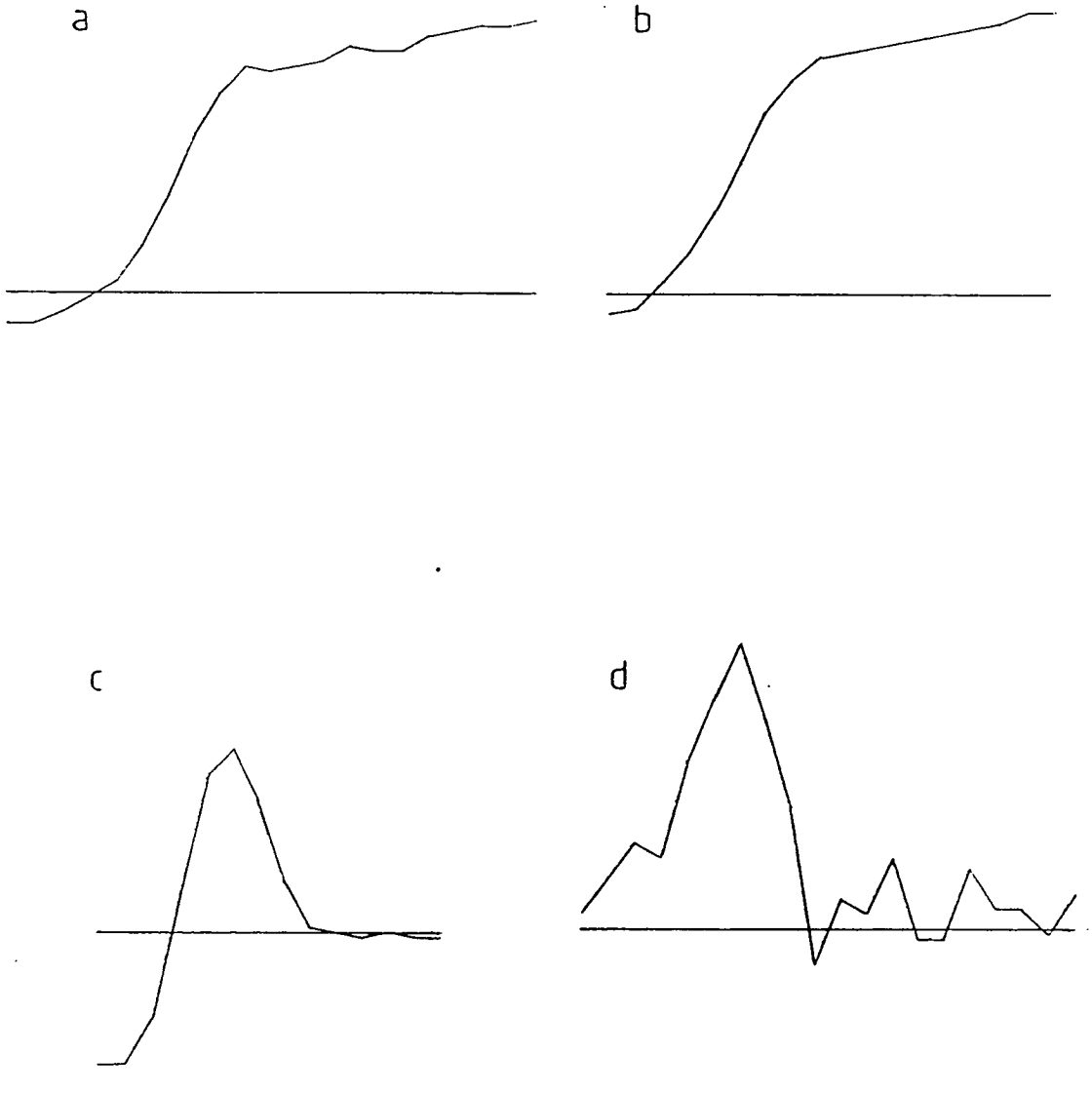

Figure 5.3 a. Sampled S-curve. b. After convolution with block operator (1.1.1.1). c. Convolved with digital equivalent of the synchronuous demodulator (-1.-1.1.1.1.1.-1.-1). d. With differential operator (1.-1).

5.2.3.4 Double Differentiation

The next step was to try a technique of differentiating the S-curve twice to produce a curve which crosses zero at the point of inflection of the original S-curve. It is then very simple to detect the position of this point using interpolation if necessary. The best differentiating operator is a linear ramp[21] and the longer this ramp is, the less the noise sensitivity, but the more the genuine features of the S-curve will tend to be smoothed out. Another problem is that convolution of a curve of n points with an operator of m points yields a curve of $n-m+1$ points so, with S-curves of only a few sampled points, if the operator is too long there is only a very short resultant curve for analysis.

To differentiate twice, the same operator can simply be applied again. In fact the operation of convolution is associative so the two differentiating operators can be combined to produce a double differential operator which can then be used on the sampled data in a single stage process - this is the method which was adopted. An S-curve of 21 sampled points was settled on, covering a filter grid range of 20V in 1V steps. Double differential operators of varying numbers of points were tried (figure 5.4). A routine was then added to measure the position of the zero crossing of the resulting curve using linear interpolation between the 1V steps.

The programs developed so far allow selection by the user of many parameters such as number of sample points, operator type and length, etc etc. The results from this work showed that, at least in the cases tested, using a 21 point S-curve and a 5 or 7 point operator it was possible to measure the curve position easily and repeatably with an error well below 1V which was quite good for the moment.

The specimens used for this work were all test chips built in the department and measurements were made on test tracks down to 10μm wide.

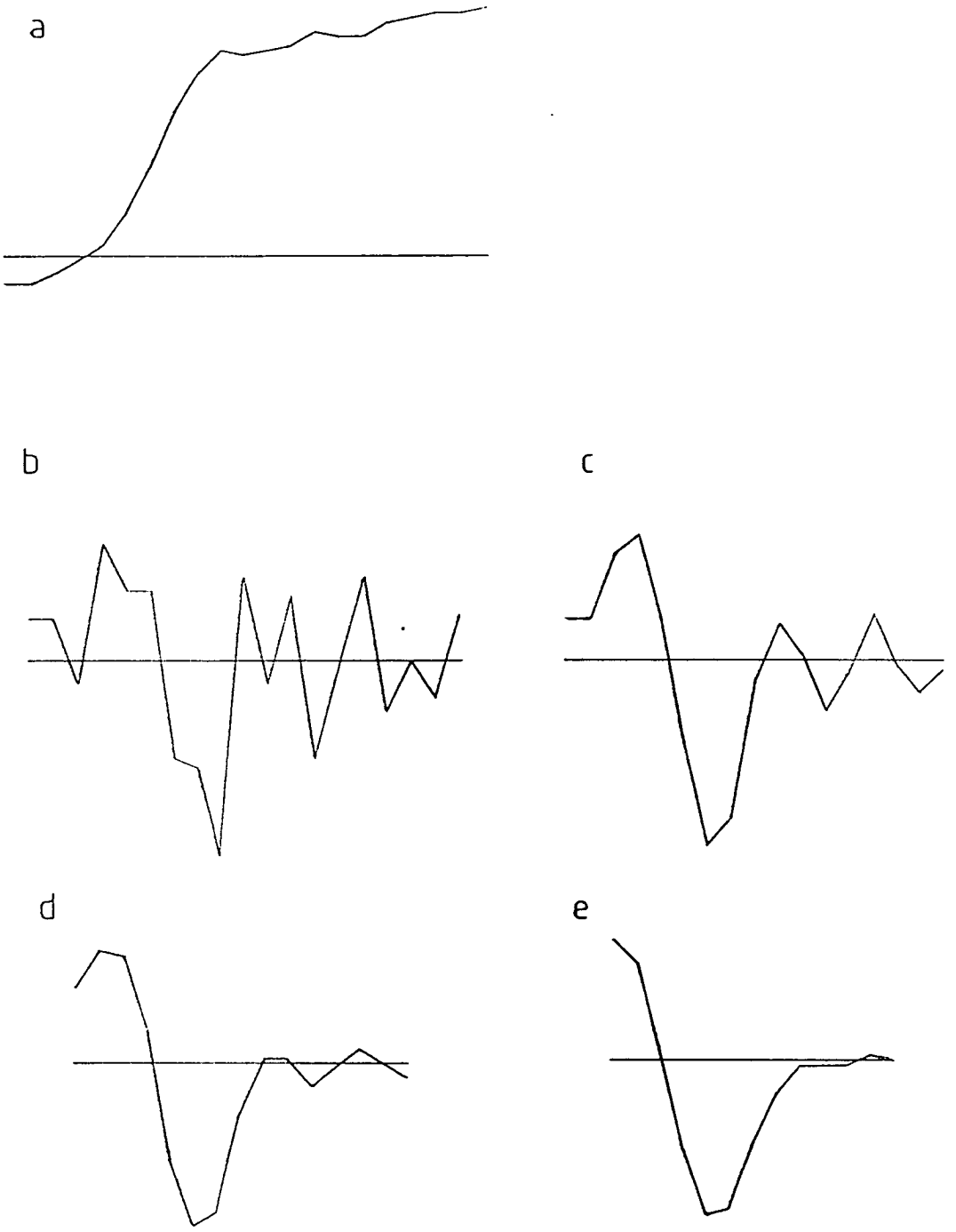

Figure 5.4 Sampled S-curve convolved with double differential operators of various lengths. a. Original curve. b. 3 point operator (1,-2,1). c. 5 points (1,0,-2,0,1). d. 7 points (9,6,-5,-20,-5,6,9). e. 9 points (4,4,1,-4,-10,-4,1,4,4).

Chapter 6

Results

Note. Some of the results in this chapter were previously published in two papers in Scanning[22] [23].

Having arrived at the setup described in the preceding chapters a great many variations on the basic programs were written. In all programs the same method of sampling an S-curve in the shortest possible time, followed by processing using convolution of the sampled data with some operator, was used. But the number of points sampled, the particular operator used, any further stages of processing and the presentation of computed results were varied for different experiments.

6.1 Specimen and Operating Conditions

For all the experimental work the IC was a test specimen consisting of a pattern of aluminium tracks on a plain SiO_2 chip. Two different test layouts were made by the Edinburgh Microfabrication Facility for this purpose. Both are similar in principle - only the geometry varies. Unless otherwise stated S-curves shown were taken from a relatively wide track of 10-20 μm with a primary beam energy of 500V (narrower tracks are difficult to focus on reliably with this microscope at this beam energy).

6.2 First Testing

Figure 6.1*a* shows a typical 21 point S-curve as sampled from a test specimen. By convolving this with a 5 point differential operator - a simple ramp (-2, -1, 0, 1, 2) the curve of figure 6.1*b* is generated. Extending the operator to 9 points gives the curve of figure 6.1*c*. It can be seen that the first curve appears more noisy but that the second lacks some useful detail.

The first differential is not in fact very useful but by using an

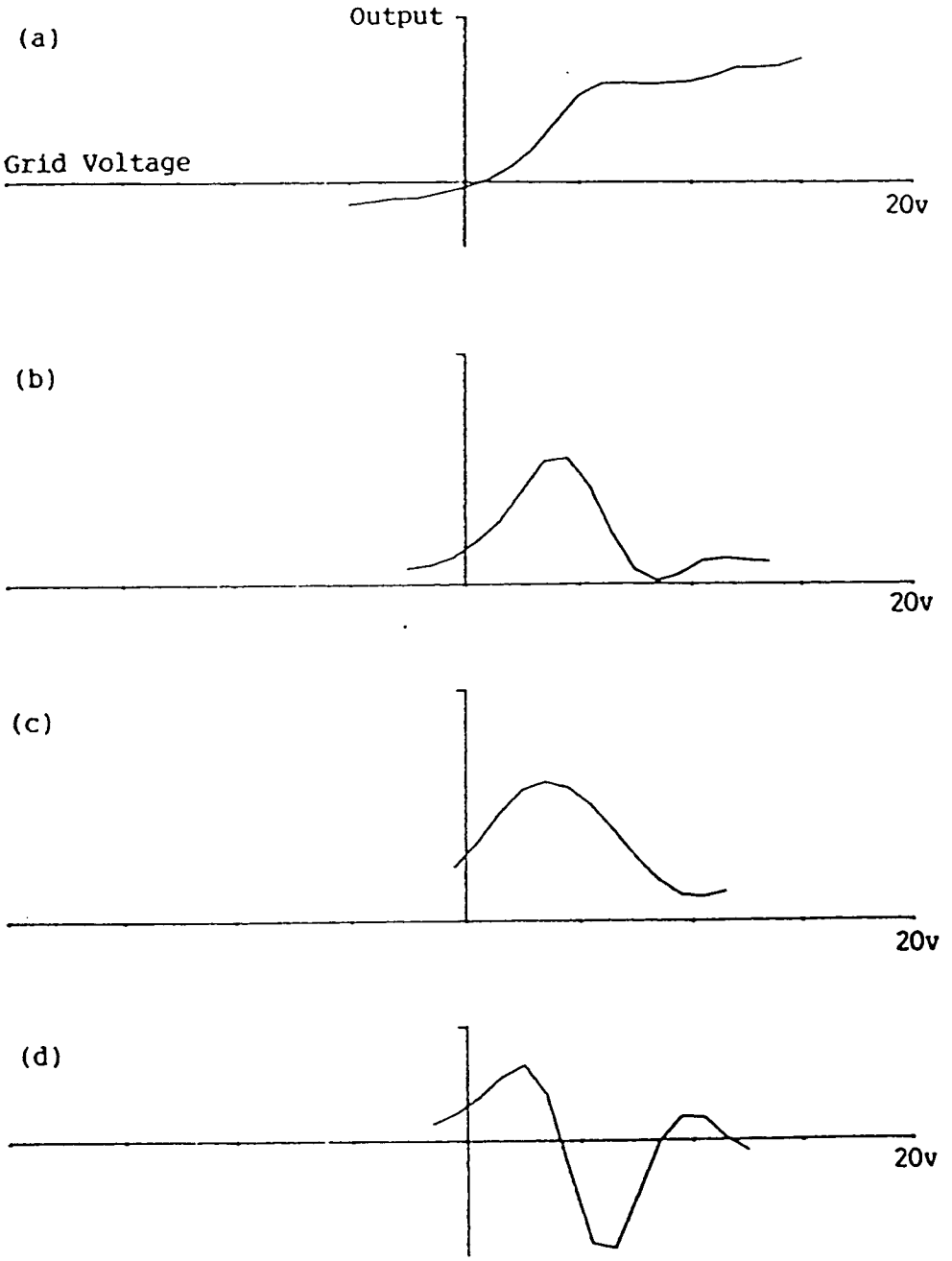

Figure 6.1 a. Sampled S-curve. b. and c. convolved with 5 and 9 point differential operators. d. Convolved with 7 point double differential operator. (Y axis in all curves has been autoscaled by the program).

operator to generate the double differential (simply the first differential operator applied to itself) the curve of figure 6.1*d* was produced - in this case a 7 point operator was used. This curve has a very obvious zero crossing corresponding to the inflection on the original S-curve. It is a simple matter to interpolate the position of this point.

6.3 Linearity Test

To test the linearity of the method a program was written to adjust the specimen voltage then sample and process the S-curve for each value. Figure 6.2 shows a typical output from this program: *a* shows a family of S-curves sampled for track voltages ranging from 0V to 5V in steps of 1V. *b* shows their calculated second derivatives, and the interpolated positions of the zero crossing points plotted against specimen voltage are shown in *c*. The dashed line in this diagram shows the ideal unity gradient response plotted through the first point. These curves were sampled with very little setup time and show that this has great potential as a usable method for voltage measurement.

6.4 Extraction Voltage and Oxide Charging

In the course of previous work it was observed that charging of exposed areas of oxide appeared to be related to extraction voltage and that this could affect the quality of S-curves quite drastically. Studies were carried out to examine the mechanism of oxide charging and its influence on voltage contrast measurements.

6.4.1 Theory

Assuming that the secondary emission co-efficient (the ratio of emitted secondary electrons to absorbed primaries) of SiO_2 is greater than One, when the specimen is scanned there will be a net loss of electrons in the form of secondaries which will be drawn away by the positive extraction electrode and the surface will begin to charge positively. As the surface potential rises the

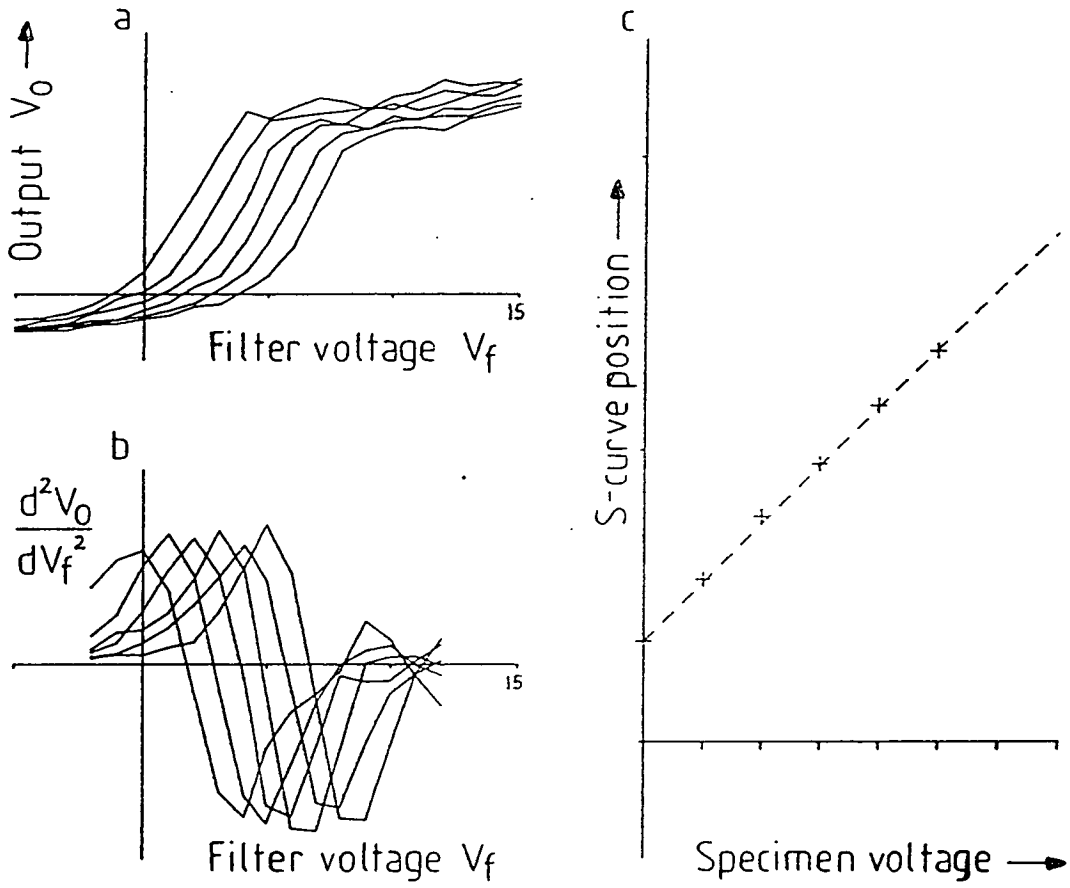

Figure 6.2 Family of S-curves sampled for specimen voltages varying from 0-5V. a. Samples s-curves. b. Their calculated second derivatives. c. The zero crossing points of the curves in b plotted against specimen voltage. The dotted line is the ideal unity gradient.

extraction field will become weaker and secondaries will be more likely to return to the specimen. Eventually equilibrium will be reached when the extraction field is such that the number of secondaries extracted is balanced by the number returning to the surface plus the number of absorbed primaries. As the secondary electrons have an energy of a few eV equilibrium would be expected to occur when the surface is a few volts *above* the extraction electrode. In practice a host of other factors come into play, such as the effect of secondaries created by back-scattered electrons, charge leakage across or into the surface, effects around the edge of the scanned area and of the IC and the influence of any other conductors in the vicinity.

6.4.2 Experimental results

Using a similar program to the one in the previous experiments a series of S-curves were sampled directly from exposed oxide for varying values of extraction voltage - allowing time for equilibrium to be reached before each S-curve was sampled. The specimen used is shown in figure 6.3.

To begin with, a large area of oxide was scanned and readings taken from its centre (region A figure 6.3). The results are shown in figure 6.4 the dashed line being unity gradient as before. The measured oxide potential rises by approx 0.48 Volt per Volt of extraction voltage - shown by the dotted line.

6.4.2.1 Effect of Scanned Area

Reducing the area being scanned first to B and then to C (figure 6.3) produced the results of Figs 6.5 & 6.6 respectively. Here the measured changes in oxide potential with extraction voltage were 0.41 and 0.24 respectively, tending to agree with the above model because as the scanned area is reduced and becomes small compared with the distance to the extraction electrode, so the extraction voltage will become less significant and the voltage of the surrounding (uncharged) oxide will dominate the local field.

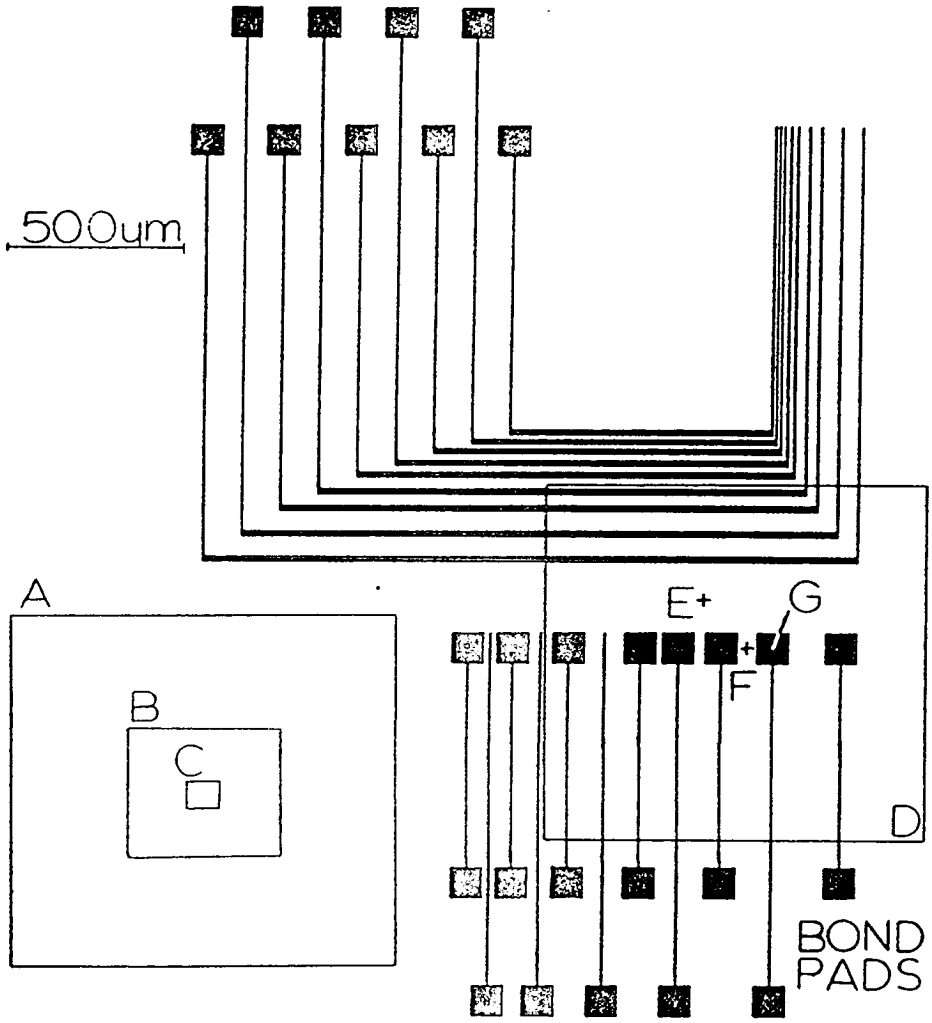

Figure 6.3 Test specimen used in studies of oxide charging.

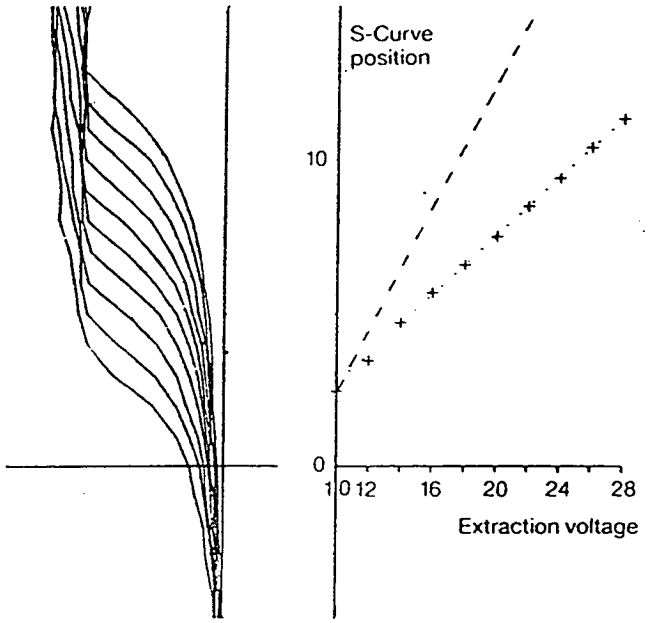

Figure 6.4 Oxide voltage versus extraction potential for central point of region A (fig 6.3).

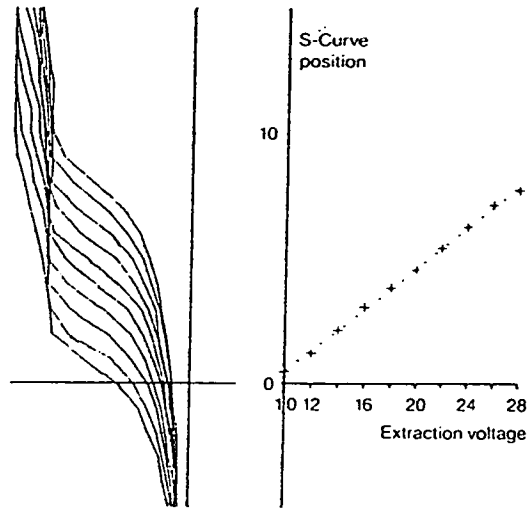

Figure 6.5 Oxide voltage versus extraction potential for centre of region B (fig 6.3).

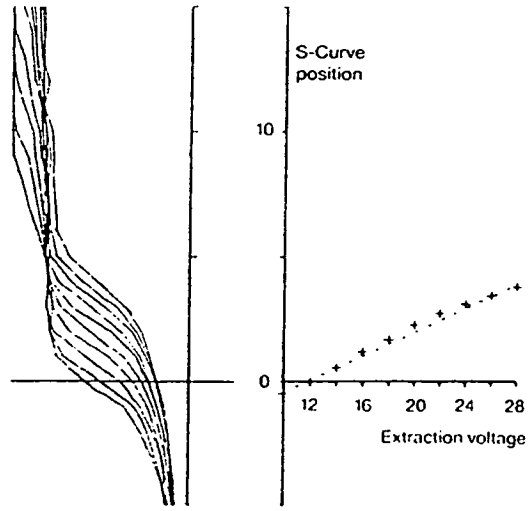

Figure 6.6 Oxide voltage versus extraction potential with scanned area reduced to region C (fig 6.3).

6.4.2.2 Effect of Nearby Conductors on Oxide Charging

The region scanned was now changed to D in figure 6.3 which includes a number of aluminium conductors - all grounded. In this region a series of readings were first taken from point E. Because the apparatus restricts the output swing in one set of readings to 20V these and subsequent results had to be split into a series of three sets of curves. The readings from point E are shown in figure 6.7*a*, *b* and *c* with extraction voltage ranging from 0-20V, 20-40V and 40-60V respectively. The measured S-curve positions are all plotted together in figure 6.7*d* where the gradient is approximately 0.15 after an initially sharp rise. The corresponding graph for point F is shown in figure 6.8 where the gradient has now fallen to 0.06.

These graphs confirm that nearby conductors strongly affect the relationship between extraction voltage and oxide charging and in the case of F where the adjacent conductors are very close the extraction field effect has become quite small. This is what we would expect since as the SiO_2 begins to charge above the voltage on these conductors a strong field attracting secondaries back towards the oxide will form at the surface.

In order to show these measured curve shifts were not simply a spurious phenomenon induced in the energy analyser as a result of changing the extraction grid potential, rather than genuine changes in oxide voltages, a series of curves were sampled from a grounded conductor (point G figure 6.3) for varying extraction voltage. The sampled curves (figure 6.9) show negligible shift but a slight flattening - and consequent loss of resolution - at higher values.

6.4.2.3 Oxide Potential and Voltage Contrast Linearity

Surface fields have a strong effect on the accuracy of voltage contrast measurements and in some cases oxide charging will obviously make a large contribution to these fields. A series of

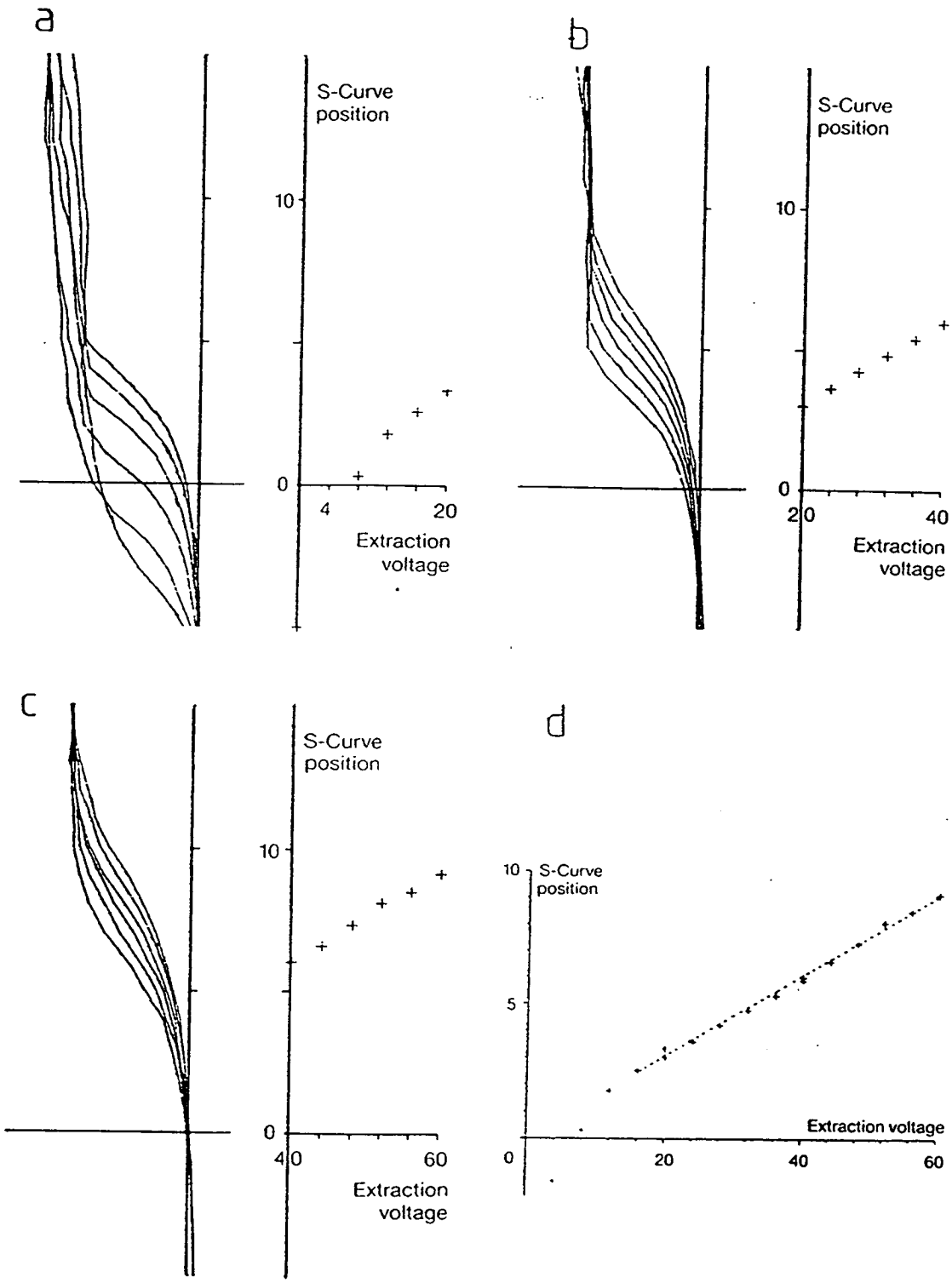

Figure 6.7 Oxide voltage versus extraction potential for point E - region D scanned (fig 6.3) surrounding conductors are grounded. a. b. c. different extraction field ranges. d. Collected results from a. b. c plotted together.

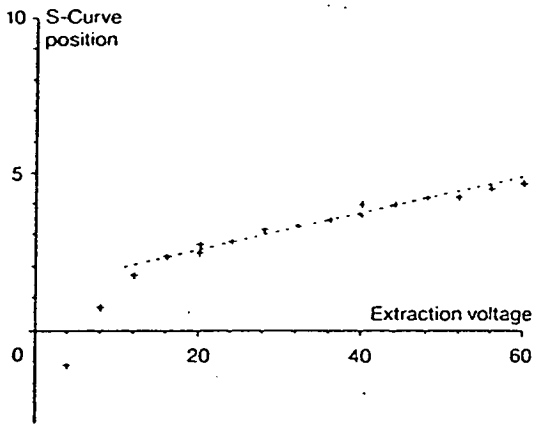

Figure 6.8 Oxide voltage shifts collected for point F. Extraction voltage varying from 4V to 60V in three stages.

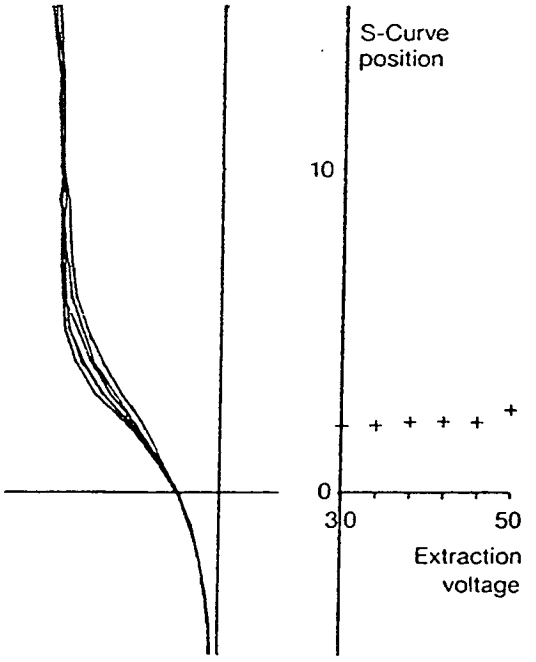

Figure 6.9 S-curve collected from grounded pad G for differing extraction fields.

voltage contrast linearity measurements of the type in section 6.3 were taken from point G (figure 6.3) for a number of different extraction potentials. The results are shown in figure 6.10*a-e*). At lower extraction voltages the measured value tracks the actual voltage well, up to a point at which the S-curve begins to collapse and measured voltage then rises much more slowly. This turning point, or elbow, occurs at a voltage closely related to oxide potential and indicates that as the track becomes more positive than the surrounding oxide a retarding microfield is created which causes the secondary electrons, particularly those with lower energies, to be lost. Examination of the S-curves of figure 6.10*a* shows that there is a clear cutoff energy corresponding to a filter grid voltage of around 6V (shown by dashed line).

6.4.2.4 Estimation of Absolute Value of Oxide Voltage

S-curve shift can only show relative potential and in the case of oxide cannot easily be related to a known value to get an absolute measure. Referring the curves to a conductor can give a guide value but this presumes that the secondary electron energy distribution function is the same for SiO_2 as it is for aluminium. A correction could be made based on the formula given in section 1.3 if the work functions of the two materials are known. An alternative means to arrive at a value is to deduce it from the position of the elbow in the graphs of figure 6.10 which would be expected from the theoretical model to occur at or close to the oxide voltage.

6.4.3 Conclusions

The picture that emerges from these results is of irregular charging of oxide which will tend to charge to an equilibrium voltage determined by local fields - where conductors at the surface are distant this voltage will be greatly influenced by extraction field and can get quite high. Near conducting tracks though the field at the surface will be dominated by the conductor

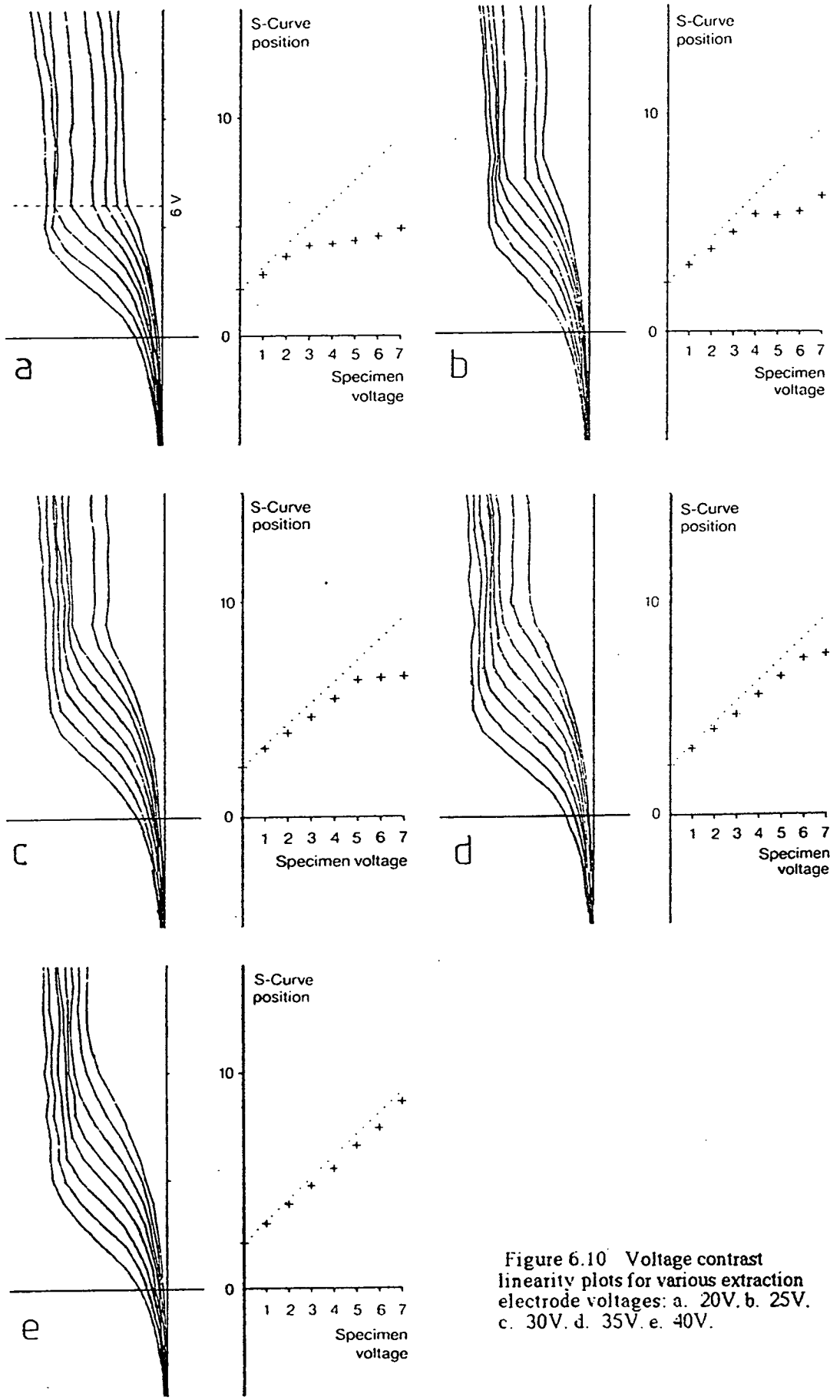

Figure 6.10 Voltage contrast linearity plots for various extraction electrode voltages: a. 20V. b. 25V. c. 30V. d. 35V. e. 40V.

and the oxide will charge to a voltage close to that on the track. This can be observed qualitatively as brightness changes on the oxide near to conductors under normal viewing conditions. Towards the edge of the viewing area un-scanned oxide will have a similar effect. The results shown in figure 6.10 show that low oxide voltages can cause problems with loss of the S-curve. The fact that nearby positive voltages improve extraction when we might expect them to preferentially attract the secondary electrons points to the fact that it is the field at and very close to the surface which is important. This field will always be perpendicular to the surface and, in the case of nearby positive voltages, accelerate electrons away from their emission point. Once clear of the surface the extraction voltage is more effective in attracting them into the spectrometer. The conclusion is that extraction voltage should be high enough to prevent loss of the S-curve but otherwise kept as low as possible to prevent high and sharply varying charging voltages which cause strong local fields. These fields extend beneath the surface and can easily affect circuit operation.

A further point to note is that when tracks are closer together these will dominate the microfields in a manner similar to the oxide voltage in these studies and the voltage on these tracks cannot be controlled by changing the extraction electrode.

In general attempts to make voltage measurements from a point in close proximity to more negative voltages is liable to run into the sort of S-curve collapse shown in figure 6.10.

Chapter 7

Conclusions, New Developments and Suggestions for Further Research

Any e-beam testing system to be used in routinely and extensively for diagnosis of ICs will need to have a much simpler and more robust user interface than those currently available, in order to achieve a reasonable throughput and repeatability of results. The research detailed here has gone a long way towards answering a number of aspects of this problem - however further work needs to be done in some of the areas covered whilst in others work elsewhere has superseded or obviated the need for the apparatus constructed here. Later in this chapter is a summary of some of the progress made in relevant fields since this project was carried out, and then some pointers to areas needing further study arising from this thesis.

7.1 Conclusions

7.1.1 Spectrometer

At the heart of any e-beam testing system is the secondary electron energy analyser. The spectrometer of chapter 3 has proved better than anything else I have tried of its kind in terms of ease of use in real situations. Its novelty lies not in its principle of operation, which is the same as many others, but in the engineering of its construction. It introduces no noticeable astigmatism, produces clean S-curves and its construction is extremely cheap and simple - a new one can be made in a couple of hours work - and would lend itself to common industrial construction processes. Its drawbacks are a slightly longer working distance than some other models and in common with all purely electrostatic high pass energy analysers, it is sensitive to local microfields at the surface of the specimen.

7.1.2 Control Electronics and Computer

A large effort was put into circuitry for computer control of the e-beam tester which was necessary for the rest of the project. Much of the resulting circuitry has been duplicated elsewhere, in outward effect if not in detail and with increasing use of digital microelectronics many SEMs are now controlled by central microprocessors. However for serious voltage contrast use it is imperative that these computers either be programmable directly to implement appropriate algorithms, or have some sort of remote control interface to allow a separate voltage contrast computer to operate the microscope functions. In particular control of the scan generator is vital.

In the detail of the scanning system developed some novel methods were used and the scan amplifiers in particular are far superior to those found in many commercial microscopes, especially when the improvements suggested in section 4.1.3.6 are taken into account. The scan generator is not such a success as it was never made completely glitch free and, as section 4.1.1.15 suggests, its hardware could have been considerably simpler. The great strength of the scan generator is its remote control interface which allows rapid practical control over all scanning functions from the voltage contrast computer using very simple program statements. This was certainly not available elsewhere at the time it was built and - so far as I know is still not.

7.1.3 Summary

The effectiveness of the integrated system is clearly shown by its use in generating the results of chapter 6 which represent only a very short time actually operating the apparatus. The principal reason for this improvement is the computer control of the scan generator and analyser and the good performance of the latter. S-curve sampling is a simple "point and shoot" operation taking a fraction of a second, during which time drift due to charging changes and contamination are insignificant. It also allows

readings to be taken from a large number of points very easily.

7.2 New Developments

Since the work described in this thesis was done a number of relevant developments have occurred in the field. Several companies are now producing e-beam testers which are purpose built from scratch and optimised for the conditions necessary for voltage contrast, in particular for stable high beam currents with high resolution at very low beam energies[24]. They also have energy analysers and beam chopping built into them and other features such as specimen chambers designed to take wafer probers and many high frequency electrical connections.

The results in section 6.4.2.3 show that microfields at the specimen surface can play havoc with voltage contrast readings. Even though extraction voltage can be used to control oxide charging it is impossible on a real device to control the voltages on adjacent conductors reliably and these will have a similar effect in creating local fields which may be beneficial or obstructive. This is widely acknowledged to be the biggest problem with conventional electrostatic spectrometers and most research in this field is now concentrating on energy analysers using both magnetic and electrostatic fields to improve the performance. Many of these designs also place the spectrometer above or within the final lens, guiding the secondaries back through the lens to reach it. These designs show some success in reducing microfield effects and in doing so also reduce errors caused by secondary electrons passing through the spectrometer at an angle to the ideal normal. Through lens analysers can also help reduce the working distance and so improve resolution. No device yet proposed though can eliminate microfield effects entirely.

K Nakamae et al[25] distinguish between two effects of microfields: The first MFE1 is caused when secondary electrons cannot overcome local retarding fields and never reach the detector. The second effect MFE2 is caused by secondaries which

are affected by microfields but detected nevertheless, causing errors in the S-curve measurement. The results in section 6.4 display MFE1 clearly but show little sign of MFE2. In all the cases described however the local fields are roughly symmetrical either side of the point of measurement. Transverse and asymmetrical microfields would be expected to cause much stronger MFE2.

7.3 Suggestions for Further Research

7.3.1 Improvements to Signal Processing Algorithm

This system has shown that digital analysis of sampled S-curves can calculate voltage shift quickly and accurately. The algorithm used was arrived at empirically and gives results quickly and reliably. No statistical analysis was done to analyse the accuracy or to optimise this algorithm and as the results of figure 6.10 show, if conditions are wrong the S-curve can collapse rendering the readings virtually meaningless. Examination of these graphs shows that although the S-curve changes shape drastically in these conditions, the point at the lower end of the curve where the output just begins to rise appears to be much less influenced by local fields. This region corresponds to the higher energy electrons which are more likely to escape from adverse microfields. By more detailed mathematical analysis it should be possible to derive and optimise an algorithm, possibly using correlation or regression, which detects the position of this turn rather than of the point of inflection. Although more recent analysers have improved immunity to microfields they still suffer from them so the same or a very similar algorithm would still apply.

7.3.2 A Proposal for a New Computer Based Electron Beam Tester

The e-beam tester described has shown the strength of a system in which disruption to uniform scanning is minimised. Taking this to its logical conclusion we would arrive at the situation where scanning is not interrupted at all and the sample is taken as the beam passes through the point of interest. This is

precisely what is happening, on a massive scale, when the microscope image is captured in a digital frame store - which is a very common component of more modern SEMs and e-beam testers. Furthermore framestores usually include some sort of averaging scheme to improve picture quality, which would be ideal for noise reduction of sampled data.

I propose a system in which the electron detector output is fed straight into a framestore. The main computer would have direct access to the stored image, sufficient memory to hold several images at once and the ability to transfer images to and from some bulk storage device such as a Winchester disc (this means a lot of memory but memory is already very cheap and continually falling in price). Under control of the computer a series of suitably noise reduced pictures would be acquired and saved for a number of different filter grid voltages. Once this process has been completed (at 128 frames averaged per image and 20 images this would take under a minute) the voltage information for any point in the field of view could be deduced with no further reference to the microscope!

7.3.2.1 Theoretical Discussion

Gopinath[26] has related the voltage resolution of a voltage contrast system with a given bandwidth Δf to beam current with the formula:

$$\Delta\phi_s^2 = K^2\frac{\Delta f}{I_b}$$

Where $\Delta\phi_s$ is the smallest detectable change in surface potential and K is a constant for the detector. The theoretical value of K for a retarding field analyser has been calculated[27] and using these equations recent work by Khursheed[28] has derived an expression for the number of electrons N_p needed to make a measurement at any given resolution σ_v:

$$N_p = \frac{K^2}{2e\,\sigma_v^2}$$

Where e is the charge on an electron. The value of K depends on the operating conditions and the secondary emission characteristics of the specimen but Khursheed has derived a minimum value for $K^2/2e$ of 32 at optimum conditions. This implies that for a resolution of 0.1V not less than 3200 electrons would be required. In practice the experimental value of K is found to be several times higher than that derived theoretically, and conditions are unlikely to be optimised for this alone. Taking this into account a figure of 10^5 electrons would be more appropriate and the minimum sampling time is then:

$$\frac{10^5 e}{I_b}$$

For a typical beam current of 1nA[29] [30] this gives a sampling time of 1.6×10^{-5} s.

In a framestore with a horizontal resolution of 768 pixels and an active line time of 50μs one pixel time is 65ns so around 250 samples would be required. This represents 10 seconds with an interlaced TV scan with a full frame time of 40ms. Bearing in mind that in this time data are collected for nearly 400,000 points 10s is fast. In fact, of course there is a great deal of redundancy involved since in many places adjacent points will be on the same conductor and at the same potential, or on oxide and not normally useful at all. Furthermore this assumes that the sampling gate is open for the full pixel time.

The high spatial redundancy could be used to reduce collection time further by summing samples from all pixels close to the point of interest which are known to be on the same conductor. This process need not be carried out in real time.

A typical system might operate by sampling 16 images with each image being integrated over 16 frames. This is well within the capabilities of many framestores and the number of frames could easily be increased by a factor of 4 or 8.

Consideration of the possibilities of such a system brings other features to light:

7.3.2.2 Optimisation

By proper analysis of the S-curve detection algorithm such things as length of convolution operator, image averaging time and number of images stored could be optimised with respect to memory requirements or acquisition time.

7.3.2.3 Microfield Compensation

Not only could the advanced algorithm proposed in section 7.3.1 be used to improve immunity to microfields but, since values for all surrounding potentials would also be available, the microfields themselves could be deduced and compensated for! Using this technique, which might require a series of iterations akin to relaxation of networks, the set of images for one sweep of the filter grid could be reduced to a single voltage map image which would greatly reduce storage problems. For full compensation much more detailed mathematical modelling of the precise effects of microfields would need to be undertaken.

7.3.2.4 Image Processing

Further image processing techniques could then be used to derive or display all sorts of information, for example by plotting equipotentials, highlighting intermediate "illegal" logic states in logic circuits, or comparison with known good devices, automatic detection of broken tracks (with abrupt potential changes along their lengths) etc, etc.

7.3.2.5 Window Scanning

A technique known as window scanning is sometimes used to prevent damage caused by the e-beam to sensitive areas on the IC (such as exposed gate oxide). This works by blanking the beam as the scan crosses the protected area[31]. Many commercial framestores incorporate graphic overlay planes to allow text and/or graphics to be superimposed on the stored image at the

same resolution. By simply connecting one bitplane of this overlay to the blanking circuitry, window scanning would be a trivial matter.

7.3.2.6 User Interface

Use of text and graphics overlays would also allow the user interface to be suited to the occasional or non expert user. For example the cursor, generated by hardware with great effort in my system would simply become a software generated cross in the graphic plane. Instructions, menus and diagrams could all be superimposed on the the image at will.

7.3.2.7 AC Measurements

All the techniques so far described have been for DC static voltage contrast, for AC measurements stroboscopy and sampling are used (see section 1.3.2). The frame store based system could be used in stroboscopy in two different ways: If the signal on the IC is asynchronous to the frame scan frequency, then by chopping the beam and averaging the picture over a long period a stroboscopic picture will be built up for a single point in the specimen's cycle. This is the same as conventional stroboscopy with the addition of noise reduction through picture averaging, and with sufficient time a series of images for differing filter values can be captured and processed as before. If, on the other hand, the specimen signal is synchronised with the video scan then, without chopping the beam at all, different phases will appear at fixed locations across or down the image. By changing the phase relationship between signal and scan it would be possible in theory to sample sufficient images to reconstruct all phase steps at all points on the image. To do this fully this might be prohibitive in memory costs but in many cases nothing like this amount of information is required. This second method is elegant in that the beam is on all the time so there is no time overhead due to the low duty cycle when chopping the beam, but it is limited in the range of

signals which could be examined. The difference between adjacent pixels in a typical digitised TV picture is around 80ns so the maximum frequency which could be examined by this method would be less than 6 MHz. High scan rate framestores could improve the situation slightly but they are expensive and non standard.

7.4 Work with Digital Equipment Corporation

After completion of this project a step was taken along the lines discussed in the last section in collaboration with Digital Equipment Ltd, Ayr (DEC). They have a semi-dedicated e-beam testing system made by Cambridge Instruments which incorporates a frame store as well as an energy analyser, beam chopping hardware and computer control. An interface was built which allows full frame images to be transferred in both directions between the frame store and a powerful computer graphics workstation. The interface is a direct memory access link which can transmit a complete picture in under a second. The computer is a MicroVAX workstation, a powerful mini/micro computer with special graphics facilities for which high quality image processing software is available. This computer would be ideally suited to the kind of tasks described above. The e-beam tester is itself fully computer controlled and the frame store contains yet another microprocessor. Unfortunately these two dedicated microprocessors are not readily programmable or remotely controllable and Cambridge Instruments did not wish to co-operate with development of the link to the VAX. It is unlikely that would allow access to their programs. However the VAX/e-beam testing system as set up is now routinely used for capture, display and manipulation of images from the SEM[32].

Appendix 1

The GPIB

A1.1 Overview

The GPIB (General purpose interface bus) was conceived by Hewlett-Packard (as the HPIB or Hewlett-Packard Interface Bus) as a rapid and flexible means for interconnecting instruments and control computers over short distances such as in a typical laboratory. The original specification was then adopted with minor alterations as the IEEE488 standard in 1975 and revised in 1978.

A1.2 Physical Medium

Physically the bus consists of 24 conductors carrying 8 data and 8 control signals, the remaining 8 wires being signal grounds and shielding. The standard allows up to 16 devices to be connected to the bus at one time and provides a complex protocol for exchanging data between devices. Each device (instrument) on the bus is assigned a 5 bit binary address, usually by means of switches near the GPIB connector. So although there are only 16 physical devices allowed, up to 31 logical device addresses are possible (the 32nd is reserved for special functions). Connection is by means of cables with special connectors consisting of a plug and socket back to back so that two or more cables may be stacked together at one device. There is no restriction on the topology of the network - which can be in a "daisy chain" or "star" connection or a combination of the two - except that the total length of cable must be less than 20m. Figure A1.1 shows the outline of a GPIB connector and the signals carried.

The active signals that make up the bus are 8 data, 3 handshake, and 5 control lines.

The 8 data lines DIO1 to DIO8 not only carry data between devices but are used in the control protocol to carry command and address information

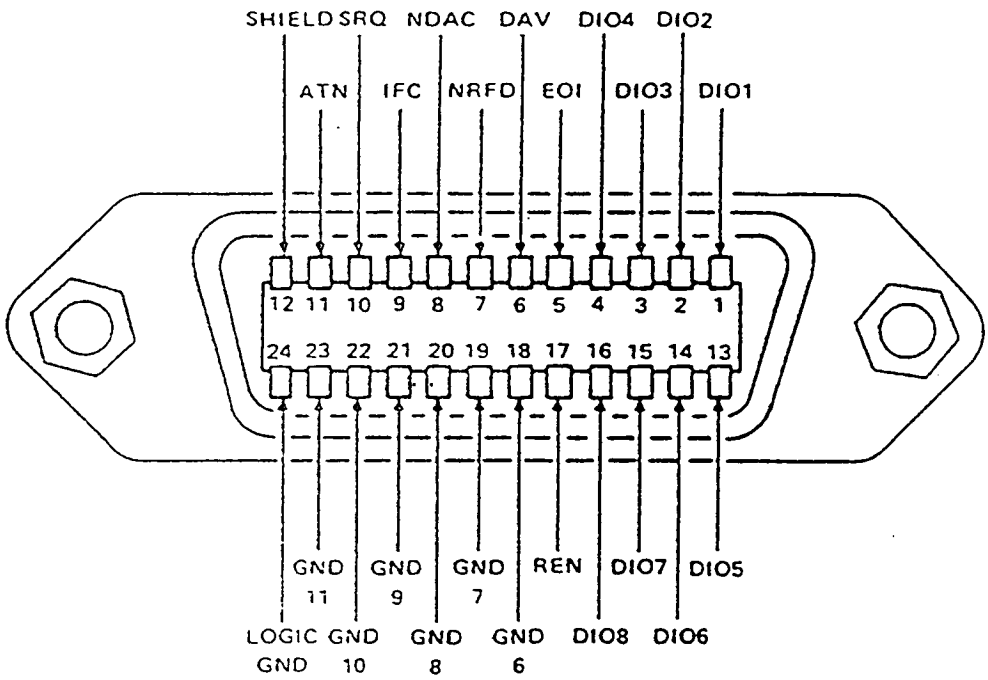

Figure A1.1 The GPIB interface connector outline and connections.

3 Handshake lines are DAV (data valid), NRFD (not ready for data) and NDAC (not data accepted). These are used to control the transfer of bytes of data on the DIO lines. By using three wires instead of the more usual two it is possible to transfer data asynchronously between one transmitter (the Talker) and any number of receivers (the Listeners) simultaneously. By using "wired or" logic, only when all active listeners are ready does NRFD go false allowing the talker to put the data on the bus and assert DAV. Again all listeners must remove NDAC before the cycle can begin again, so transfer progresses at the rate of the slowest active listener at any moment. This handshake allows broadcasting of commands and addresses (and data if so desired) to several or all devices at once.

The remaining 5 signals are additional control lines. ATN (attention) is driven by the controlling device to distinguish between command/address and data transfer operation. SRQ (service request) can be asserted by any device requiring some kind of service. IFC (interface clear) is used to reset the bus hardware (but not the devices connected to it). EOI (end or identify) is a dual purpose signal used to mark the end of a string of data bytes when passing data, and as a rapid status poll of up to 8 devices in parallel. Finally REN (remote enable) is used in switching instruments between remote control via the GPIB and local (front panel) operation.

A1.3 Logical Operation

The specification of the GPIB defines a very complex set of commands and operations in terms of messages and state diagrams. Connections can range from simple connection of one talker and one listener to a network with full bus control passing between several of the devices on it. Data can be transferred between a talker and several listeners with a completely separate controller. Instruments on the bus may interrupt the controller via the service request facility. A number of control messages are defined

including ones for triggering devices, polling device status in two ways, locking out local controls, clearing devices, passing control between devices etc etc. As well as the primary addresses mentioned above any device can have a number of secondary addresses which might typically relate to different functions within one instrument.

As can be seen the GPIB is a very powerful means of interconnecting instruments and at full speed (up to 1Mbyte/second) can transfer large quantities of information very quickly. It's difficulties arise partly because of it's flexibility and because although the hardware and basic transfer protocols are rigorously defined, the format of the data transferred and its meaning, together with the subset of the bus commands implemented within individual instruments, are entirely up to the instrument designers. This is partly inevitable in any interface which sets out to connect together anything from waveform analysers to power supplies to scanning electron microscopes; it does mean though that any software written for controlling a GPIB device will be completely device dependent - a program to control one oscilloscope will probably be meaningless with another.

Appendix 2

The UCSD p-System

A2.1 Description

Initially developed at the University of California, San Diego - hence the name - the UCSD p-System is an operating system for mini and micro-computers. The major aim in developing the operating system was complete portability of object code between different machines. To achieve this a theoretical computer architecture - the p-machine (for pseudo machine) was defined and all programs are compiled to produce code for this machine (p-code). To run programs on a particular computer a p-machine emulator must be written in the native code of the target processor. Once this p-code interpreter is available the operating system - which is entirely in p-code can be loaded and any programs which are also in p-code may be run.

The only other native machine code element of the system is the section which handles input and output. To facilitate writing of the I/O section a set of standardized subroutine calls is defined for each device which are accessed by the operating syatem via a table. The very low level device drivers are further organised into the SBIOS - for Simplified Basic Input/Output Subsystem - and generally to adapt the operating system to a particular target machine this is the only code which must be rewritten (as p-code interpreters are readily available for most common processors).

The p-System is written almost entirely in Pascal with a set of extensions to improve such things as I/O, string handling and low level machine access for system functions. UCSD Pascal also includes extensions to allow separate compilation of program modules - the greatest weakness of standard Pascal.

The operating system comes with a Pascal compiler, text editor and assembler for the host machine as well as a number of utility programs.

Appendix 3

The Digital Scan Generator

A3.1 Introduction

The unit consists of a main digital board, two D to A converter boards, a video processor board and a front panel together with a remote cursor control box, all mounted in a 19 inch card frame with a power supply. An optional scan rotation unit was constructed by a third year student project group which plugs in to the same rack.

The scan generator is controlled by a 6809 microprocessor which implements both front panel and remote control functions. Remote control is via an IEEE 488 interface bus (GPIB) and allows control of all front panel functions as well as various additional operations.

A3.2 Hardware

A3.2.1 Main Board

The main board is a double height, extended Eurocard which is mounted horizontally in the rack. It is a wire-wrapped board which contains virtually all the digital electronics - mostly consisting of low-power shottky TTL ICs (LS TTL) - and all the microprocessor functions The circuit is shown in figs A3.1 to A3.4.

Figure A3.1 shows the timing circuitry: a 10.25 MHz oscillator feeds a programmable clock divider to generate a pixel rate clock. The same oscillator drives a Ferranti sync pulse generator IC which generates the necessary line and frame signals for TV rate operation.

The X and Y (line and frame) scans are generated by two 12 bit counters shown in figure A3.2. The amount by which these counters increment at each clock may be varied from 0 to 15 to give a variable number of pixels per line and lines per frame. The counters may also be cleared to ensure flyback to zero, or loaded

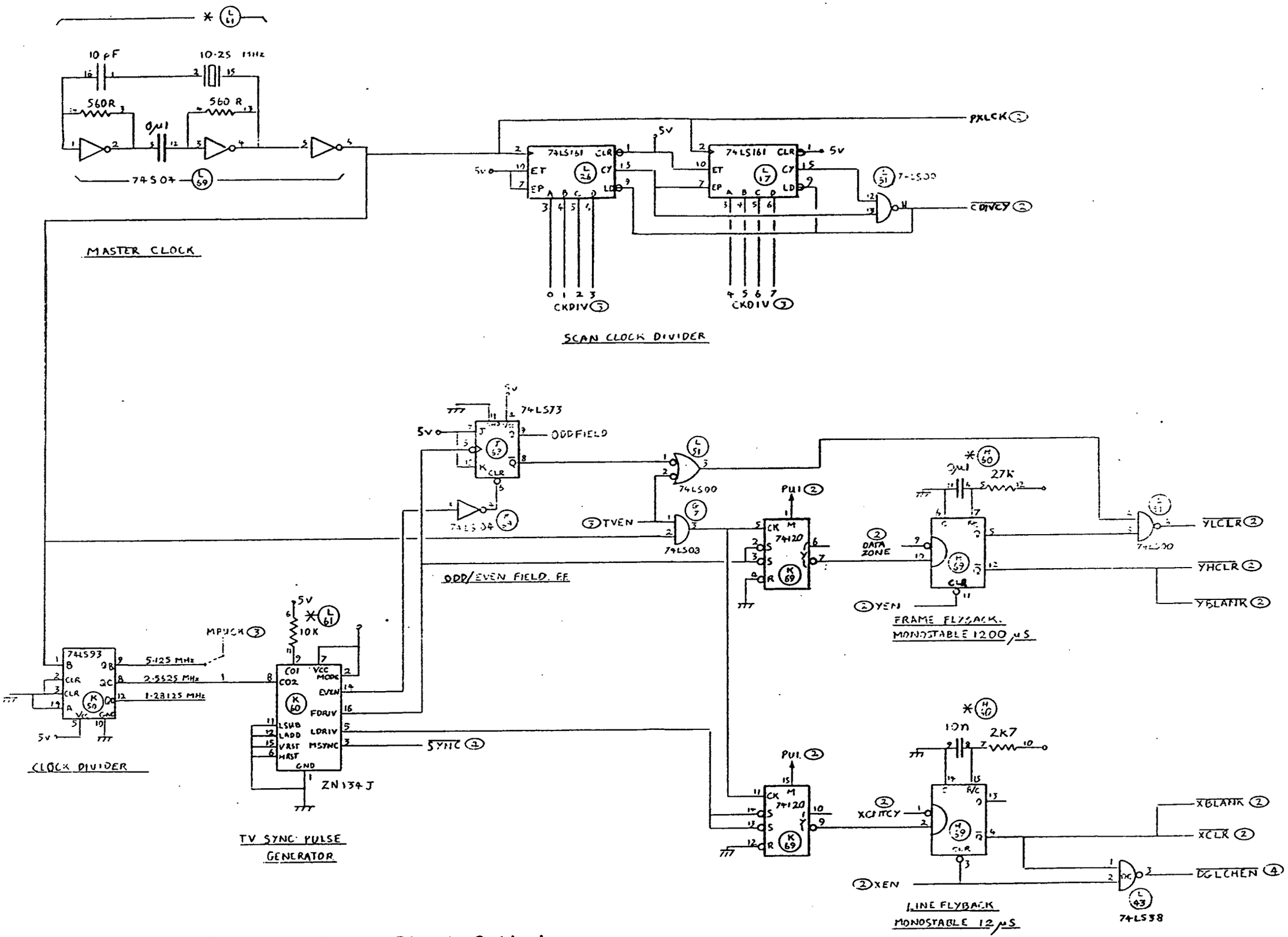

Figure A3.1 Clock & timing

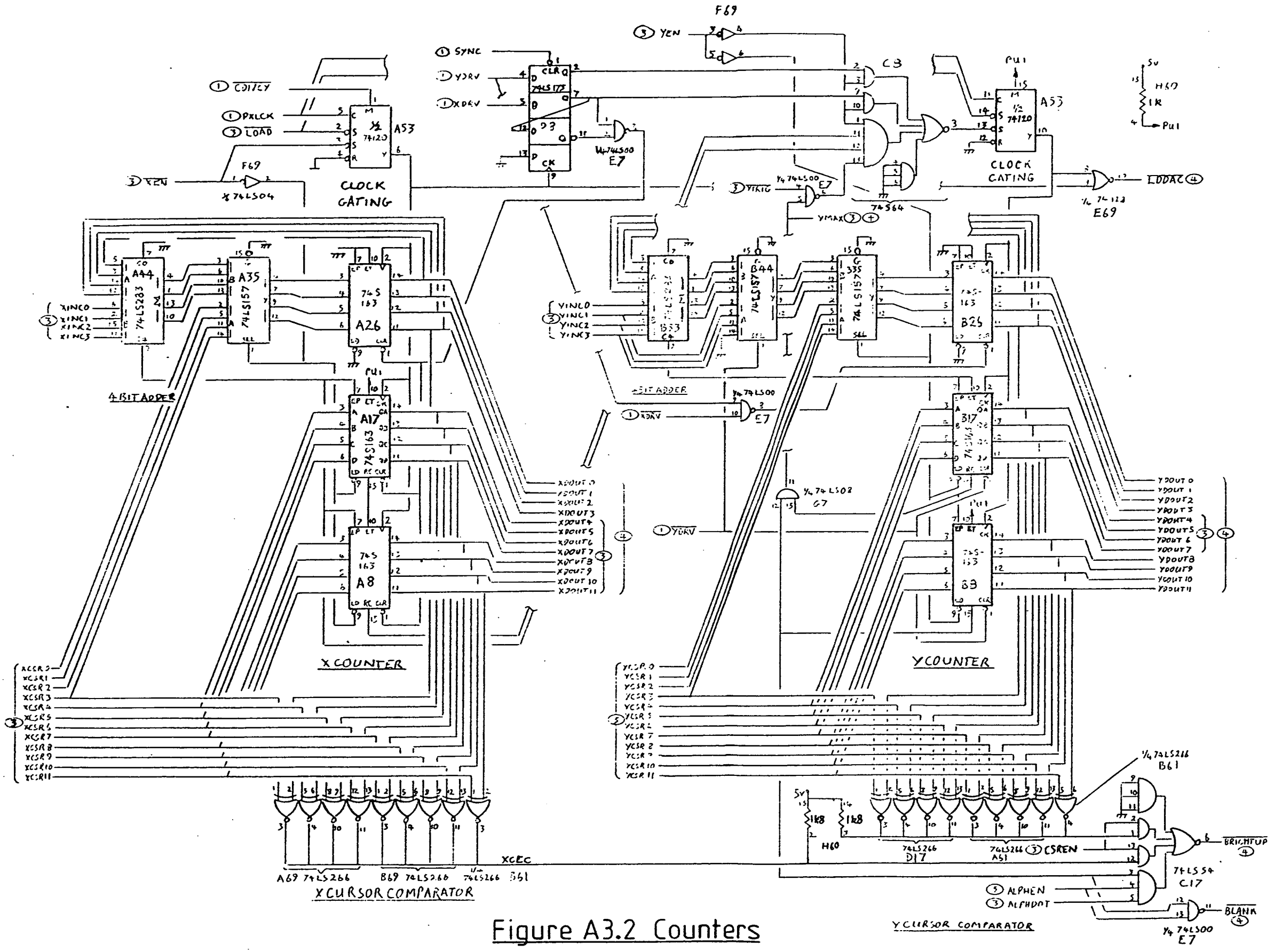

Figure A3.2 Counters

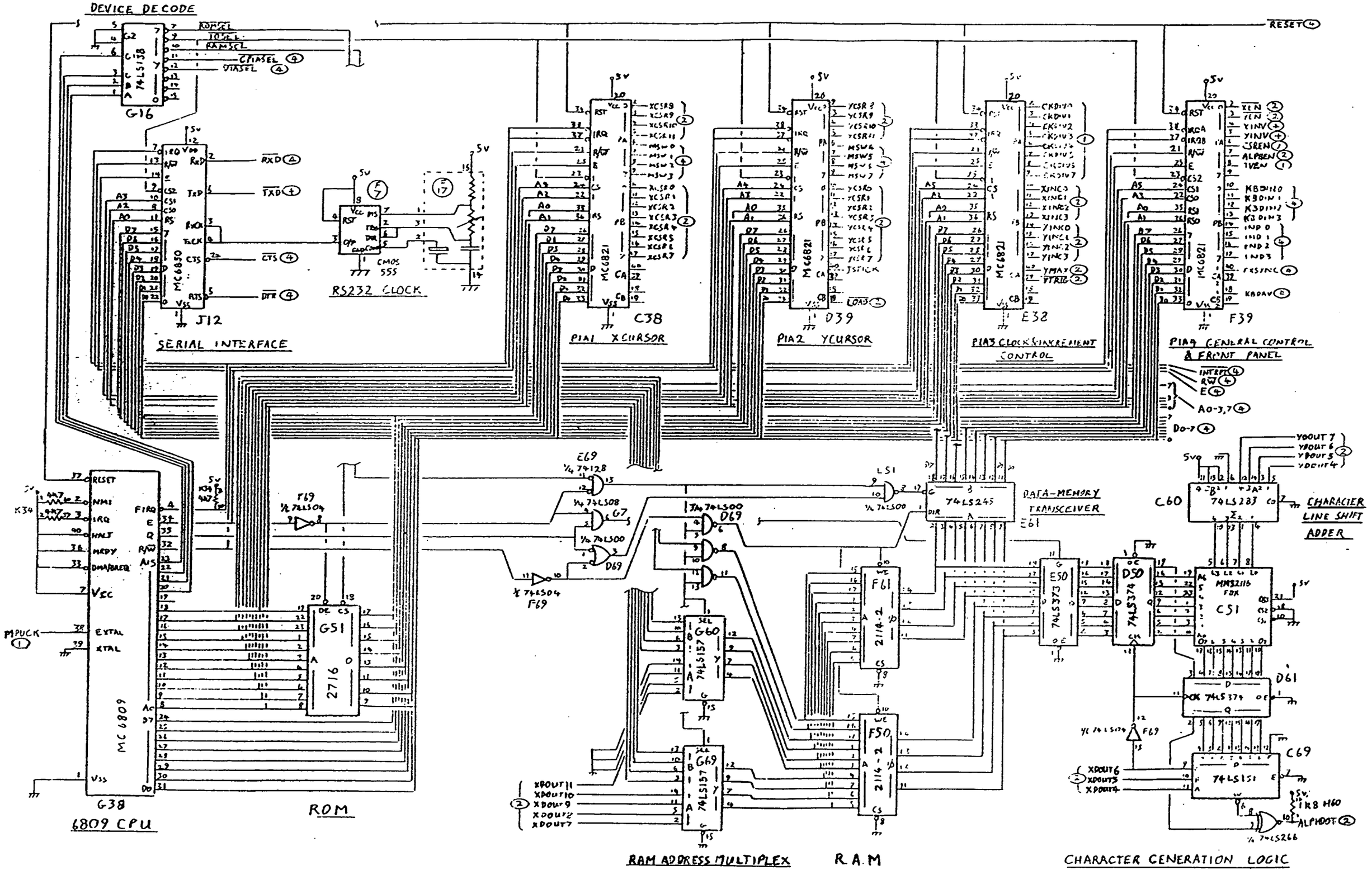

Figure A3.3 Microprocessor

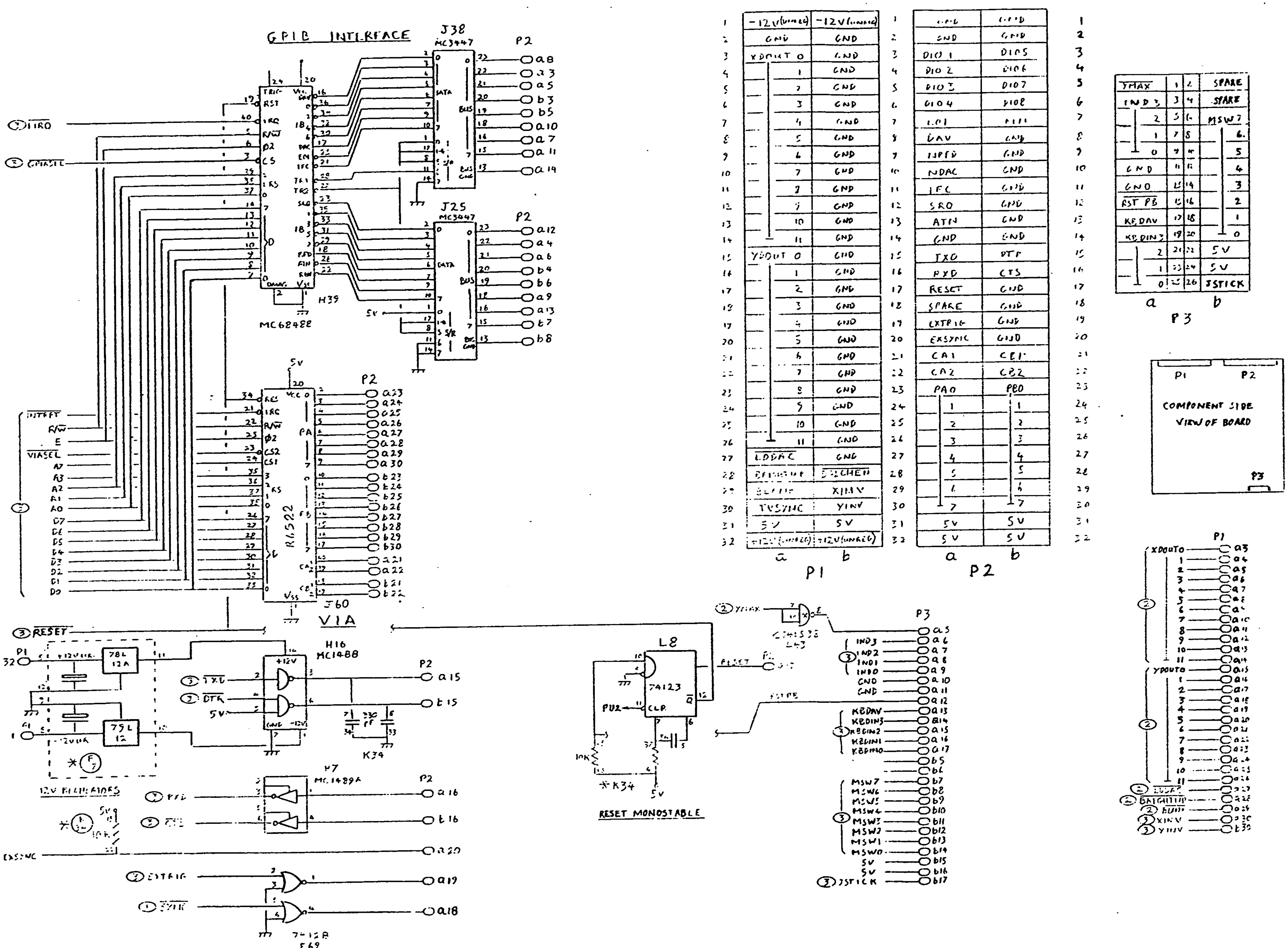

Figure A3.4 GPIB & Connectors

with a preset value (cursor) to allow position control in spot and line modes. The digital count values are compared (most significant 9 bits only) with the cursor value to produce a pulse as the scan passes through the cursor value, which is used to generate the crosswires on the display. To allow full 625 line interlacing in TV mode the high order 8 bits of the Y counter may be reset independently of the low order bits and an additional data selector loads a value of the normal Y increment at this time.

The 6809 microprocessor together with its circuitry is shown in figure A3.3. Four PIA (peripheral interface adaptor) ICs provide the necessary general purpose signals to provide the 12 bit X and Y cursors, the main clock divider control and the X and Y count increments. These are also used to interface to the local control panel providing 4 key-panel data lines, 4 led indicator control lines and 8 mode inputs from switches on the front panel; and a number of signals which control the scanning mode (record, line, spot etc). A serial (RS 232) interface is provided using a MC6850 ACIA (asynchronous communications adaptor) IC, however there is currently no support for this in the software.

The software for the microprocessor is stored in a 2716 (2 Kbyte) EPROM. RAM is provided by two 2114 static ram ICs which also provide the character data for the alphanumeric display zone at the bottom of the screen which is implemented by interleaving accesses to the first 32 bytes of memory for data display with microprocessor accesses. A character generator ROM is used to produce the character matrices from the ASCII information stored.

Fig A3.4 shows the GPIB interface which is a standard implementation, and the 6522 VIA (versatile interface adaptor) IC. The VIA provides a remote data bus for control of expansion cards and two timers which are used by the firmware.

A3.2.2 Digital to Analogue Converter Boards

The two D to A boards (one for X and one for Y) are more or less the same however additional circuitry was necessary to

provide some de-glitching of the X ramp (figure A3.5). The digital input can be negated (inverted) by logic on the board to invert the analogue scan to suit different microscopes, a register is then loaded with the modified data by the LDDAC signal, and the output of the register is fed directly into a high speed DAC whose analogue current output is converted to the necessary voltage signal by a fast OP AMP with a high power emitter follower buffer stage. De-glitching is achieved on the X output by using a slew rate limiting circuit during the ramp. The circuit is switched out during flyback and when spot mode is selected.

A3.2.3 Video Processing

The video processor board contains a video buffer amplifier with various gating inputs to provide bright up and blanking functions (figure A3.6). However on the S100 SEM this is not used as the brightup, blanking and TV sync signals are fed via a ribbon cable to appropriate points in the video chain in the microscope circuitry.

A3.2.4 Front Panel

The front panel PCB (figure A3.7) contains a CMOS keyboard controller IC controlling 16 keys, a one-of-16 decoder driving 11 LED indicators, an 8 bit "chip switch" and a reset push button. The PCB is mounted behind the aluminium front plate so that the chip switch is concealed behind a small aluminium cover and the reset push button is behind a small hole to prevent accidental reset. A BNC socket on the front plate is also provided for connection to the remote cursor control box.

A3.2.5 Remote Cursor Controller

The position of the cursor, or of the spot in spot mode, is controlled by a box with X and Y control knobs, connected by a single co-axial cable to the front panel. The circuit (figure A3.8) provides a rectangular waveform from a low power CMOS (555

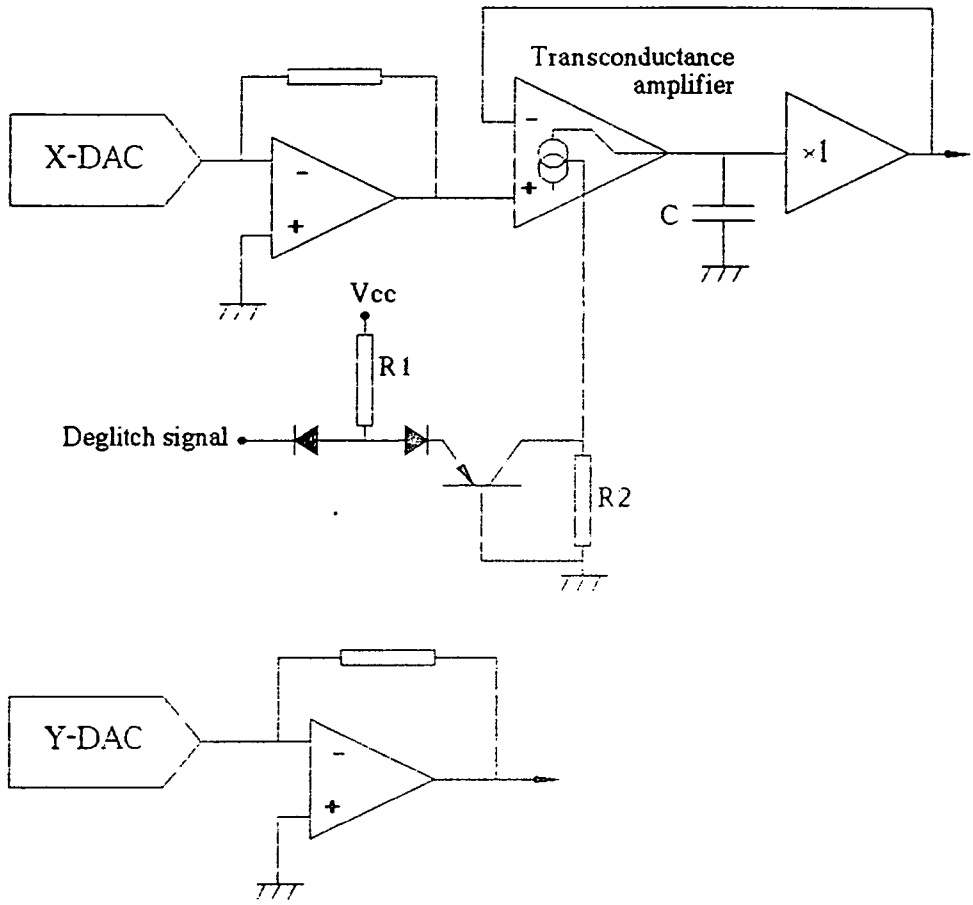

Figure A3.5 Scan ramp D to A converters - The buffer for the X (line scan) converter includes a slew rate limiting circuit: When the deglitch input is low the bias current to the transconductance amplifier is set by R2 only and slew rate is limited by the rate at which this current can charge the capacitor C. When deglitch input is high a much larger bias current flows through R1 and the transistor, so increasing the slew rate.

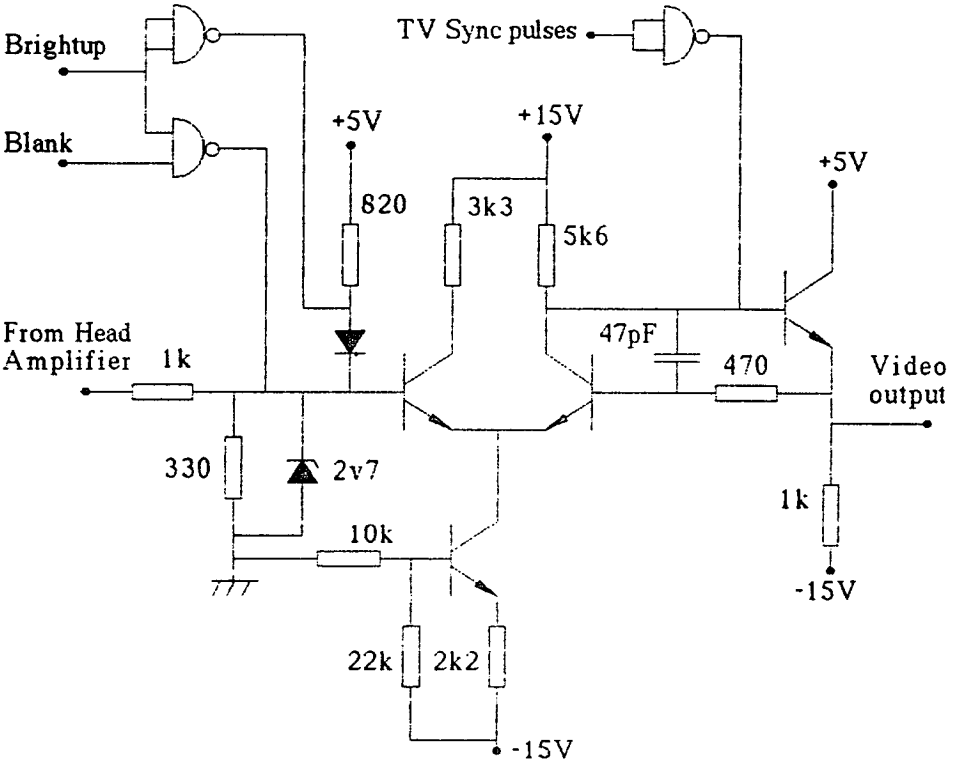

Figure A3.6 Video processing circuit

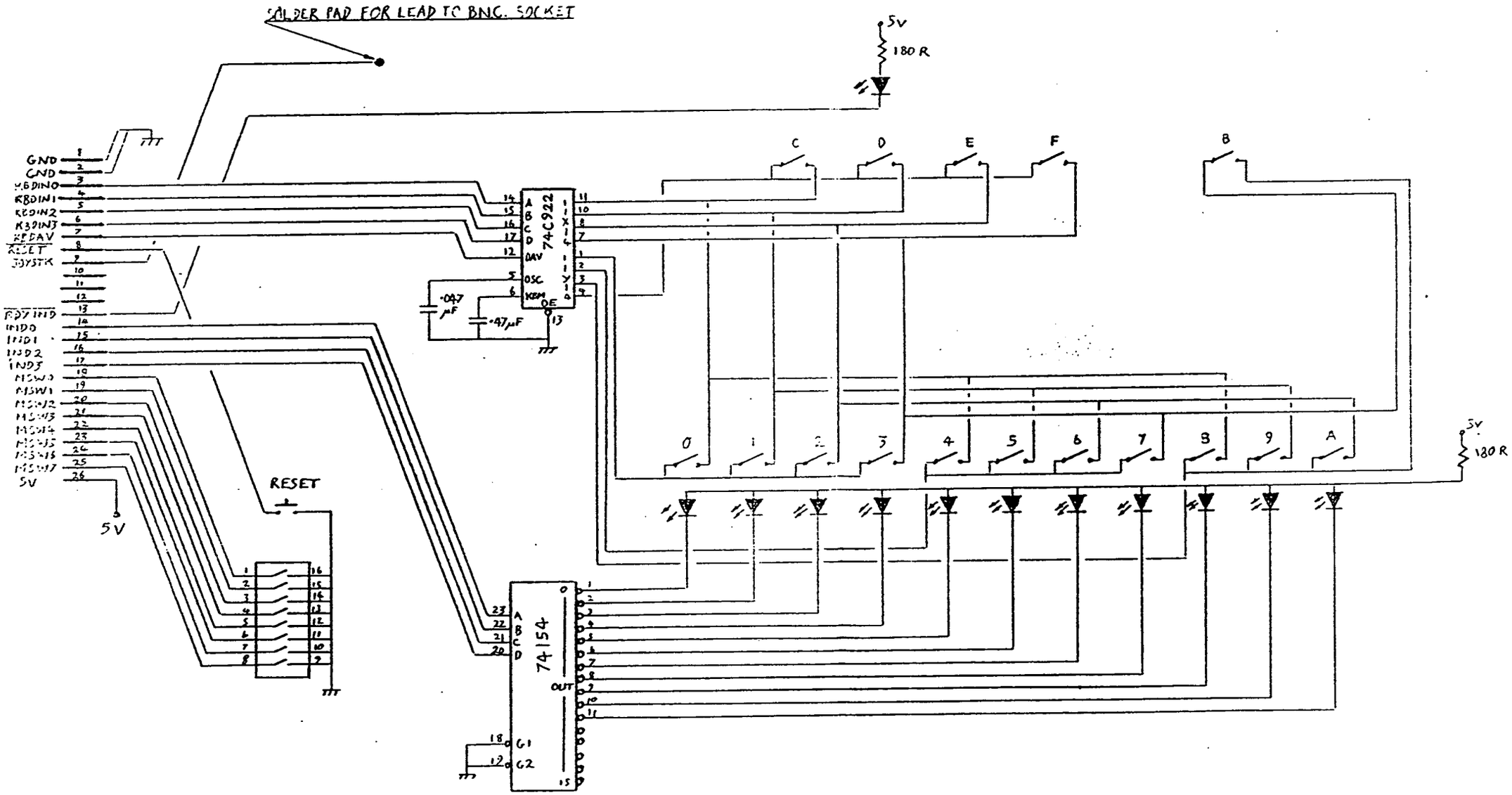

Figure A3·7 Front panel

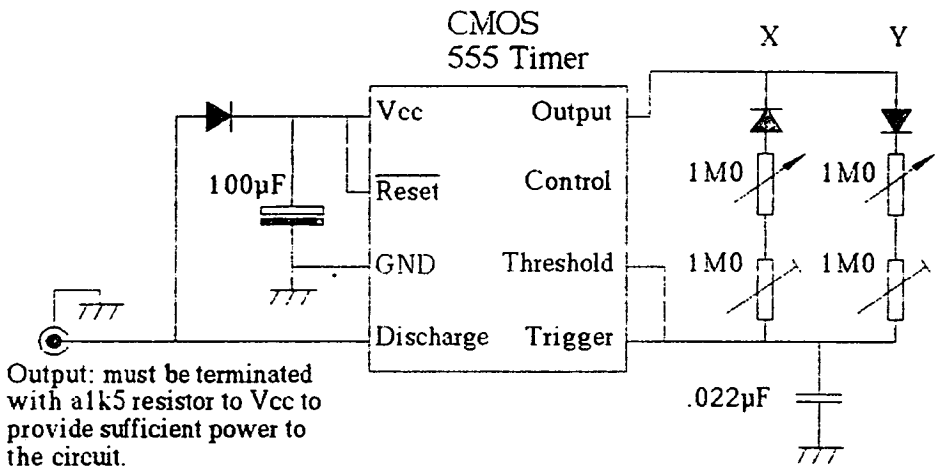

Figure A3.8 Remote cursor controller circuit

type) timer which draws its power from the signal line. Pin 3 (normally output) charges and discharges the timing capacitor via the X and Y control potentiometers respectively. Thus the mark time is proportional to X and the space time to Y. Pin 7 (normally discharge) provides an open drain output. A pull up resistor on the main circuit board completes the circuit and passes sufficient current during the mark time to power the IC via a diode and smoothing capacitor.

A3.2.6 Power Supply

The power supply which is housed in a plug in module at the left hand side of the rack, provides 5 volts at 5 amps from a commercial switched PSU module and 15 volts at 100mA unregulated which is regulated on the boards where necessary.

A3.3 Software

A3.3.1 General

Both local and remote control functions are implemented by software written in assembler for the 6809 microprocessor. Control of the scan functions is via PIA chips as outlined above, the processors address map is shown in figure A3.9

The three interrupt inputs are all used: NMI is driven by VIA IC which is set to generate on a change of level of the cursor position signal, FIRQ is driven by the GPIB interface IC and IRQ by PIA 4 in response to the data valid output from the front panel keyboard controller. All the interrupts both hardware and software (except RESET) are vectored via RAM locations so that they can be patched if required by user routines.

The low order five chip switches on the front panel are used to select the GPIB address, the remaining switches are unused.

The 32 character display area shows an initial message and version number at reset. A firmware function can maintain a numeric display of the current cursor position (0-4095) in this area, otherwise it can only be used for remotely loaded data.

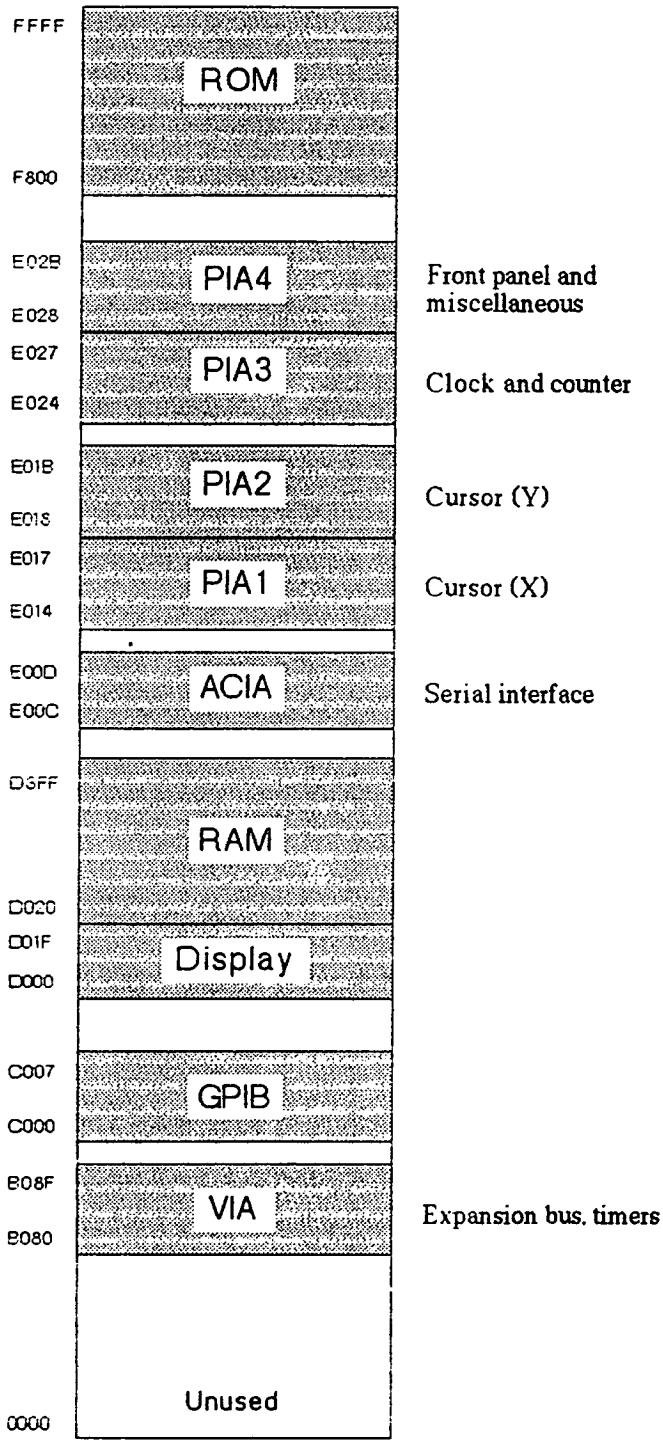

Figure A3.9 Scan Generator Memory Map - Addresses are hexade cimal. Memory is only partially decoded so addresses not shown are not necessarily unused.

A3.3.2 Front Panel Operation

The front panel has sixteen keys numbered 0-9, A-F whose layout is shown in figure A3.10. There are eleven scan rate select keys (approximate frame times are shown on the keys), four mode keys corresponding to normal scan, photo scan (single frame), line and spot modes and a grey secondary function key which is pressed before other keys to select additional display control functions.

Key	Primary Function	Secondary Function
0	TV 625 lines	
1	0.05s 512 lines	
2	0.1s 512 lines	
3	0.2s 512 lines	
4	0.5s 512 lines	Inverted horizontal scan
5	1s 512 lines	Non-inverted horizontal scan
6	2s 512 lines	Inverted vertical scan
7	5s 1024 lines	Non-inverted vertical scan
8	10s 1024 lines	Enable numeric display of cursor position
9	25s 1024 lines	Disable numeric display of cursor position
A	60s 2048 lines	Clear the alphanumeric buffer area
B	Secondary function	
C	VISUAL mode	Switch cursor crosswires on
D	RECORD mode	Switch cursor crosswires off
E	LINE scan	Switch alphanumeric display on
F	SPOT mode	Switch alphanumeric display off

The TV scan rate timing is determined by the sync pulse generator IC, there are approximately 585 active lines in one TV frame. The line and frame flyback times are set by two monostables and are fixed for all scan rates.

When record mode is first selected the scan is set to standby and the ready LED is lit. Pressing RECORD again triggers a single frame scan whenever this LED is on.

Inversion of X and Y scans is performed by hardware as described above. They are both inverted after a reset to suit the S100 SEM.

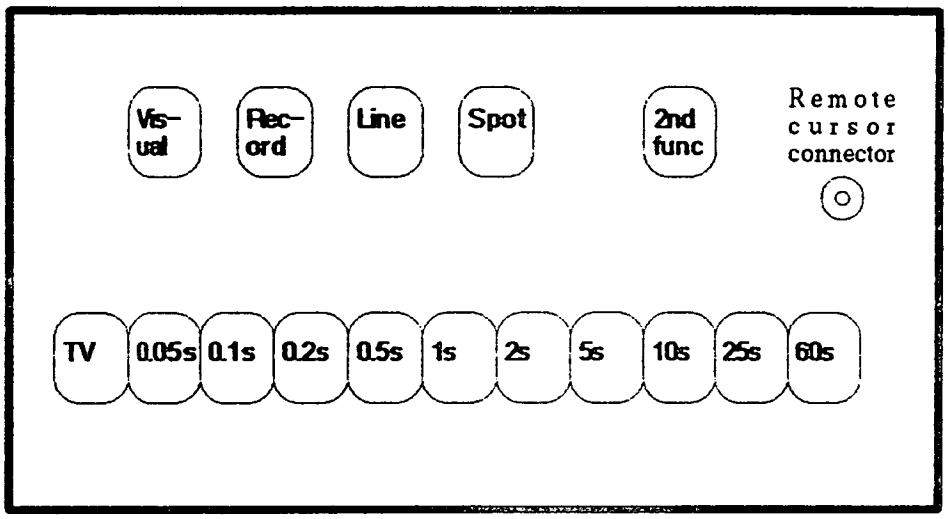

Figure A3.10 Front panel

The numeric cursor display, when selected, is continuously updated and will overwrite any other data.

Switching the cursor crosswires off only affects the display. The cursor control continues to operate and will continue to determine the spot or line position. Similarly switching the alphanumeric display off does not change the data in the display area which will re-appear when the alphanumerics are turned on again.

A3.3.3 Remote Control

The software provides a very wide range of remote control functions which are received via the GPIB. The user should be familiar with the general operation of the GPIB before attempting more complex programming (on the whole the "style" of the GPIB interface matches that of the GPIB driver for the SuperBrain).

GPIB Messages The GPIB END message is the normal method to terminate variable length commands and can also be used to terminate many commands prematurely. The service request (SRQ) message can be generated by the SG at the start of every frame if desired. The device clear (DCL) and selected device clear (SDC) messages have the same effect as a hardware reset except that the GPIB address is not read from the front panel switches and the start up message is not re-displayed.

Output via the GPIB To prevent the system from hanging when output over the GPIB is required, all output data is put in a buffer. When the SG is addressed to talk it will output bytes continuously starting from the beginning of the buffer. Once all valid data have been transmitted the SG will transmit garbage until it is unaddressed.

Command Format All remote commands consist of a single ASCII command character followed by various other data which may be in the form of further ASCII characters, as 8 bit binary data bytes or as 16 bit binary data words which are transmitted as two bytes with the least significant byte first. In variable length

commands where the number of bytes is not fixed, the command is usually terminated with the END message. In the following chart <char> represents an ASCII character, <byte> is an 8 bit binary byte and <word> is a 16 bit word. Square brackets: [] imply that the item may occur any number of times (including zero).

Command	Description
A [chars]	Alphanumeric display - all characters are displayed in the alphanumeric buffer until the command is terminated by END.
C <word><word>	Cursor set The two data words give the X and Y cursor positions (12 bits each, the high order bits are ignored). This command disables local control of the cursor. To re-enable the cursor the command must be terminated with END before any data are sent (i.e. the END is sent with the command character)
E <byte><byte>	Expansion output The first byte is put on the VIA B-data lines as an address, then the second byte is output on the A-data lines and the CA2 line pulsed to load the data into a peripheral.
F [chars]	Front panel emulation - followed by a string of hexadecimal digits representing front panel key strokes (see key numbers above) terminated by END or any character which is not a legal Hex digit.
G <addr>	Go to user routine at the given address - A "rts" instruction will return to the main program provided that no major RAM areas have been corrupted.
I <byte>	Input from expansion card through the VIA - the byte is put on the VIA B-data lines as an address, then a single byte is read from the A-data port and the CA2 line pulsed to signal that the data has been accepted. The received byte is then inserted into the GPIB output buffer.
L	Load data into memory from the serial port (Tektronix format hex data) - this is untested!
M <word>[bytes]	Modify memory Starting at the address specified by the first word, all following data bytes are stored sequentially in memory until the command is terminated by END.

O <byte> Operating mode - allows setting of the mode control byte - be careful as some combinations do not work.

R <byte><byte> Rate set
Direct setting of the scan rate: the first byte is the two's complement of the clock divisor, the second byte contains the X and Y counter increments (Y in high order 4 bits).

S State - places the following information in the GPIB output buffer: X cursor position (2 bytes), Y cursor position (2 bytes), Operating mode (1 byte), Clock divisor and counter increments (2 bytes).

T <char> Timing mode: the character must be '1' to set timing mode on or '0' to turn it off - with timing mode on a SRQ is generated on the GPIB at the start of every frame.

V <word> View memory - simply sets the output buffer pointer to the address given by the data word so that data will be output starting from this address when the SG is addressed to talk.

r Cursor right 8 places - (There are 4096 places across the display in both directions)

l Cursor left 8 places

u Cursor up 8 places

d Cursor down 8 places

A3.3.4 Scan Rotation

The scan rotation board built by a third year student project group plugs into the backplane of the scan generator. The column scan signals form the DAC boards are then fed through the rotation board to produce rotated scan signals. The display scan signals are not fed through the rotation unit. For full details see the appropriate student project report.

Appendix 4

SuperBrain - GPIB Interface

This circuit - shown in figure A4.1 is a fairly standard connection of the SuperBrain's expansion connector (which is in fact simply the un-buffered memory interface of the main z80 microprocessor) with the Texas Instruments TMS9914 GPIB interface IC [33] 34 [35]. Extra logic is provided to access an 8 way DIP-switch within the address space of the GPIB controller (A gap in it's address space is provided by the IC's designers for this purpose). Address decoding is carried out by one 74LS138 IC while the second one decodes the DIP-switch address. A clock for the TMS9914 is provided by a 5 Mhz quartz crystal oscillator and the GPIB signals are buffered by Texas Instruments IC's designed for this purpose. The only components not shown in this figure are a number of decoupling capacitors to reduce power supply noise.

The circuit was constructed using wire wrap connections on a single Eurocard size circuit board. It was mounted inside the Superbrain not only for neatness but also to minimise the length of the connections to the unbuffered expansion bus to which it was connected using ribbon cable. A standard GPIB connector was mounted in the computers back panel and connected to the board again using ribbon cable.

This interface gave no problems at all over several years life.

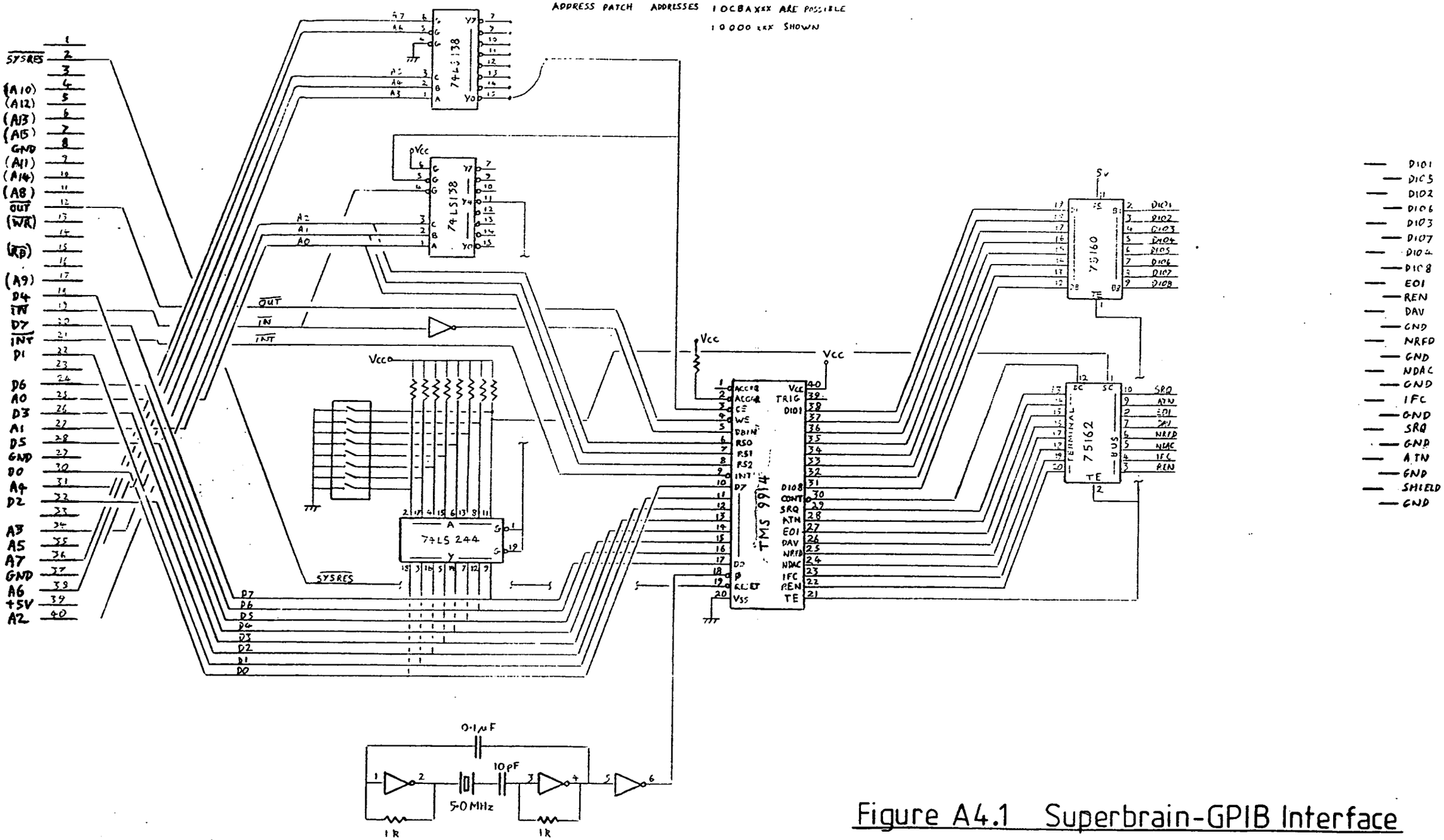

Figure A4.1 Superbrain-GPIB Interface

Appendix 5

Voltage Contrast Software Details

A5.1 Introduction

The results described in chapters five and six are outputs from not one program in particular but a series which were developed and modified as the techniques were refined in order to investigate particular phenomena. This appendix describes in more detail some of the algorithms used.

A5.2 Program Structure

All programs were structured in a similar way which was heavily influenced by the style of the operating system. The p-System's user interface presents the user with a menu of alternative actions which may be selected by typing a single character. Selection of a menu option typically takes the user into a more detailed menu or runs a program or routine within a program. The library of procedures and functions which come with the system's Pascal compiler include a whole suite of routines for manipulation of these on screen menus.

The highest level of the program performs any necessary initialisation - principally setting the scan generator and spectrometer into a known state. It then enters a simple loop which presents the user with a menu of options. These typically include: Set or modify S-curve parameters - The filter grid voltage range and number of points; Capture and display a single S-curve - useful for checking gain and offset levels to ensure adequate signal levels without clipping; Set spot position - switches the SEM's cursor display on and enables the remote control. Individual programs included a wide range of other options along these lines. To begin with many parameters such as size and values for convolution operators, and delays (to allow conditions to settle) between sampling were changable but as optimum values

were discovered they became embedded in subsequent programs which then performed further more complex processing. The three most important stages common to all programs are sampling of the S-curve, convolution with a short operator and in later programs where the use of a double diferential operator was fixed the detection of the position of the zero crossing on the resulting curve.

A5.3 S-curve sampling

Two external routines are defined in the device dependent module for driving the multiprogrammer:

```
procedure setgrid(v : real);
function pmout : integer;
```

which set the filter grid voltage, via the multiprogrammer, to v volts and return the head amplifier output voltage as an integer respectively (the head amp scaling depends on the hardware but is unimportant here). Using these two routines S-curve sampling is performed by a very simple program fragment in Pascal:

```
const
    n = 20; {number of points}
    stepv = 1; {step size in volts}
    startv = -5; {start of sweep in volts}

var
    S : array[0..n] of integer; {the s-curve}
    i : integer;
....

    write(scangen, 'FF '); {set spot mode}
    for i := 0 to n do
    begin
        setgrid(startv+i*stepv);
        S[i] := pmout
    end;
    write(scangen, 'FC '); {revert to scanning}
```

The two write statements control the scan generator - see Appendix 3.

A5.4 Convolution

The single most important routine common to all programs is the process of convolving an array of sampled and sometimes processed data with a shorter operator see section 5.2.3.3. Assuming an S-curve has been sampled and stored in an array in memory $S_0..S_n$ (this is an $n+1$ point curve) to convolve it with a prestored operator $C_{-m}..C_m$ ($2m+1$ points) and place the result in array $R_m..R_{n-m}$ the formula is:

$$R_i = \sum_{j=-m}^{m} S_{i-j}C_j$$

this is programmed directly in Pascal by a routine something like:

```
var C : array[-m..m] of integer; {operator}
    S : array[0..n] of integer;  {S-curve}
    R : array[m..n-m] of integer; {Result}
    i,j : integer;  {index counters}

....

    for i := m to n-m do
    begin
        R[i] := 0;
        for j := -m to m do
        begin
            R[i] := S[i-j]*C[j]
        end
    end
```

A5.5 Zero Crossing Detection

The final stage in the process of measuring S-curve position is to detect the zero crossing point Z. This was done by tracing the resulting curve from low to high and simply finding the first point with a positive value. The points of interest are found by the simple routine:

```
var R : array[m..n-m] of integer; {convolution result}
    i : integer;  {index}
    Z : real; {the calculated zero crossing}

....

    i:=m;
    while R[i]<0 do i := i+1;
    Z := i - R[i]/(R[i]-R[i-1]);
```

The last line performs simple linear interpolation between the two known points on the resulting curve which lie either side of zero.

SCANNING™
Journal of Scanning Electron Microscopy and Related Methods

Reprints

FACM Publishing. Inc.

SCANNING Vol. 7, 113–116 (1985)

Received: December 17, 1984

Original Paper

Digital Techniques for Improved Voltage Measurements

P. Nye and A. R. Dinnis

Edinburgh University, Department of Electrical Engineering, Kings Buildings, Mayfield Rd, Edinburgh EH9 3JL, Scotland

Introduction

The principle of making quantitative voltage contrast measurements using an electron energy spectrometer has been discussed extensively. However, in real situations accurate measurements are very difficult using existing techniques, and the usefulness of such systems is often impaired because of the time required to set up operating conditions and take readings. This paper describes a new technique, using digital signal processing, which has several major advantages:

1) Inaccuracies caused by amplitude changes in the cumulative energy distribution curve (S-curve) are eliminated.
2) A simple algorithm is used to find the point of inflection of the S-curve.
3) The system uses a very simple electron energy spectrometer, and could be used with most currently available models.
4) Measurements are made very rapidly making operation much simpler.
5) The fact that the electron beam is only stopped at one point for a fraction of a second introduces several other benefits: Specimen damage is reduced. Contamination buildup leading to drift in the S-curve is virtually eliminated. The effect of changing surface field, due to charge on exposed oxide leaking away when the scan is stopped, is minimised.

Background

The method used in almost all current quantitative voltage-contrast measurement systems consists of an accelerating – retarding (high pass) electron energy spectrometer in a simple feedback arrangement as shown in Fig. 1 (*Menzel* and *Kubalek* 1983). The retarding voltage is continuously adjusted to maintain the output at some constant reference level, thus a shift in the S-curve should be tracked exactly by a shift in the retarding voltage. The most important disadvantage with this arrangement is that variations in the amplitude of the S-curve can affect readings as much as shifts in its position do. Also the beam must be directed at the point to be measured for some time while the gain or reference level is adjusted. The action of stopping the scan can cause specimen damage and contamination buildup and, most importantly, a constantly changing surface field is experienced for several seconds as the charge on surrounding oxide leaks away. More complicated systems such as that described by *Gilhooley* and *Dinnis* (1983), which uses AC modulation of the retarding voltage and signal processing to detect the position of the S-curve, overcome the problem of varying S-curve height but still require much adjustment for each measurement, and are very inflexible.

The new system developed uses a conventional energy analyser, but a digital computer is used for control, acquisition and processing of voltage contrast information.

SCANNING Vol. 7, 113–116 (1985)

Received: December 17, 1984

Original Paper

Digital Techniques for Improved Voltage Measurements

P. Nye and A. R. Dinnis

Edinburgh University, Department of Electrical Engineering, Kings Buildings, Mayfield Rd, Edinburgh EH9 3JL, Scotland

Introduction

The principle of making quantitative voltage contrast measurements using an electron energy spectrometer has been discussed extensively. However, in real situations accurate measurements are very difficult using existing techniques, and the usefulness of such systems is often impaired because of the time required to set up operating conditions and take readings. This paper describes a new technique, using digital signal processing, which has several major advantages:

1) Inaccuracies caused by amplitude changes in the cumulative energy distribution curve (S-curve) are eliminated.
2) A simple algorithm is used to find the point of inflection of the S-curve.
3) The system uses a very simple electron energy spectrometer, and could be used with most currently available models.
4) Measurements are made very rapidly making operation much simpler.
5) The fact that the electron beam is only stopped at one point for a fraction of a second introduces several other benefits: Specimen damage is reduced. Contamination buildup leading to drift in the S-curve is virtually eliminated. The effect of changing surface field, due to charge on exposed oxide leaking away when the scan is stopped, is minimised.

Background

The method used in almost all current quantitative voltage-contrast measurement systems consists of an accelerating – retarding (high pass) electron energy spectrometer in a simple feedback arrangement as shown in Fig. 1 (*Menzel* and *Kubalek* 1983). The retarding voltage is continuously adjusted to maintain the output at some constant reference level, thus a shift in the S-curve should be tracked exactly by a shift in the retarding voltage. The most important disadvantage with this arrangement is that variations in the amplitude of the S-curve can affect readings as much as shifts in its position do. Also the beam must be directed at the point to be measured for some time while the gain or reference level is adjusted. The action of stopping the scan can cause specimen damage and contamination buildup and, most importantly, a constantly changing surface field is experienced for several seconds as the charge on surrounding oxide leaks away. More complicated systems such as that described by *Gilhooley* and *Dinnis* (1983), which uses AC modulation of the retarding voltage and signal processing to detect the position of the S-curve, overcome the problem of varying S-curve height but still require much adjustment for each measurement, and are very inflexible.

The new system developed uses a conventional energy analyser, but a digital computer is used for control, acquisition and processing of voltage contrast information.

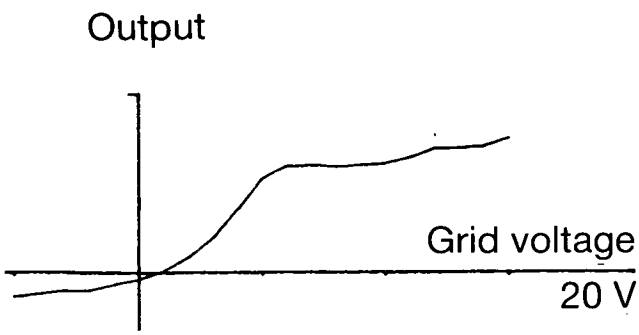

Fig. 3a

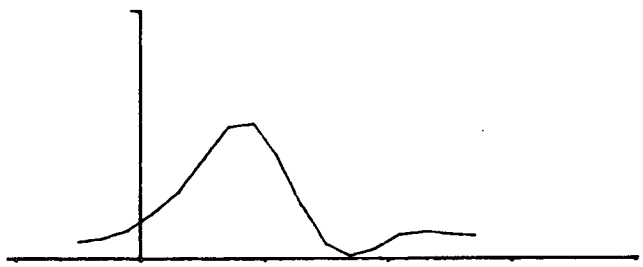

Fig. 3b

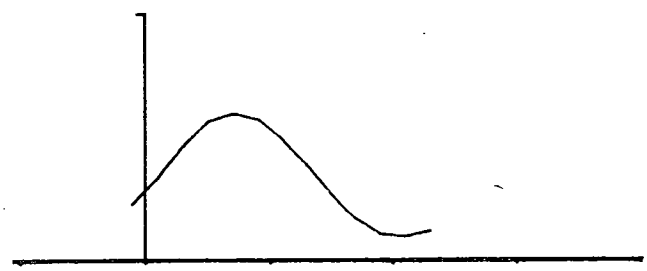

Fig. 3c

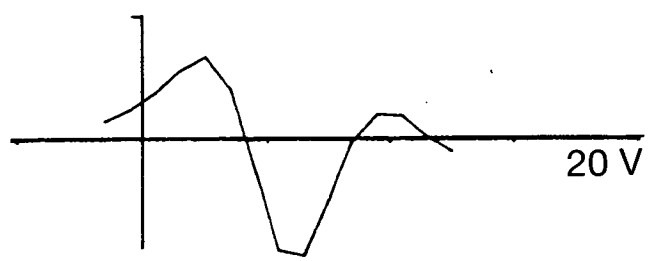

Fig. 3d

Fig. 3 (a) Sampled S-curve; (b) after convolution with 5 point ramp; (c) with 9 point ramp; (d) with 7 point double differential operator.

With the statistically small numbers of points involved, care must be taken in processing the curve. Convolution with a simple differentiating operator – a linear ramp (*Arthur* et al. 1980) – should provide a peak at the steepest point on the S-curve. The problem here is that it is not easy to deduce the position of the peak of the resulting curve with a resolution better than the 1 V step size. Differentiating a second time though will produce a curve with a zero crossing corresponding to the point of inflection on the original S-curve, and its position may be estimated by interpolation. In all cases convolving with a longer operator will give a less noisy result (analogous to low pass filtering) but reduces the number of points, and if this filtering is too severe it will tend to smooth out the details of the S-curve which we are trying to locate. To illustrate these points Fig. 3 shows an S-curve (a) together with the results of convolving it with 5 and 9 point ramp (differential) operators (b and c) and with a 7 point double-differencing operator (d). It can be seen that the curve of Fig. 3d has a very clearly defined zero crossing corresponding to the steepest point on the S-curve.

Finally Fig. 4a shows a family of S-curves, sampled with the track of interest on the specimen varying from 0 to 5 V in 1 V steps. The results of convolving these curves with the same 7 point double-differential operator are shown in Fig. 4b. It can be seen that the zero crossings are evenly spaced and track the specimen voltage nicely. The voltages at these zero crossing points are calculated by interpolation and in Fig. 4c they are plotted against the applied specimen voltage (in this graph crosses are the calculated values and the dashed line is an ideal linear response shown for comparison).

Conclusions

The combination of computer control of the beam with digital analysis of the signal allows greatly simplified acquisition of voltage contrast information together with improved accuracy and reduced specimen damage. The equipment used for these experiments is slow and the computing power minimal. A more powerful computer has been purchased and it is hoped that converting to this system will make further improvements in the speed and versatility of the system, however the current work has demonstrated the usefulness of the technique.

SCANNING
Journal of Scanning Electron Microscopy and Related Methods

Reprints

FACM Publishing. Inc.

Original Paper

Extraction Field and Oxide Charging in Voltage Contrast Systems

P. Nye and A. Dinnis

Edinburgh University, Department of Electrical Engineering, Kings Buildings, Mayfield Rd, Edinburgh EH9, 3JL, Scotland

1. Introduction

The majority of systems for making voltage contrast measurements are based on some kind of extracting-retarding field secondary electron energy analyser and all such systems use an extraction electrode at high voltage close to the specimen to ensure that the maximum possible number of secondaries are detected (*Menzel* and *Kubalek* 1983). This extraction field is a major factor in determining the charging on any exposed oxide on the IC under test and this in turn can have great influence on quantitative measurements, due to strong local fields at the surface. The new system in use at Edinburgh University (*Nye* and *Dinnis* 1985) makes studies of quantitative voltage contrast particularly easy, and it is now possible to make direct measurements of oxide potential with minimum disturbance of this charge. Using this system, the effects of extraction field on surface charging have been investigated.

2. Equipment

A block diagram of the system is shown in Fig. 1. The microscope is a Cambridge Instruments Stereoscan-100 which is connected to an external digital scan-generator (constructed in this department) which is remotely controlled from a microcomputer. The electron energy spectrometer used is very similar to the one described by *Ranasinghe* and *Khursheed* (1983), but is of vastly simplified construction; in particular the lower surface of the analyser is very flat to create as uniform an extracting field as possible. The voltage on the retarding grid of the energy analyser is controlled from a digital to analogue converter (DAC) and the output from the detector is fed to an analogue to digital converter (ADC), both connected to the microcomputer (via an IEEE-488 interface). Further DACs are available for control of specimen voltages and extracting field.

The specimen used in all the experiments is a test specimen, consisting of aluminium tracks and pads over an oxide layer, built by the Edinburgh Microfabrication Facility. This provides a specimen on which voltages and geometries are known, but which is typical of simpler real IC's. The layout of the specimen is shown in Fig. 2.

In operation the program switches the scan-generator from scan to spot modes and directs the electron beam at the point of interest for the shortest possible time while the retarding grid of the analyser is swept and an S-curve sampled. Apart from the short time taken for this operation (about 200 ms) the specimen is subjected to continuous uniform scanning. Having sampled the S-curve, digital processing and interpolation are used to estimate the position of the curve, which should track the specimen voltage.

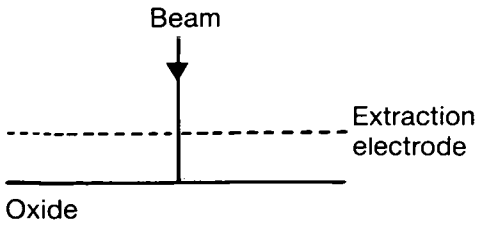

Fig. 4 Simplest case of flat extraction electrode above large area of oxide

4. Theory

When exposed oxide on an IC is irradiated with primary electrons in the SEM it emits a number of secondary electrons determined by the secondary emission coefficient. For the primary beam energies useful for voltage contrast (500-1500 eV) this is assumed to be greater than one. For the simple case of a uniform oxide surface beneath a flat extraction electrode at a positive voltage (Fig. 4) the secondaries will initially be pulled away by the extraction field, however, as this happens the surface begins to charge positively thus reducing the extracting field. Eventually an equilibrium condition will be reached such that the number of secondaries returning to the surface plus the number of absorbed primaries is equaled by the number being extracted. As the secondaries are emitted with an energy of a few eV, this condition would occur with the surface charged to a few volts *above* the extraction voltage.

In practice the surface voltage is also affected by other factors and charge tends to leak away by other mechanisms. Also on an IC beneath a real energy analyser the field at the surface is not determined solely by the extraction voltage but depends on the arrangement of tracks on the IC, and the particular geometry will have a great effect on surface charging since the surface to extraction-electrode spacing is usually large in comparison to the size of surface features. In general it is to be expected that the more remote the extraction electrode is in comparison to other elements contributing to surface field, the less will be its effect on oxide potential.

5. Experimental Results

Initial results were taken from the centre of a large area of exposed oxide; the rectangle marked A in Fig. 2 was scanned and S-curves were sampled for values of extraction voltage varying from 10 to 28V in 2V steps; the results are shown in Fig. 5. It can be seen

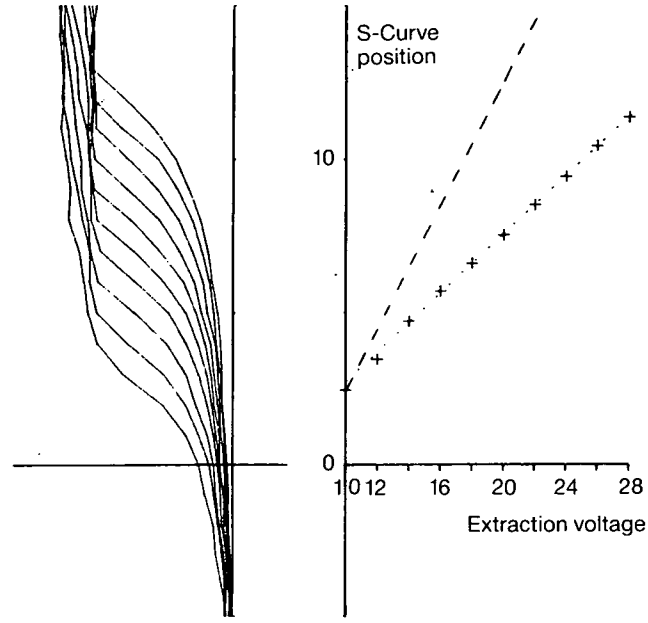

Fig. 5 S-curves sampled from centre of area A: Dashed line = 1V/V, dotted line = 0.48V/V

that the oxide potential rises but by nothing like the same amount as the extraction voltage. In this figure the dashed line shows the gradient of the extraction voltage while the gradient of the measured oxide potential is approximately 0.48V/V (dotted line).

5.1 Effect of area scanned

From the arguments outlined above (section 4) we would expect that as the scanned area is reduced and the ratio of scanned area to specimen/extraction-electrode distance becomes small the extraction voltage would have less effect on the oxide potential. To illustrate this the area scanned was reduced to rectangle B (Fig. 2) and then to rectangle C and the curves of Fig. 6 and Fig. 7 were produced; the change of oxide potential with extraction voltage being approximately 0.41 V/V and 0.24 V/V respectively.

5.2 Effect of nearby conductors

For all subsequent results the region scanned was changed to the area marked D (Fig.2). To illustrate the effects of nearby conductors, readings were taken from points E and F. The apparatus restricts the maximum output voltage swing over one set of curves to 20 V, so to obtain data for a wide range of extraction voltage it was necessary to take several sets of readings. Figure 8 (a, b and c) show 3 sets of curves for extrac-

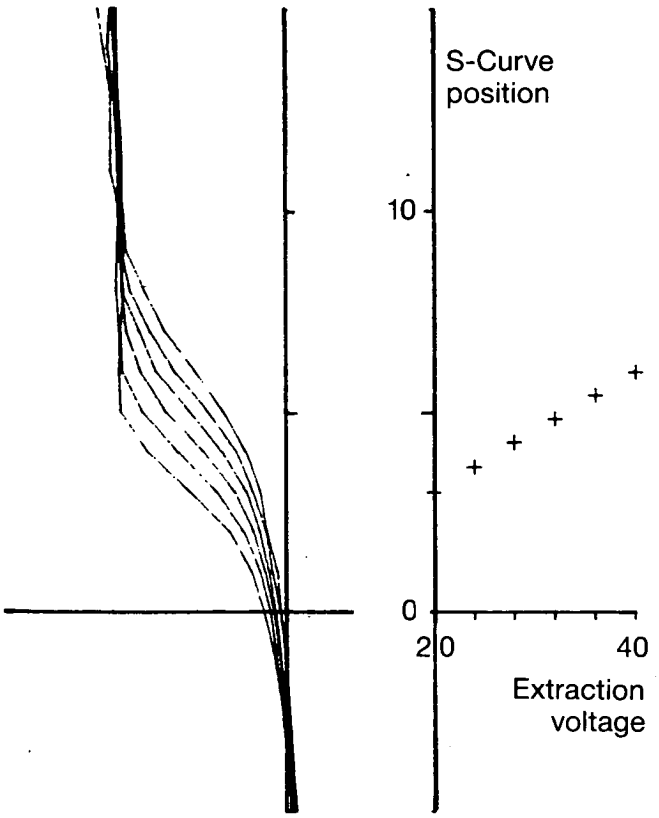

Fig. 8b

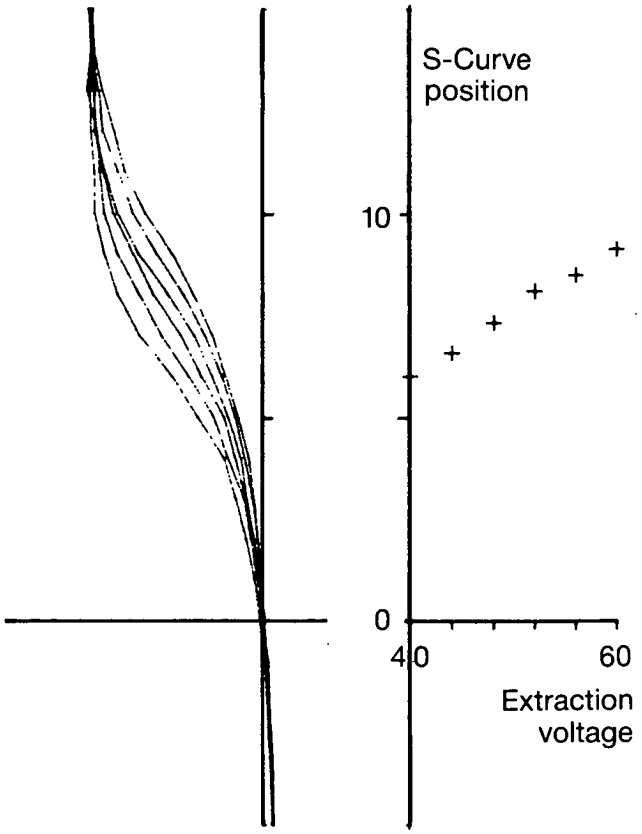

Fig. 8c

5.3 Effect of oxide potential on voltage contrast linearity

Surface fields can have a strong effect on the accuracy of voltage contrast measurements and oxide charging must make a large contribution to these fields. The setup used is ideally suited to making measurements of voltage contrast linearity as shown in Fig. 3. A series of such measurements were made from point G (Fig. 2) for a number of values of extraction voltage and the results are shown in Figs. 12-16. At lower values of extraction voltage (e.g. Fig.13) the measured value tracks the actual voltage well, up to a point at which the S-curves begin to collapse and the measured voltage continues to rise very much more slowly, if at all. This turning point, or elbow, occurs at a voltage closely related to oxide potential and indicates that as the track becomes more positive than the surrounding oxide then the secondary electrons, particularly those with lower energies, are lost. Examination of the S-curves of Fig. 12 shows that there is a clear cutoff energy corresponding to a retarding grid voltage of around 6V (shown by dashed line).

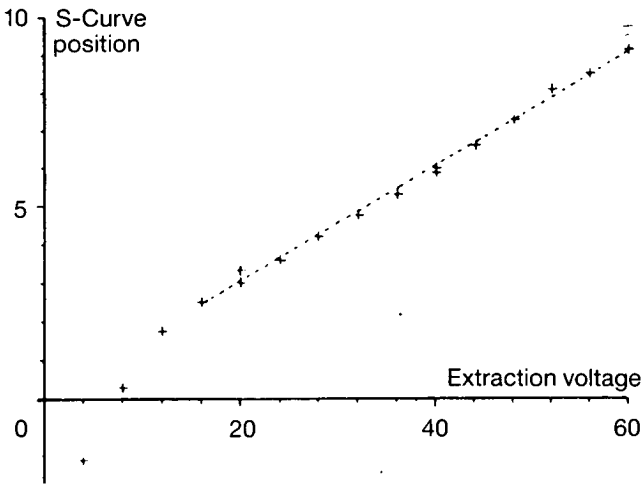

Fig. 9 Positions of S-curves from point E (from Fig. 8): Dotted line = 0.15V/V

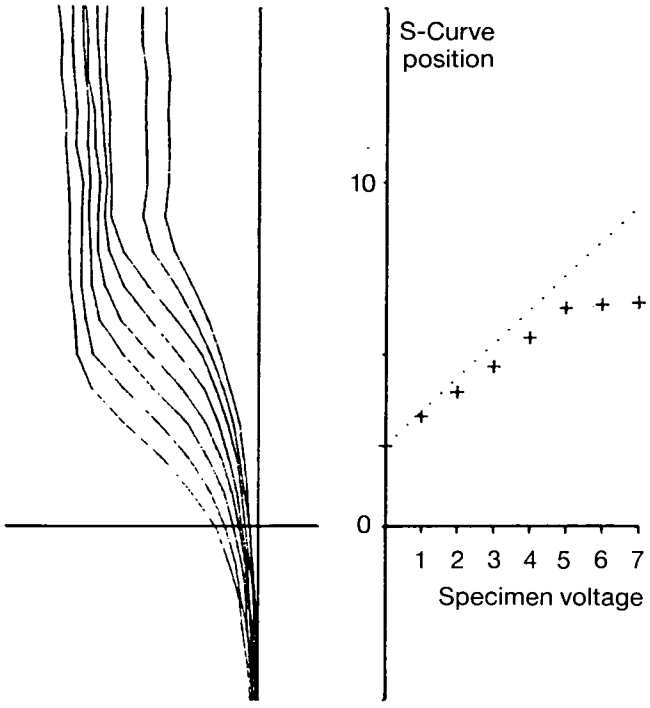

Fig. 14 Voltage contrast linearity curve (point G), extraction voltage = 30V

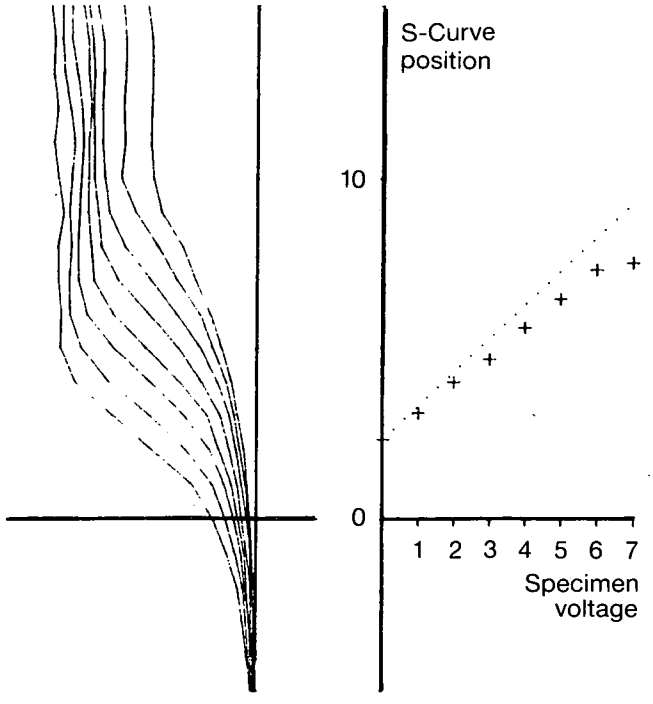

Fig. 15 Voltage contrast linearity curve (point G), extraction voltage = 35V

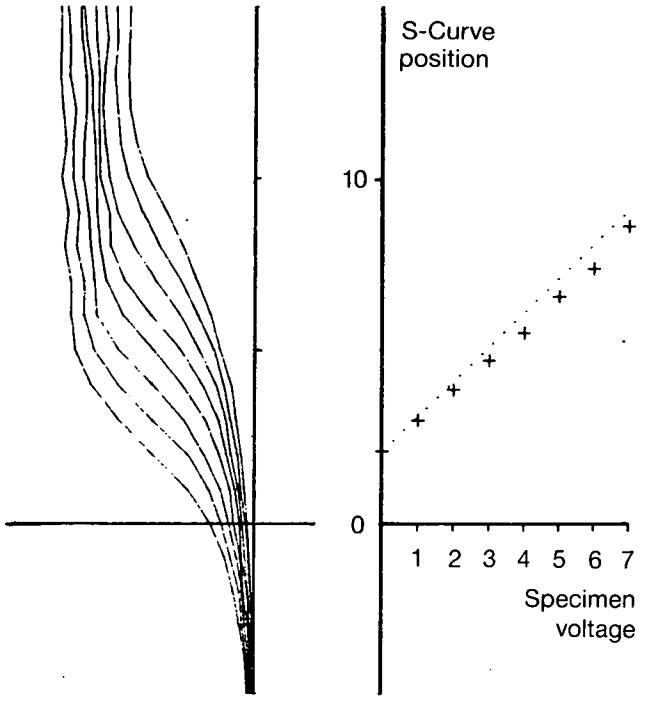

Fig. 16 Voltage contrast linearity curve (point G), extraction voltage = 40V

5.4 Estimation of absolute value of oxide voltage

These results all show relative changes in oxide potential but do not indicate any absolute value. As a guide an absolute value can be estimated by reference to curves from a conductor at a known voltage (e.g. Fig. 11). This estimation though, rests on the assumption that the secondary electron energy distribution is the same for SiO_2 as it is for aluminium. Another method for estimating the oxide voltage would be to deduce it from the position of the elbow in the curves of Figs. 12-16.

6. Conclusions

The value of oxide potential is closely connected with extraction voltage as predicted and the final figures show that this can have a drastic effect on the accuracy of voltage contrast measurements. This would seem to indicate that a high extraction field is desirable. However the resultant high surface voltage is very undesirable for the proper functioning of many

References

1 P May, J M Halbourt & G Chiu. "Non-contact High-speed Waveform Measurements with the Picosecond Photoelectron Scanning Electron Microscope". IEEE Journal of Quantum Electronics 24, 234-239 1988

2 T E Everhart and R F M Thornley. "Wide Band Detector for Micro-Ampere Low-energy Electron Currents". J. Sci. Instrum. 37, 246-250 1960

3 G V Lukianoff & G O Langner. "Electron Beam Induced Voltage and Injected Charge Methods of Testing". Scanning 5, 53-70 1981

4 M S Chung & T E Everhart. "Simple Calculation of Low-energy Secondary Electrons Emitted from Metals Under Electron Bombardment". J. Appl. Phys. 45, 707-709 1974

5 W J Tee & A Gopinath. "A Voltage Measurement Scheme for the SEM Using a Hemispherical Retarding Analyser". SEM 1976/IV 595-602 (Chicago: IIT Research Institute) 1976

6 G S Plows & W C Nixon. "Stroboscopic Scanning Electron Microscopy". J. Phys. E: Sci. Instrum. 1, 595-600 1968

7 K G Gopinathan & A Gopinath. "A Sampling Scanning Electron Microscope". J Phys. E: Sci. Instrum. 11, 229-233 1978

8 J M Hannah. "SEM Applications to Integrated Circuit testing". PhD Thesis, University of Edinburgh 1974.

9 O Wells & C G Bremer. "Improved Energy Analyser for the SEM". J. Phys. E: Sci. Instrum. 2. 1120-1121 1969

10 H P Feuerbaum. "VLSI Testing Using the Electron probe". Scanning Electron Microscopy 1979/I (Chicago: SEM inc.) pp 285-296 1979

11 G S Plows. "An Electrode System of a retarding Field Spectrometer for a Voltage Measuring Electron Beam Apparatus". European patent application number 83902278.7 Jan 7 1988

12 E Menzel, E Kubalek "Secondary Electron Detection Systems for Quantitative Voltage Measurements". Scanning 5. 151-171 1983

13 A Khursheed & A Dinnis. "A Comparison of Voltage Contrast Detectors" Scanning 6, 85-95 1984

14 D W Ranasinghe & A Khursheed. "Design of a High Efficiency Secondary Electron Collector". Proc 3rd Oxford Conf on Microscopy of Semiconducting Materials. p 433. Institute of Physics 1983

15 P Nye. "Digital Scan Generator - Users Manual" internal document. University of Edinburgh. Department of Electrical Engineering. 1987

16 Third year undergraduate project report. University of Edinburgh, Department of Electrical Engineering. 1982

17 B Gilhooley. "A Quantitative Voltage Contrast Test and Measurement System". PhD Thesis, University of Edinburgh 1984

18 R Schmitt, D Winkler, M Brunner, J M Dortu. "Application of High Speed Electron Beam Testing in Solid State Electronics". Proceedings Microcircuit Engineering Conference, Cambridge 1989.

19 Saad Alshaban. "Instrumentation for Observation of High Frequency Signals in the Scanning Electron Microscope". PhD Thesis. University of Edinburgh 1983

20 TDI Ltd. Bristol. UCSD p-System for Intertec SuperBrain.

21 J W Arthur, C F N Cowan & J Mavor. "Analogue Real Time Statistical Analyser Using CCD's to Implement a Decision Algorithm". IEEE Transactions on Instrumentation and Measurement. March 1980

22 P Nye & A R Dinnis. "Digital Techniques for Improved Voltage Measurements" Scanning 7, 113-116 1985

23 P Nye & A R Dinnis. "Extraction Field and Oxide Charging in Voltage Contrast Systems" Scanning 7, 117-125 1985

24 E Plies. "Electron-Optical Components for E-Beam Testing". To be published Proc. 2nd European Conf. on Electron Optical Beam Testing of Integrated Circuits. Duisburg October 1989.

25 K Nakamane. H Fujioka & K Ura. "Local Field Effects on Voltage Contrast in the Scanning Electron Microscope". J. Phys. D: Appl. Phys. 14. pp1939-1960 1981

26 A Gopinath. "Estimate of Minimum Measurable Voltage in the SEM". J. Phys. E: Sci. Instrum. 10. 911-913 1977

27 L Dubbeldam. "A Voltage Contrast Detector With Double Channel Energy Analyser in a Scanning Electron Microscope". PhD Thesis, Delft University of Technology, Netherlands 1989

28 A Khursheed & A R Dinnis. "A Time of Flight Detector for Voltage Contrast". J. Sci. Instrum. To be published 1990.

29 Specification of Electron Beam Tester Model S-8000, Hitachi Ltd., Tokyo, Japan

30 Specification of E-Beam Testing System 9000, Integrated Circuit Testing GmbH, D8011 Heimstetten, Federal Republic of Germany.

31 S Görlich, E. Postulka, E. Kubalek "Window Scan Mode for Testing Passivated MOS Devices". Proceedings - Microcircuit Engineering, Cambridge 1983 pp 493-500.

32 Lionel Levy. "The Development of an E-Beam Testing System With Industrial Applications in the Debug of Advanced Semiconductors". PhD Thesis, University of Edinburgh, 1990.

33 Zilog Inc. Z80 Microprocessor Technical Manual. 1978

34 Texas Instruments Ltd. TMS9914 Data Manual.

35 Texas Instruments Application Report B213: General Purpose Interface Adaptor TMS9914.